New Wrinkles on Black Hole Perturbations: Numerical Treatment of Acoustic and Gravitational Waves

Valery Tenyotkin

A dissertation submitted to the faculty of the University of North Carolina at Chapel Hill in partial fulfillment of the requirements for the degree of Doctor of Philosophy in the Department of Physics and Astronomy.

Chapel Hill
2009

Approved by:

Charles R. Evans

J. Christopher Clemens

Jianping Lu

Laura Mersini-Houghton

Y. Jack Ng

Abstract

VALERY TENYOTKIN: New Wrinkles on Black Hole Perturbations: Numerical Treatment of Acoustic and Gravitational Waves.
(Under the direction of Charles R. Evans.)

This thesis develops two main topics. A full relativistic calculation of quasi-normal modes of an acoustic black hole is carried out. The acoustic black hole is formed by a perfect, inviscid, relativistic, ideal gas that is spherically accreting onto a Schwarzschild black hole.

The second major part is the calculation of sourceless vector (electromagnetic) and tensor (gravitational) covariant field evolution equations for perturbations on a Schwarzschild background using the relatively recent $\mathcal{M}^2 \times \mathcal{S}^2$ decomposition method. Scattering calculations are carried out in Schwarzschild coordinates for electromagnetic and gravitational cases as validation of the method and the derived equations.

Acknowledgments

I thank all those who were close to me during my tenure at UNC Chapel Hill for emotional support; my advisor for sharing his knowledge and experience; and my office-mates for comic relief.

Table of Contents

List of Figures

List of Tables

Chapter 1

Introduction

"It is a capital mistake to theorize before one has data. Insensibly one begins to twist facts to suit theories, instead of theories to suit facts."

– Sir Arthur Conan Doyle.

If anything is to be inferred from the quote above it is that Sherlock Holmes would disapprove of this work, for it seeks to aid the search of a natural phenomenon by *a priori* assumption of its existence.

1.1 Overview

Presented in this thesis are two seemingly distinct yet subtly connected themes. One deals with a classical notion, sound, in a relativistic environment, in the immediate vicinity of a Schwarzschild black hole; the second replaces the scalar, acoustic perturbation with electromagnetic – vector, and gravitational – tensor ones.

1.1.1 The Acoustic Black Hole

An acoustic black hole forms when an accelerating fluid becomes supersonic. At certain locations the fluid accelerates and exceeds the local speed of sound for which said fluid is the medium, forming an *acoustic event horizon*; no acoustic event can travel upstream from that point on. A simplified example is a river culminating in a waterfall. Surface water waves propagate slowly and acceleration caused by the waterfall easily exceeds the water wave speed creating a *water wave event horizon*; if a pebble is thrown into the water beyond the horizon – surface wave information of the event will not propagate upstream to the rest of the river.

In this part of the thesis, the quasinormal modes of one such system are computed. Quasinormal modes are the resonance-like frequencies of energy dissipation, which are excited when a perturbation is introduced (pebble is thrown) into the medium (water) before the event horizon.

In addition, it is shown that in a special limit of the [perfect] fluid whose equation of state is given[1] by $p = \rho$, as in [41], the solution limits on the quasinormal modes of the Regge-Wheeler scalar wave.

1.1.2 $\mathcal{M}^2 \times \mathcal{S}^2$ Decomposition

One oftentimes encounters a phrase "cracking a peanut with a sledgehammer." The phrase exists for the sole purpose of drawing attention to the fact that perhaps a tool more suited for peanuts can be used instead, such as a nutcracker. The problem with both tools is that they are the extremes: one too general and the other too specific.

The blessing and the curse of General Relativity is that it is, perhaps, too general. Its statements are sledgehammers until a coordinate system is adopted, and they

---

[1]Where ρ is the total energy density.

quickly reduce to nutcrackers once the coordinates are chosen and become more or less single-use formulae with little chance of more widespread implementation, even more so if a specific gauge is selected.

In this part of the thesis, a relatively novel treatment of the equations of General Relativity, which seeks to strike a balance between the overwhelmingly general and the ephemerally specific is introduced. The so-called $\mathcal{M}^2 \times \mathcal{S}^2$ decomposition assumes Schwarzschild space but, not Schwarzschild coordinates and preserves complete covariance in the r, t sector ($\mathcal{M}^2$) while settling on use of spherical coordinates on the sphere ($\mathcal{S}^2$).

1.1.3   Electromagnetic Waves on Schwarzschild Background

As a test of the $\mathcal{M}^2 \times \mathcal{S}^2$ decomposition, the electromagnetic vector potential A_μ is cast on Schwarzschild background and covariant equations describing the electromagnetic field are derived. A coordinate system is then selected and reflection/ transmission of the electromagnetic radiation from/through the Schwarzschild curvature is [numerically] computed. Results match those previously obtained via traditional calculations.

1.1.4   Gravitational Waves on Schwarzschild Background

Successful application of the new $\mathcal{M}^2 \times \mathcal{S}^2$ decomposition method leads to an attempt at the implementation of this method on a perturbation of the metric tensor, $h_{\mu\nu}$, a.k.a. the gravitational wave. Requiring significantly more analytic calculation and producing substantially more complicated equations, gravitational radiation reflection form the Schwarzschild curvature is computed numerically. Results obtained match traditional calculations.

1.2 The Acoustic Black Hole

1.2.1 Accretion

Following Stephen Hawking's prediction [17] of black hole evaporation in 1974, short of direct measurement, attempts to verify the concept using simpler approach have been made. In part, the acoustic black hole[2] literature exists to bring us closer to the understanding the nature of Hawking Radiation, albeit in the confines of a model that can neither confirm nor deny the reality of Hawking's assertion.

In 1980, V. Moncrief [30] showed the stability of a relativistic, spherically accreting, perfect fluid. In the process, he developed a formalism governing the propagation of sound in a fluid flow, which centered on an acoustic metric describing the causal structure of sound propagation:

$$\mathfrak{g}^{\mu\nu} = \frac{h}{\sigma} v \left(g^{\mu\nu} - \frac{u^\mu u^\nu}{u_c^2} \right),$$
(1.1)

where u^μ is the 4-speed of the flow and u_c is the local 4-speed of sound

$$u_c^2 = \frac{v_c^2}{1 - v_c^2};$$
(1.2)

$$= \left(\frac{\partial \rho}{\partial p} - 1 \right)^{-1}.$$
(1.3)

Shortly thereafter, W. G. Unruh demonstrated [45] that transsonic fluid flow [acoustically] radiates similar to the thermal emissions of a black hole calculated by Stephen Hawking [17].

---

[2]a.k.a. dumb hole, sonic black hole, or mute hole

1.2.2 Quasinormal Modes

Unlike spherical accretion, classical study of which began with H. Bondi [9], continued [most notably] in [8, 10, 14, 16, 35, 46, 24, 41, 36, 47] *et al.*, and is still ongoing; the matter of quasinormal modes of specific acoustic black holes has not received as much attention at all [1, 37, 39, 34, 12, 21, 6]. The majority of studies either assume a canonical accretion[3], or classical gas/fluid, or both. In this study, a physical[4] accretion flow on a Schwarzschild black hole of a relativistic ideal gas is computed. The equation of state of such gas is given by

$$p = (\gamma - 1)\rho, \tag{1.4}$$

where $\gamma \in [1, 2]$. $\gamma = 1$ represents non-interacting particles, *e.g.* dust. It can be shown that $\gamma = 2$ is a scalar wave traveling at the speed of light.

1.3 Gravitational Waves on Schwarzschild background

"No amount of experimentation can ever prove me right; a single experiment can prove me wrong."

– Albert Einstein.

Einstein's theory of gravity has been tested again and again from the relatively simple problem of the precession of the perihelion of Mercury and bending of light in gravitational fields, to frame-dragging of massive, rotating bodies[5]. The triumph of

---

[3]*e.g.* force the speed of the flow to be, say, $v \propto \dfrac{1}{r^2}$.

[4]As opposed to canonical.

[5]See Gravity Probe B

General Relativity is the accurate prediction and subsequent detection[6] of gravitational radiation.

1.3.1   Extreme Mass Ratio Inspiral

Because we do not [yet] possess the technology to generate gravitational waves of significant magnitude to be detected by even the most precise equipment, we must rely on natural sources of gravitational radiation. Such sources usually comprise a collision of two massive objects at distances parsecs away. For example: a black hole swallowing a star; two neutron stars coalescing, etc. Accelerating masses radiate, lose energy, and *fall* as a result. Spacetime disturbances[7] created by such phenomena are meager at best. Elaborate detection apparatus have been constructed[8] around the planet in search of gravitational radiation emanating from coalescing binary systems. Unfortunately, everything from seismic and thermal noise to imperfections in the miles-long detection machinery buries the gravitational disturbances, requiring sophisticated numerical post-processing in order to extract the signal. A template of the signal greatly enhances its detectability. Thus, one of the ultimate goals of the Extreme Mass Ratio Inspiral (EMRI) community is to produce accurate detection templates, *i.e.* the trajectory as a function of time of a small body spiraling into a large body[9]. Why extreme mass ratio? – Because it is significantly simpler to compute to than comparable mass inspiral and is a stepping-stone on the way to arbitrary, general relativistic, two-body simulations. Also, such assumption is realistic for small stars ($M \sim 1 - 10\, M_{\odot}$) spiraling into supermassive ($M \sim 10^7 M_{\odot}$) black

---

[6]Indirect measurements of binary pulsars is the only evidence to date.

[7]Gravitational waves.

[8]See LIGO, VIRGO, GEO, TAMA.

[9]$m/M \ll 1 \sim 10^{-5}$.

holes.

1.3.2 History

Seminal works on the subject of gravitational perturbations on black holes are those of Regge & Wheeler [38] and Zerilli [48]. While the most general gravitational disturbance (metric) encompasses ten seemingly independent components, adopting a specific gauge[10], Regge, Wheeler, and Zerilli show that the gravitational waves[11] can be reduced to two field functions, for the so-called *even* and *odd* parity polarizations. The resulting non-physical[12] wave functions are not easily invertible and can be used to compute quantities such as energy flux. These papers dealt with sourceless gravitational wave propagation on a Schwarzschild black hole.

The next step is the introduction of a point-mass, which orbits the central black hole and weakly perturbs the spacetime. The mechanics of such step are illustrated by Martel [26]: A point-mass represented by a four-dimensional delta function orbiting a Schwarzschild black hole. An approach often taken is to exploit the small mass ratio, $m/M \ll 1$, and weak perturbation, which leads to gradual, or adiabatic, orbital decay. That is, the inspiral may be slow enough that an outgoing energy flux (radiation) is presumed nearly constant over multiple orbits and is used to acausally remove the energy from the binary system resulting in an inspiral. Such methods suffice whenever the orbit-to-orbit changes are small but, the technique tends to break down when the mass enters its late stages of inspiral.

An upgrade, instead of the evolution of non-physical field functions of Regge &

---

[10]Schwarzschild spacetime and Schwarzschild coordinates are also used but, not required.

[11]As well as electromagnetic, vector waves.

[12]*Non*-physical does not mean *un*-physical; whereas the latter implies impossibility, the former merely points out the lack of physical interpretation.

Wheeler and Zerilli & Moncrief, is a direct evolution of the metric components origi-

inally introduced by L. Barack and C. Lousto [2]. This study attempts to produce the

ten metric evolution differential equations via application of the $\mathcal{M}^2 \times \mathcal{S}^2$ formalism

to the sourceless gravitational wave equation

$$\bar{h}_{\mu\nu|\gamma}{}^{\gamma} + 2R_{\mu\lambda\nu\sigma}\bar{h}^{\lambda\sigma} = 0, \tag{1.5}$$

which shall be derived in (5.2).

1.3.3 The Connection

It is worth noting that though seemingly distinct, two main parts of this thesis:

acoustic black hole and gravitational wave propagation are related in that they both

take place on Schwarzschild background, introduce new techniques, and the acous-

tic perturbations approach Regge-Wheeler scalar field in the limit of $p = \rho$.

Chapter 2

Quasinormal Modes of An Acoustic Black Hole

2.1 Introduction

2.1.1 What are Quasinormal Modes?

Throw a small pebble into the water – radially expanding water waves carry away the energy of the perturbation. In certain physical systems the ripples measured at any point as a function of time behave like

$$A(t) = e^{-\omega'' t} \cos \omega' t, \tag{2.1}$$

i.e. exponentially decaying simple harmonic oscillator. (2.1) can be expressed concisely as

$$A(t) = e^{i\omega t}, \tag{2.2}$$

$$\omega = \omega' + i\omega'', \tag{2.3}$$

where ω is the complex frequency of a so-called quasinormal mode[1]. Put succinctly: quasinormal modes signify the oscillation and exponential decay of perturbations.

2.1.2 Why Study Quasinormal Modes?

Particle creation near the event horizon, be it a photon or a phonon, is a subtle effect. Disturbances in the vicinity of a black hole will ring down and disappear, in the form of quasinormal modes.

2.1.3 This Study

The goal of this study is to compute the quasinormal modes of one type of acoustic black hole. The system is chosen to be perfect, relativistic, ideal gas radially accreting (sinking) into a Schwarzschild black hole.

2.2 Theory

2.2.1 Properties of The Flow

Consider a uniform, steady state, radial flow with a stress-energy tensor of a perfect fluid

$$T^{\mu\nu} = (\rho + p)u^\mu u^\nu + pg^{\mu\nu}, \tag{2.4}$$

and an equation of state of a relativistic ideal gas

$$p = (\gamma - 1)\rho, \tag{2.5}$$

---

[1]Imaginary part of the amplitude is retained for mathematical convenience and is dealt with appropriately when any physical quantity is due to be calculated directly from the amplitude.

where p is the isotropic pressure, ρ is the total energy density, $g^{\mu\nu}$ is the metric, and u^{μ} is the 4-velocity of the gas subject to the constraint

$$u_{\mu}u^{\mu} = -1. \tag{2.6}$$

Mass conservation equation has the form

$$\nabla_{\mu}(\sigma u^{\mu}) = 0, \tag{2.7}$$

where σ is the rest energy density. Specific enthalpy of the fluid h is defined by

$$h = \frac{\rho + p}{\sigma}. \tag{2.8}$$

Choice of radial (irrotational, i.e. no vortex) flow implies that

$$u^{\theta} = u^{\phi} = 0, \tag{2.9}$$

a necessary condition, along with the assumption of isentropic ($s = s_0$) flow, for expressing the flow as a gradient of a scalar. To do so, consider the enthalpy current

$$hu_{\mu} = \nabla_{\mu}\psi, \tag{2.10}$$

also known as the potential flow, where ψ is some scalar function. The conservation equation (2.7) becomes

$$\nabla_{\mu}\left(\frac{\sigma}{h}\nabla^{\mu}\psi\right) = 0. \tag{2.11}$$

11

2.2.2 Relativistic Hydrodynamics

Substituting (2.4) into the matter conservation equation, which is the divergenceless stress-energy tensor

$$\nabla_\nu T^{\mu\nu} = 0, \tag{2.12}$$

yields

$$\nabla_\nu T^{\mu\nu} = \left[u^\mu u^\nu \nabla_\nu + 2u^{(\nu} \nabla_\nu u^{\mu)} \right] (\rho + p) + \nabla^\mu p = 0. \tag{2.13}$$

Projecting (2.13) along the 4-velocity yields the energy conservation equation

$$- u_\mu \nabla_\nu T^{\mu\nu} = u^\nu \nabla_\nu \rho + (\rho + p) \nabla_\nu u^\nu = 0. \tag{2.14}$$

Projecting (2.13) perpendicular to the 4-velocity yields the momentum conservation equation

$$\left(\delta^\lambda_{\ \mu} + u_\mu u^\lambda \right) \nabla_\nu T^{\mu\nu} = (\rho + p) u^\nu \nabla_\nu u^\lambda + \nabla^\lambda p + u^\lambda u_\mu \nabla^\mu p = 0, \tag{2.15}$$

where $\left(\delta^\lambda_{\ \mu} + u_\mu u^\lambda \right)$ is perpendicular to u_μ

$$\left(\delta^\lambda_{\ \mu} + u_\mu u^\lambda \right) u^\mu = 0. \tag{2.16}$$

Equation (2.15) is more conveniently expressed with the free and differentiation indices lowered

$$(\rho + p) u^\mu \nabla_\mu u_\lambda + \nabla_\lambda p + u_\lambda u^\mu \nabla_\mu p = 0. \tag{2.17}$$

Equation (2.17) is known as the relativistic Euler's equation of motion of an inviscid fluid.

2.2.3 The Acoustic Metric

Equation (2.11) is a description of a background flow. To study the waves in this medium, small perturbations are introduced

$$\sigma \quad \rightarrow \quad \sigma + d\sigma\,(t,r,\theta,\phi)\,; \tag{2.18}$$

$$h \quad \rightarrow \quad h + dh\,(t,r,\theta,\phi)\,; \tag{2.19}$$

$$\psi \quad \rightarrow \quad \psi + d\psi\,(t,r,\theta,\phi)\,; \tag{2.20}$$

$$\rightarrow \quad \psi + \varphi\,(t,r,\theta,\phi)\,. \tag{2.21}$$

Note that whereas the flow is radial, perturbations do not have to be. Inserting these perturbations into (2.10)

$$dh = -u^{\mu}\nabla_{\mu}\varphi; \tag{2.22}$$

perturbing the mass conservation equation (2.11) and keeping only the first order terms gives

$$\nabla_{\mu}\left[\frac{\sigma}{h}\left(1 + \frac{d\sigma}{\sigma} - \frac{dh}{h}\right)(\nabla^{\mu}\psi + \nabla^{\mu}\varphi)\right] = 0; \tag{2.23}$$

from (2.7) (2.8), and (2.14) one finds

$$\nabla_{\mu}\rho = h\nabla_{\mu}\sigma \quad \Leftrightarrow \quad d\rho = hd\sigma; \tag{2.24}$$

differentiating (2.8) and substituting (2.24)

$$\sigma dh = dp \quad \Leftrightarrow \quad \sigma\nabla_{\mu}h = \nabla_{\mu}p; \tag{2.25}$$

combining (2.25) and (2.24)

$$\frac{d\sigma}{dh} = \frac{d\rho}{dp}\frac{\sigma}{h}, \tag{2.26}$$

$$= \frac{1}{v^2}\frac{\sigma}{h}, \tag{2.27}$$

where v is the local speed of sound (longitudinal perturbation). Using (2.22), (2.27), and (2.10) in (2.23) yields the expression

$$\nabla_\mu \left[\frac{\sigma}{h} \left(1 - \eta \frac{u^\nu \nabla_\nu \varphi}{h} \right) (\nabla^\mu \psi + \nabla^\mu \varphi) \right] = 0, \tag{2.28}$$

where

$$\eta = \frac{1}{v^2} - 1. \tag{2.29}$$

Expanding (2.28)

$$\nabla_\mu \left[\frac{\sigma}{h} \left(\nabla^\mu \psi + \nabla^\mu \varphi - \nabla^\mu \psi \frac{\eta}{h} u^\nu \nabla_\nu \varphi - \frac{\eta}{h} u^\nu \nabla_\nu \varphi \nabla^\mu \varphi \right) \right] = 0. \tag{2.30}$$

The first term is zero because of (2.11), last term is zero because only the linear perturbations are analyzed ($\nabla_\nu \varphi \nabla^\mu \varphi \approx d\varphi^2 \approx 0$), thus with aid from (2.10), (2.30) reduces to

$$\nabla_\mu \left[\frac{\sigma}{h} \left(\nabla^\mu \varphi - \eta u^\mu u^\nu \nabla_\nu \varphi \right) \right] = 0. \tag{2.31}$$

It is known that for any vector A^α

$$\nabla_\alpha A^\alpha = \frac{1}{\sqrt{-g}} \partial_\alpha \left[\sqrt{-g} A^\alpha \right], \tag{2.32}$$

therefore, (2.31) can be expressed as

$$\frac{1}{\sqrt{-g}} \partial_\mu \left[\sqrt{-g} \frac{\sigma}{h} (g^{\mu\nu} - \eta u^\mu u^\nu) \nabla_\nu \varphi \right] = 0, \tag{2.33}$$

and because φ is a scalar, covariant derivatives can be replaced with partial derivatives ($\nabla_\nu = \partial_\nu$)

$$\frac{1}{\sqrt{-g}}\partial_\mu\left[\sqrt{-g}\frac{\sigma}{h}(g^{\mu\nu} - \eta u^\mu u^\nu)\partial_\nu\varphi\right] = 0. \tag{2.34}$$

It is also known that for any scalar S

$$\mathfrak{D}_\mu\mathfrak{D}^\mu S = \frac{1}{\sqrt{-\mathfrak{g}}}\partial_\mu\left[\sqrt{-\mathfrak{g}}\mathfrak{g}^{\mu\nu}\partial_\nu S\right], \tag{2.35}$$

where $\mathfrak{D}_\mu$ is a covariant derivative[2] compatible with metric $\mathfrak{g}_{\mu\nu}$ Comparing (2.35) and (2.34) one can see that $S = \varphi$ and

$$\sqrt{-\mathfrak{g}}\mathfrak{g}^{\mu\nu} = \sqrt{-g}\frac{\sigma}{h}(g^{\mu\nu} - \eta u^\mu u^\nu), \tag{2.36}$$

where $g^{\mu\nu}$ is the background spacetime metric and $\mathfrak{g}^{\mu\nu}$ is the sought acoustic metric. The perturbation equation (2.34) can now be written in a concise form

$$\frac{1}{\sqrt{-\mathfrak{g}}}\partial_\mu\left[\sqrt{-\mathfrak{g}}\,\mathfrak{g}^{\mu\nu}\partial_\nu\varphi\right] = 0, \tag{2.37}$$

$$\mathfrak{D}_\mu\mathfrak{D}^\mu\varphi = 0. \tag{2.38}$$

After some algebra, one finds the acoustic metric

$$\mathfrak{g}^{\mu\nu} = \frac{h}{\sigma}v\,(g^{\mu\nu} - \eta\,u^\mu u^\nu), \tag{2.39}$$

and

$$\mathfrak{g} = g\left(\frac{\sigma}{h}\right)^4\frac{1}{v^2}. \tag{2.40}$$

---

[2]Germanic lettering is used to illustrate the generality of this statement.

2.3 Relativistic Accretion Flow

So far, the discussion has been general and did not specifying the background space-time or flow. This section begins the exploration of a particular accretion flow, on a particular background geometry. For this study, Schwarzschild geometry is used

$$g_{\mu\nu} = \mathbf{diag}\left(-f, \frac{1}{f}, r^2, r^2 \sin^2\theta\right), \tag{2.41}$$

where

$$f = 1 - \frac{2m}{r}. \tag{2.42}$$

One can get a sense for the acoustic horizon by looking at $\mathfrak{g}_{tt}$ (2.39)

$$\mathfrak{g}_{tt} \propto -\left(1 - \frac{2m}{r} - u_t^2\eta\right). \tag{2.43}$$

$\mathfrak{g}_{tt}$ turns zero at $r > 2m$, *i.e.* the acoustic horizon is before the event horizon of the Schwarzschild black hole, which is both expected and desired.

2.3.1 Mathematical Description

Recall (2.7), it expands to

$$\frac{1}{\sqrt{-g}}\partial_\mu\left(\sigma\sqrt{-g}u^\mu\right) = 0, \tag{2.44}$$

$$\partial_\mu\left(\sigma r^2 \sin\theta u^\mu\right) = 0. \tag{2.45}$$

The stationary requirement removes the temporal derivative ($\mu = t$), (2.9) removes the angular derivatives ($\mu = \theta, \phi$), and all that remains is the radial derivative ($\mu = r$)

$$\partial_r\left(\sigma r^2 u^r\right) = 0, \tag{2.46}$$

$$\sigma r^2 u^r \;=\; \alpha, \tag{2.47}$$

where α is an integration constant. It is convenient to write this equation in terms of proper 4-speed

$$u = \sqrt{g_{rr}}\, u^r, \tag{2.48}$$

then

$$r^2 f^{1/2} u \sigma = \alpha. \tag{2.49}$$

Using (2.7) and (2.8) in (2.17), one finds

$$u^\mu \nabla_\mu (h u_\nu) + \nabla_\nu h = 0, \tag{2.50}$$

setting $\nu = t$ leads to

$$h u_t \;=\; \beta, \tag{2.51}$$

where β is another integration constant. Applying (2.6) and (2.48) to (2.51) yields

$$h^2 f(1 + u^2) = \beta^2. \tag{2.52}$$

The specific enthalpy (2.8), together with the equation of state (2.5) gives

$$h = \gamma \frac{\rho}{\sigma}, \tag{2.53}$$

and then (2.24) becomes

$$\frac{d\rho}{d\sigma} \;=\; h = \gamma \frac{\rho}{\sigma}, \tag{2.54}$$

$$\rho \;=\; C\sigma^\gamma, \tag{2.55}$$

17

$$h = C\gamma\sigma^{\gamma-1}. \tag{2.56}$$

where C is yet another integration constant. Equation (2.56) is the link between conservation equations (2.49) and (2.52)

$$1 + u^2 = \xi r^{4(\gamma-1)} f^{\gamma-2} u^{2(\gamma-1)}, \tag{2.57}$$

where ξ is a combination of all integration constants.

2.3.2 Physical Interpretation

(2.57) is an equation for stationary flow as a function of r. Unknown constant ξ is found by studying the derivative of u

$$\frac{du}{dr} = \frac{1}{2} \frac{\xi q'(r)}{u^{3-2\gamma} - \xi q(r)(\gamma - 1)u^{-1}}, \tag{2.58}$$

where

$$q(r) = r^{4(\gamma-1)} f^{\gamma-2}. \tag{2.59}$$

Equation (2.58) has three critical points:

(**a**). *Numerator is zero* – implies a limiting speed.

(**b**). *Denominator is zero* – implies a limiting radius.

(**c**). *Numerator and Denominator are both zero* – a unique combination of both of the above.

All three cases are plotted in Figure 2.1. Setting the numerator to zero

$$\xi q'(r) = 0, \tag{2.60}$$

18

$$r_c = m\left[1 + \frac{\gamma}{2(\gamma - 1)}\right],$$ (2.61)

where r_c shall be called a *critical radius*. Setting the denominator to zero yields ξ

$$0 = u^{3-2\gamma} - \xi q(r_c)(\gamma - 1)u^{-1},$$ (2.62)

$$\xi = \frac{1}{\gamma - 1}\left(\frac{m}{2}\right)^{4(1-\gamma)}\left(\frac{3\gamma - 2}{\gamma - 1}\right)^{2-3\gamma}.$$ (2.63)

ξ given by (2.63) offers a unique solution to the flow equation (2.57) and it is plotted in Figures 2.1 and 2.2 with solid lines. Because direction of the flow is not specified, i.e. matter can either fall in or blow out, at any given r there are two possible flow solutions:

(**a**). Accretion (infall);

(**b**). Wind (outflow, e.g. the solar wind).

Inserting r_c into (2.57) yields the speed corresponding to critical radius, or *critical speed*.

$$u_c^2 = \frac{\gamma - 1}{2 - \gamma}.$$ (2.64)

Thus far, r_c and u_c have been ambiguously referred to as *critical*, however their physical significance remains a mystery. Consider the following: classical speed of longitudinal perturbations (sound) in a medium is given by

$$v_s^2 = \frac{\partial p}{\partial \rho}.$$ (2.65)

Substituting the equation of state (2.5) gives

$$v_s^2 = \gamma - 1,$$ (2.66)

19
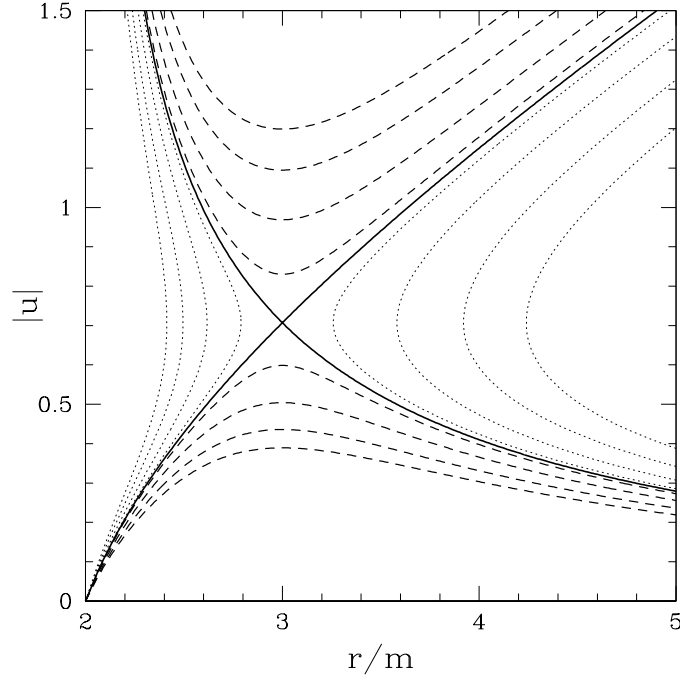
Figure 2.1: Solutions of (2.57) with ξ given by (2.63) for $\gamma = 4/3$ folded onto the positive y-axis. Dotted curves on the sides are the unphysical solutions, dashed curves on top and bottom are the ram (matter being pushed into the black hole) and breeze (matter spewing out of black hole, e.g. the Solar wind) solutions respectively. Dashed solutions are generated from $\xi \pm 0.0025$, ± 0.01, ± 0.02, ± 0.03. Crossing of the wind and accretion, solid lines, is the acoustic event horizon.
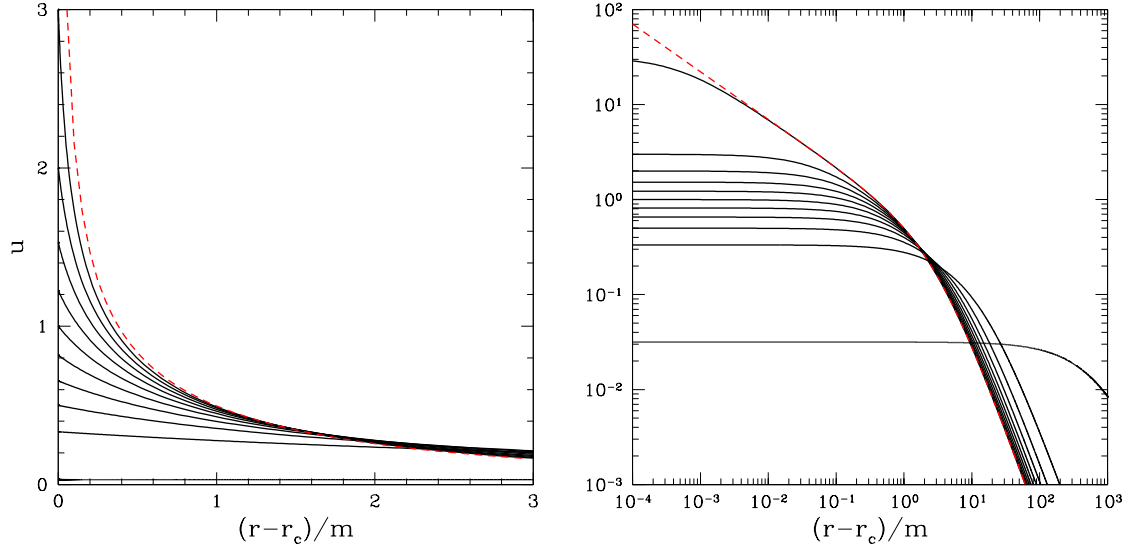
Figure 2.2: Solutions of (2.57) with ξ given by (2.63) for $\gamma = (1.001, 1.1, 1.2, 1.3, 1.4, 1.5, 1.6, 1.7, 1.8, 1.9, 1.999)$ vs. the distance from their respective acoustic event horizons; higher curves for higher γ. $\gamma = 1.999$ curve is not shown in the linear (left) plot because it almost exactly overlays the dashed line, significance of which shall become apparent later.

which is the Newtonian speed, proper (relativistic) speed is given by

$$u_s^2 = \frac{v^2}{1 - v^2} = \frac{\gamma - 1}{2 - \gamma} = u_c^2 = \frac{1}{\eta}. \tag{2.67}$$

If u_c is the speed of sound, then r_c is where flow begins to exceed that speed; therefore, r_c is the *acoustic event horizon*.

2.4   The Scattering Equation

Wave equation (2.38) is an elegant representation of acoustic perturbations on a given spacetime. However, before any useful physics can be extracted, it must be cast into standard form

$$- \ddot{z}(t, x) + z''(t, x) - V(x)z(t, x) = 0. \tag{2.68}$$

According to (2.34), the unsimplified version of (2.38)

$$\partial_\mu \left[r^2 \sin\theta \frac{\sigma}{h} \left(g^{\mu\nu} - \frac{u^\mu u^\nu}{u_c^2} \right) \partial_\nu \varphi \right] = 0. \tag{2.69}$$

$\dfrac{\sigma}{h}$ is computed using (2.47) and (2.51)

$$\frac{\sigma}{h} = \frac{\alpha}{\beta} \frac{1}{r^2} \left(1 + \frac{1}{u^2} \right)^{1/2}, \tag{2.70}$$

substituting into (2.69)

$$\partial_\mu \left[\sin\theta \left(1 + \frac{1}{u^2} \right)^{1/2} \left(g^{\mu\nu} - \frac{u^\mu u^\nu}{u_c^2} \right) \partial_\nu \varphi \right] = 0. \tag{2.71}$$

Expanding μ and ν summations

$$
\begin{aligned}
0 \;=\; & -A(r)\partial_t^2\varphi + v(r)\partial_r\left[C(r)\frac{1}{v(r)}\partial_r\varphi\right] - B(r)\partial_t\partial_r\varphi - v(r)\partial_r\left[B(r)\frac{1}{v(r)}\partial_t\varphi\right] + \\
& + \frac{1}{r^2\sin\theta}\partial_\theta\left(\sin\theta\partial_\theta\varphi\right) + \frac{1}{r^2\sin^2\theta}\partial_\phi^2\varphi,
\end{aligned}
\tag{2.72}
$$

where

$$
A(r) \;=\; f^{-1}\left(1 + \frac{1+u^2}{u_c^2}\right); \tag{2.73}
$$

$$
B(r) \;=\; \frac{u\sqrt{1+u^2}}{u_c^2}; \tag{2.74}
$$

$$
C(r) \;=\; f\left(1 - \frac{u^2}{u_c^2}\right); \tag{2.75}
$$

$$
v(r) \;=\; \left(1 + \frac{1}{u^2}\right)^{-1/2}. \tag{2.76}
$$

The last two terms in (2.72) are identical to the angular part of the flat space Laplacian, solutions to which are spherical harmonics. Angular part is therefore separated from φ

$$
\varphi = \varphi_l(t, r)Y_{lm}(\theta, \phi). \tag{2.77}
$$

(2.72) becomes

$$
-A\partial_t^2\varphi_l - 2B\partial_r\partial_t\varphi_l + C\partial_r^2\varphi_l + v\left(C\frac{1}{v}\right)'\partial_r\varphi_l - v\left(B\frac{1}{v}\right)'\partial_t\varphi_l - \frac{l(l+1)}{r^2}\varphi_l = 0. \tag{2.78}
$$

Next, a coordinate transformation is sought to simplify the form of the wave equation. The following change of coordinates takes place

$$
\tau \;=\; t + w(r); \tag{2.79}
$$

$$
\partial_t \;\rightarrow\; \partial_\tau; \tag{2.80}
$$

22

$$\partial_r \quad \to \quad \partial_r + w'(r)\partial_\tau, \tag{2.81}$$

where $w(r)$ a function to be determined by demanding a simpler form of (2.78). In terms of the new temporal coordinate τ, (2.78) becomes

$$
\begin{aligned}
0 \; = \; & \left[-A - 2Bw' + Cw'^2\right]\partial_\tau^2\varphi_l + C\partial_r^2\varphi_l + v\left(C\frac{1}{v}\right)' \partial_r\varphi_l + \left[-2B + 2Cw'\right]\partial_\tau\partial_r\varphi_l + \\
& + \left[Cw'' - v\left(B\frac{1}{v}\right)' + v\left(C\frac{1}{v}\right)'w'\right]\partial_\tau\varphi_l - \frac{l(l+1)}{r^2}\varphi_l,
\end{aligned}
\tag{2.82}
$$

which is actually more complicated than before the transformation. However, if the coefficient of the mixed derivative $\partial_\tau\partial_r$ is required to vanish

$$-2B + 2Cw' \; = \; 0, \tag{2.83}$$

$$w' \; = \; \frac{B}{C}, \tag{2.84}$$

serendipitously, the coefficient of ∂_τ vanishes as well and (2.82) turns to

$$-\partial_\tau^2\varphi_l + D\partial_r(E\partial_r\varphi_l) + F\varphi_l = 0, \tag{2.85}$$

with

$$D = \quad f\left(\frac{u_c^2 - u^2}{u_c^2 + 1}\right)v; \tag{2.86}$$

$$E = \quad f\left(1 - \frac{u^2}{u_c^2}\right)\frac{1}{v}; \tag{2.87}$$

$$F = \quad - \quad f\left(\frac{u_c^2 - u^2}{u_c^2 + 1}\right)\frac{l(l+1)}{r^2}. \tag{2.88}$$

Second transformation scales φ

$$z = \lambda(r)\varphi_l, \tag{2.89}$$

where $\lambda(r)$ is a function to be determined

$$-\partial_\tau^2 z + \lambda D \, \partial_r \left(\frac{E}{\mu\lambda} \mu \partial_r z - z \frac{E}{\lambda^2} \partial_r \lambda \right) + Fz = 0, \tag{2.90}$$

and where $\mu(r)$ is an assist function, also unknown. After some algebraic manipulation, best choices for $\mu(r)$ and $\lambda(r)$ are revealed

$$\mu = \sqrt{DE}; \tag{2.91}$$

$$\lambda = \left(\frac{E}{D} \right)^{1/4}, \tag{2.92}$$

casting (2.85) into

$$-\partial_\tau^2 z + \mu \partial_r (\mu \partial_r z) + \left[F - \frac{\mu}{\lambda} \partial_r (\mu \partial_r \lambda) \right] z = 0. \tag{2.93}$$

Third, and last adjustment is the modification of the radial coordinate r

$$r_* = k(r), \tag{2.94}$$

$$\partial_r = k' \partial_{r_*}. \tag{2.95}$$

In terms of r_*, (2.93) becomes

$$-\partial_\tau^2 z + \mu k' \partial_{r_*} (\mu k' \partial_{r_*} z) + \left[F - \frac{\mu}{\lambda} k' \partial_{r_*} (\mu k' \partial_{r_*} \lambda) \right] z = 0. \tag{2.96}$$

Requiring $\mu k' = 1$ simplifies (2.96)

$$-\partial_\tau^2 z + \partial_{r_*}^2 z - \left[\sqrt{v} \, \partial_{r_*}^2 \frac{1}{\sqrt{v}} - F \right] z = 0, \tag{2.97}$$

where

$$\frac{dr}{dr_*} = \sqrt{\gamma - 1} f \left(1 - \frac{u^2}{u_c^2} \right). \tag{2.98}$$

The variable r_* is known as the *acoustic tortoise coordinate*. It is different for each γ but, has the same horizon-removal effect as the Schwarzschild tortoise coordinate; it is plotted in Figure 2.3; $u(r_*)$ is shown in Figure 2.4. (2.72) is now in its standard form

$$- \partial_\tau^2 z(\tau, r_*) + \partial_{r_*}^2 z(\tau, r_*) - V(r)z(\tau, r_*) = 0, \tag{2.99}$$

with the potential (Figure 2.5) given by

$$V(r) = \left(1 + \frac{1}{u^2} \right)^{-1/4} \partial_{r_*}^2 \left(1 + \frac{1}{u^2} \right)^{1/4} + f \left(\frac{u_c^2 - u^2}{u_c^2 + 1} \right) \frac{l(l+1)}{r^2}. \tag{2.100}$$

Note that despite all of the transformations undergone by the coordinates and the wavefunction, original time derivative in (2.72), though renamed to τ, has not been modified, which implies that if nothing else, frequency of the oscillation is preserved.

2.4.1 Connection to the Regge-Wheeler potential

Potential (2.100) bears a non-trivial resemblance to Regge-Wheeler potential[38]. In fact, it is straight-forward to show that (2.100) reduces to Regge-Wheeler potential as $\gamma \to 2$ (Figure 2.6), which represents a scalar wave traveling at the speed of light. Consider (2.57) in the limit as $\gamma \to 2$

$$\lim_{\gamma \to 2} \left\{ 1 + u^2 \right\} = \lim_{\gamma \to 2} \left\{ \frac{1}{\gamma - 1} \left(\frac{m}{2} \right)^{4(1-\gamma)} \left(\frac{3\gamma - 2}{\gamma - 1} \right)^{2-3\gamma} r^{4(\gamma-1)} f^{\gamma-2} u^{2(\gamma-1)} \right\}, \tag{2.101}$$

$$u^2 = \frac{1}{\left(\dfrac{r}{2m} \right)^4 - 1}. \tag{2.102}$$

25
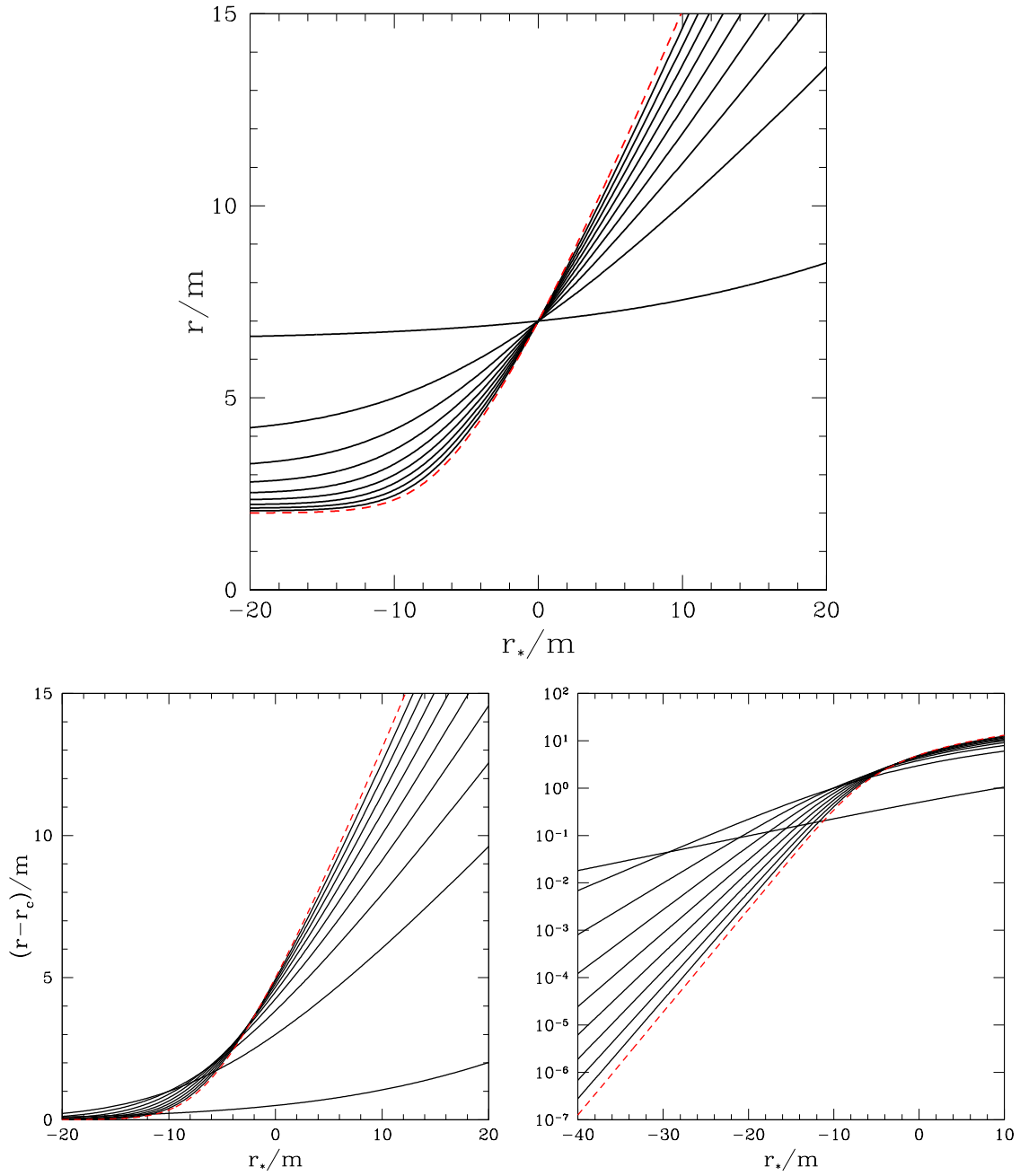
Figure 2.3: Schwarzschild r vs. the acoustic tortoise coordinates r_* (2.98) for $\gamma = (1.1, 1.2, 1.3, 1.4, 1.5, 1.6, 1.7, 1.8, 1.9)$, and $r(r_* = 0) = 7m$; steeper curves for larger γ. Dashed line is the Schwarzschild tortoise coordinate. Top plot is the Schwarzschild r is plotted vs. each of the tortoise coordinates. The intersection of all curves is the [semi-arbitrary] initial condition $r(r_* = 0) = 7m$. Bottom two plots are top plot with each curve lowered by its event horizon r_c.

It should be noted that plotting tortoise coordinates (or any other γ-dependent curves) on the same r_* axis and/or with the same initial conditions makes only partial sense because each tortoise coordinate is unique and its r_* location is arbitrary. It is done here, and throughout this chapter, to illustrate the key differences among the curves and their overall trends.
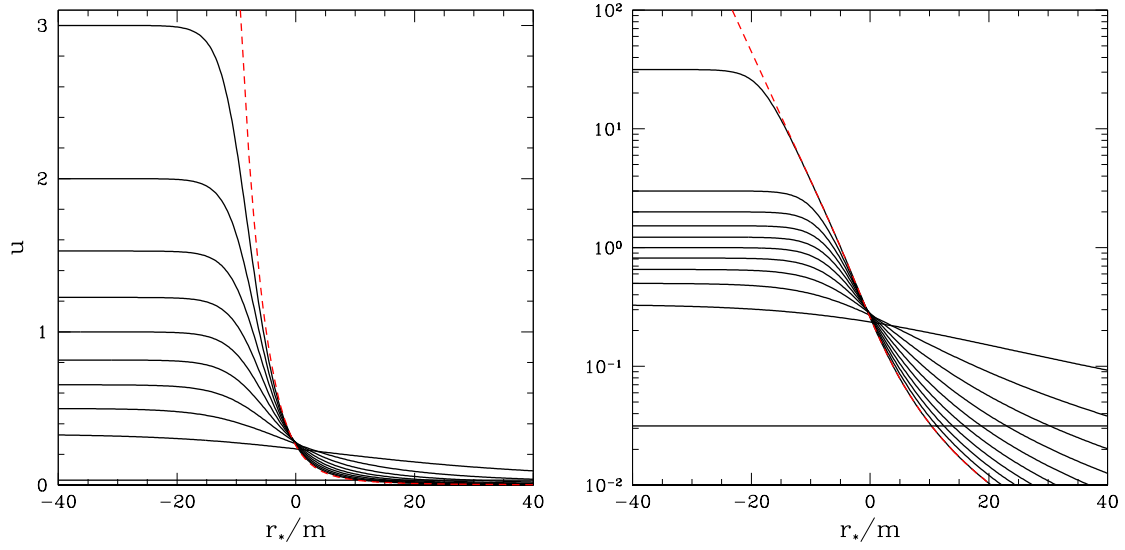
Figure 2.4: Solutions of (2.57) with ξ given by (2.63) for $\gamma =$(1.001, 1.1, 1.2, 1.3, 1.4, 1.5, 1.6, 1.7, 1.8, 1.9, 1.999), and $r(r_* = 0) = r_c + 2m$ vs. their respective acoustic tortoise coordinates r_*; $\gamma = 1.999$ curve is not shown in the linear (left) plot; higher curves for higher γ. Dashed line is the Schwarzschild ($\gamma = 2.0$) 4-speed (2.102)...even though there's no such thing.
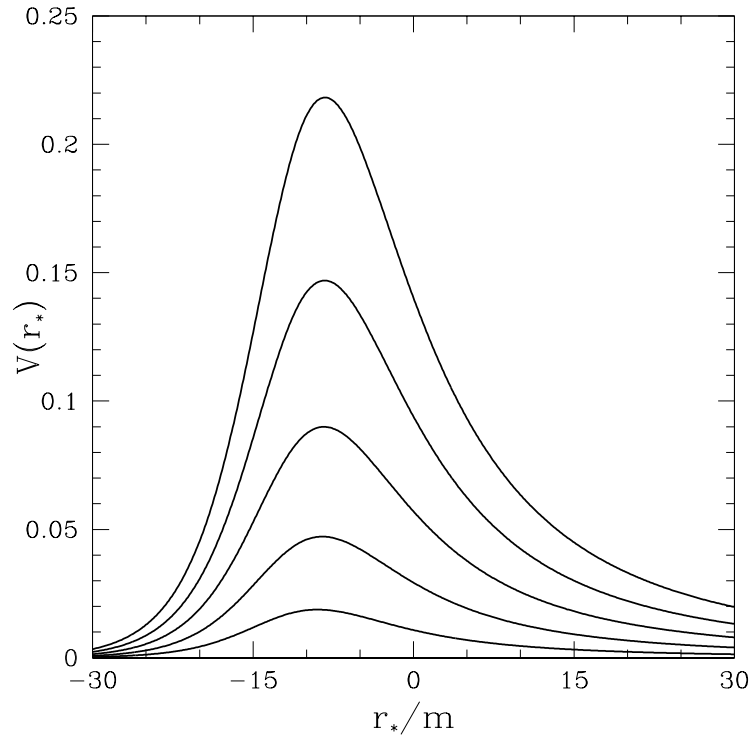
Figure 2.5: Acoustic black hole scattering potential (2.100) as a function of the acoustic tortoise coordinate (2.98) for $\gamma = 4/3$, $r(r_* = 0) = 7m$, and $l = 1, 2, 3, 4, 5$; lower curves for lower l.

27
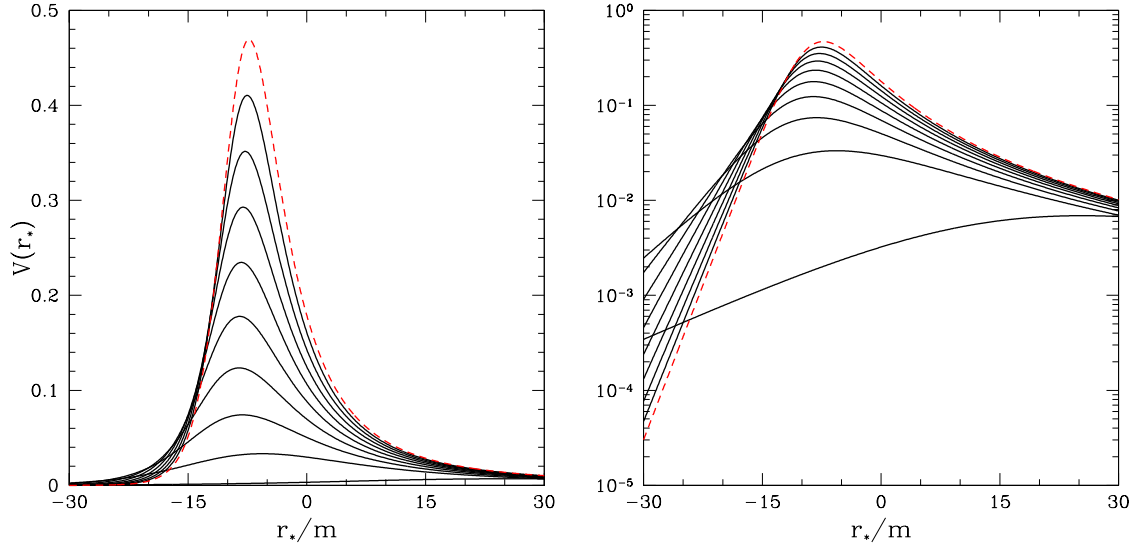
Figure 2.6: Acoustic scattering potential vs. the acoustic tortoise coordinates for $\gamma = (1.1, 1.2, 1.3, 1.4, 1.5, 1.6, 1.7, 1.8, 1.9)$, $r(r_* = 0) = 7m$, and $l = 3$; lower curves for lower γ. Dashed line is the Regge-Wheeler scalar potential (2.106).

Consider (2.64) and (2.66) in the limit as $\gamma \to 2$

$$\lim_{\gamma \to 2} u_c^2 = \lim_{\gamma \to 2} \frac{\gamma - 1}{2 - \gamma} \to \infty, \tag{2.103}$$

$$\lim_{\gamma \to 2} v_c^2 = \lim_{\gamma \to 2} \gamma - 1 \to 1, \tag{2.104}$$

i.e. the perturbation travels at the speed of light. Substituting these limits into (2.98) and (2.100) yields

$$\frac{dr}{dr_*^{(RW)}} = f; \tag{2.105}$$

$$V^{(RW)} = f\left[\frac{l(l + 1)}{r^2} + \frac{2m}{r^3}\right], \tag{2.106}$$

which are the Schwarzschild tortoise coordinate and Regge-Wheeler potential for a scalar (spin 0) wave. Figure 2.3 graphically illustrates how the acoustic tortoise coordinate gradually becomes the Schwarzschild tortoise coordinate as $\gamma \to 2$.

28

2.5 Quasinormal Modes

2.5.1 How to Compute Quasinormal Modes?

Time-Evolution

The simplest method of approximating the first quasinormal mode is to time-evolve
the wave equation in standard form (2.99) with some arbitrary initial perturbation,
say

$$z(\tau = 0, r_*) = e^{-r_*^2}; \tag{2.107}$$

$$\dot{z}(\tau = 0, r_*) = 0, \tag{2.108}$$

and measure the amplitude of any point, $z(\tau, r_* = 0)$ for example, as a function of
time. However, damped oscillations are difficult to fit to equation (2.1), so it is ad-
visable to take the natural log of the obtained time-series and plot $\ln |z(\tau, r_* = 0)|$ vs.
τ as in Figure 2.7. There are two drawbacks to this method.

First, an arbitrary perturbation will not excite only the first quasinormal mode, it
will excite them all. Only the first mode is visible because the second excited mode
decays approximately three times faster, and is buried beneath the first mode. To see
the second mode one has to fiddle with the shape of the initial perturbation (2.107)
to void the first mode, i.e. excite all modes *but* the first – a tedious and difficult
procedure.

Second, at best the mode is known to 2-3 significant figures; partially because
other modes are present below, and partially because oscillation does not go on for-
ever – order of 10 oscillations (small sample size) is available.

29
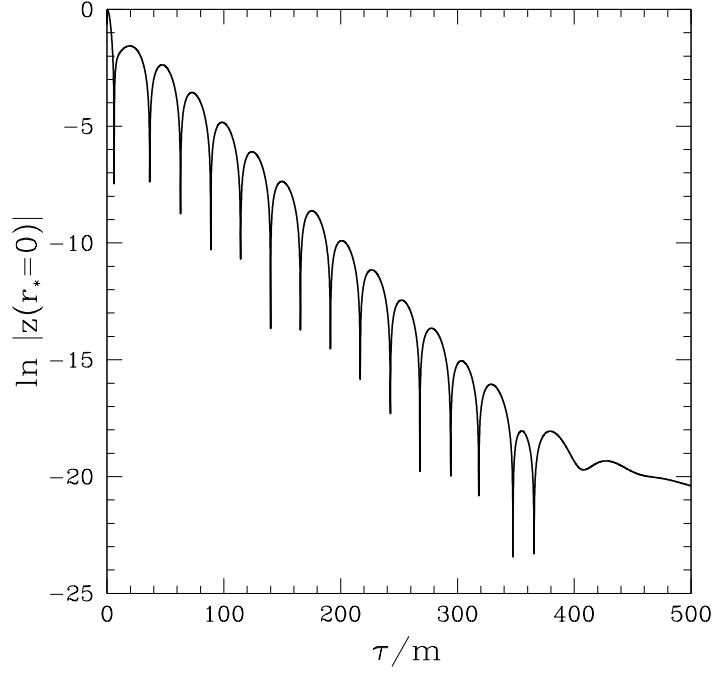
Figure 2.7: Time-evolution of the wave equation (2.99) with potential given by (2.100), $\gamma = 4/3$, $l = 1$. One can almost read-off the first quasinormal mode from this graph: peak-to-peak time is half-period, slope is the decay rate. $\omega \approx 0.12 - 0.05i$.

Wave Matching

This technique requires a frequency-decomposed wave equation in standard form. Let

$$z(\tau, r_*) = z(r_*)e^{i\omega\tau}, \tag{2.109}$$

substituting into (2.99) yields

$$z''(r_*) + \left[\omega^2 - V(r)\right]z(r_*) = 0. \tag{2.110}$$

Various flavors of this technique rely on the fact that if one looks far to the left of the point where the perturbation took place (or in the language of subseciton 2.1.1: where pebble hit the water), hereafter referred to as the origin, one only sees left-traveling waves, vice-versa for the right side. Consider the scattering equation

30

(2.110)

$$z(-\infty \leftarrow r_*) \rightarrow e^{+i\omega r_*}, \tag{2.111}$$

similarly, for the right side

$$z(r_* \rightarrow +\infty) \rightarrow e^{-i\omega r_*}, \tag{2.112}$$

due to the fact that

$$V(r_* \rightarrow \pm\infty) \rightarrow 0. \tag{2.113}$$

These limits are treated as boundary conditions, ω is guessed, solution is integrated from points numerically comparable to $\pm$infinity[3] and the two resulting waves are compared at some arbitrary location on the r_*-axis, preferably the origin. Since only quasinormal modes have such boundary conditions, if the waves match within a multiplicative constant and a phase[4], then the guessed ω is a quasinormal mode.

This method has no apparent drawbacks, except one major shortcoming discussed in the next subsection.

The anti-Stokes' Lines

When ω is complex, and it is complex, z in (2.110) is also complex. It is a second order equation with two solutions at any given point. Consider the boundary conditions (2.111) and (2.112) written explicitly in terms of real and imaginary parts of ω

$$z(r_* \rightarrow \pm\infty) \quad \rightarrow \quad e^{\mp i(\omega' + i\omega'')r_*}, \tag{2.114}$$

$$\rightarrow \quad e^{\mp i\omega' r_*} e^{\pm \omega'' r_*}. \tag{2.115}$$

---

[3]See section on Numerical Implementation for explanation.

[4]Basically a test of linear dependence, i.e. the Wronskian.

One of those solutions exponentially decays toward the origin, the other exponentially grows. By enforcing the boundary conditions it would seem that growing solution is eliminated but, small error (numerical roundoff error for example) exponentially exaggerates close to the origin and engulfs the important, exponentially decaying wave.

To remedy this situation, one may, instead of integrating along the real r_*-axis, integrate along some path in the complex plane, that is to say

$$r_* \rightarrow x + iy, \tag{2.116}$$

substituting into boundary conditions (2.111) and (2.112) yields

$$z(r_* \rightarrow \pm\infty) \quad \rightarrow \quad e^{\mp i(\omega' + i\omega'')(x+iy)}, \tag{2.117}$$

$$\rightarrow \quad e^{\mp i(\omega'x - \omega''y)}e^{\pm(\omega'y + \omega''x)}. \tag{2.118}$$

If the real exponent is set to zero, at large distances away from the origin growth/decay disappears

$$\frac{y}{x} = -\frac{\omega''}{\omega'}. \tag{2.119}$$

This path is known as the anti-Stokes' line. It is only valid far away from the origin. However, near the origin the wavefunction is of order unity and does not pose any problems. Adopting this path requires re-parameterization of the acoustic tortoise coordinate

$$r_* = se^{i\theta}, \tag{2.120}$$

where θ is the angle cast by (2.119), and s is the new acoustic tortoise coordinate. Integration along this altered path will produce the same result as the integration along the real r_*-axis, if it was possible, as guaranteed by Cauchy's Theorem so long
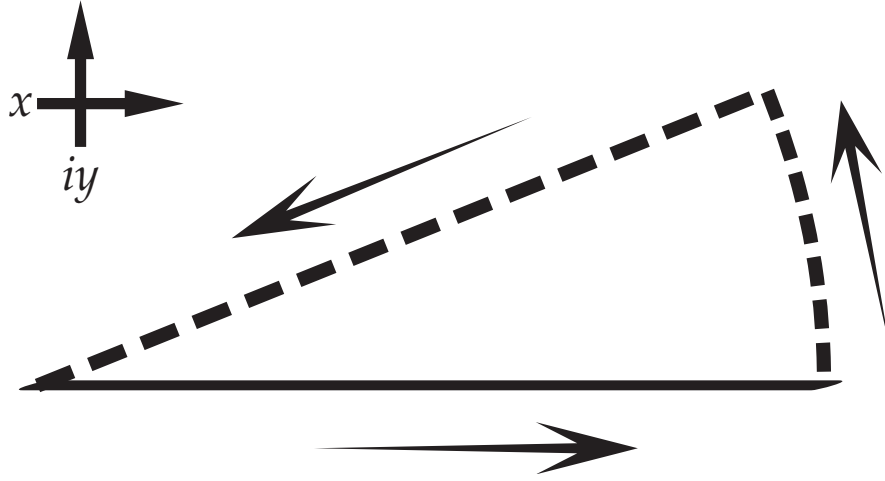
Figure 2.8: Cauchy's Theorem (2.121) guarantees that an integral of a well-behaved function $f(z)$ along the path depicted above conforms to $\int_{\rightarrow} + \int_{\uparrow} + \int_{\leftarrow} = 0$, or $-\int_{\rightarrow} = \int_{\uparrow} + \int_{\leftarrow}$. In other words, integration along the solid line is equivalent to integration along the dashed segments.

as the function is analytic, with no poles, no singularities enclosed by the integration path, and the limits of the integral remain the same

$$\oint f(z)\, dz = 0. \tag{2.121}$$

Integrating along the anti-Stokes' line insures that if an error is made at the boundaries, and error is inevitable, it will not grow exponentially; Figure 2.8.

Moving into the complex plane introduces another dimension (literally) to the calculations. Figure 2.9 illustrates the complex tortoise coordinate. Figures 2.10 and 2.11 illustrate the complex 4-speed.

Variation on Wave Matching: Riccati Transformation

Riccati-like[5] transformations, in general, reduce the order of a differential equation at the expense of turning it non-linear

$$P = \frac{z'}{z}, \tag{2.122}$$

$$P' = \frac{z''}{z} - P^2, \tag{2.123}$$

rewritten with P, (2.110) becomes

$$P' + P^2 + \left[\omega^2 + V(r_*)\right] = 0, \tag{2.124}$$

or, in terms of the new acoustic tortoise coordinate s along the anti-Stokes' line

$$P' + e^{i\theta}\left\{P^2 + \left[\omega^2 + V(se^{i\theta})\right]\right\} = 0, \tag{2.125}$$

where the prime now denotes a derivative with respect to s. Still compliant with anti-Stokes' analysis, this form of the scattering equation offers major advantages:

(**a**). It is advantageous numerically because the solution doesn't oscillate as much (or at all);

(**b**). First order reduces the coding load as compared to the second-order;

(**c**). Because equation is non-linear, wave matching at the origin reduces to comparing two complex numbers;

Riccati-transformed version of the frequency-decomposed wave equation (2.110) is used in this study.

---

[5]alternatively spelled as Ricatti.
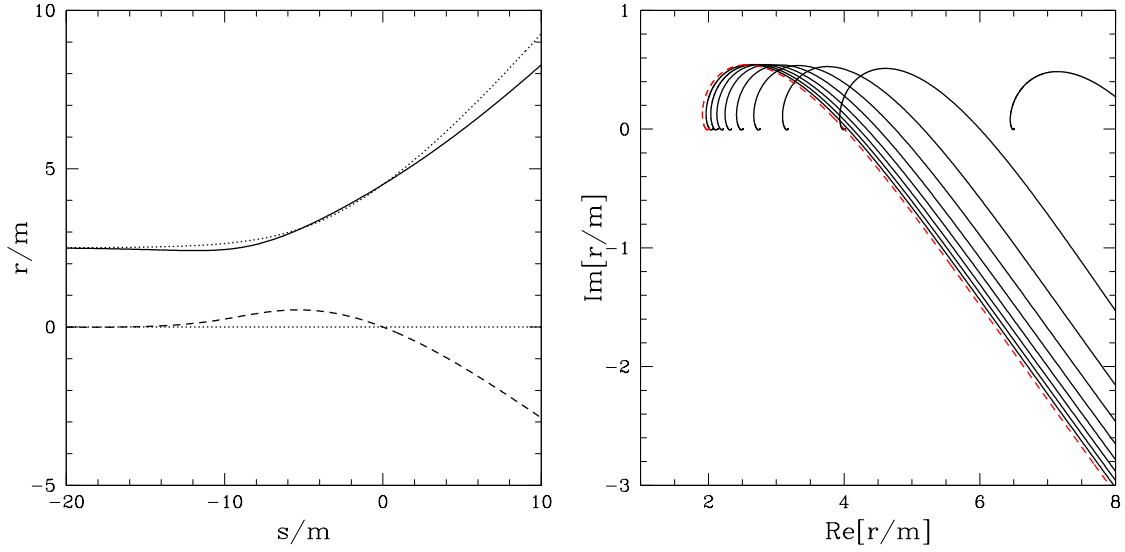
Figure 2.9: Left: real (solid) and imaginary (dashed) parts of r as a function of the new tortoise coordinate s, (2.120), for $\gamma = 1.5$, $\theta = 32°$, and $r(s = 0) = r_c + 2m$, against r for $\theta = 0°$ (real acoustic tortoise coordinate) and the same γ (dotted), (2.98). Right: complex parametric plot of r for $\gamma = (1.1, 1.2, 1.3, 1.4, 1.5, 1.6, 1.7, 1.8, 1.9)$; curves for higher γ are closer to the left. Dashed line is the Schwarzschild r.

2.6 Numerical Implementation

2.6.1 The Accretion Flow

Recall equation (2.57)

$$1 + u^2 = \xi r^{4(\gamma-1)} f^{\gamma-2} u^{2(\gamma-1)}, \qquad (2.126)$$

solution of this equation (u) is needed in (2.98) and (2.100). In both equations it appears squared, then it is only necessary to solve for u^2. Let

$$w = u^2, \qquad (2.127)$$
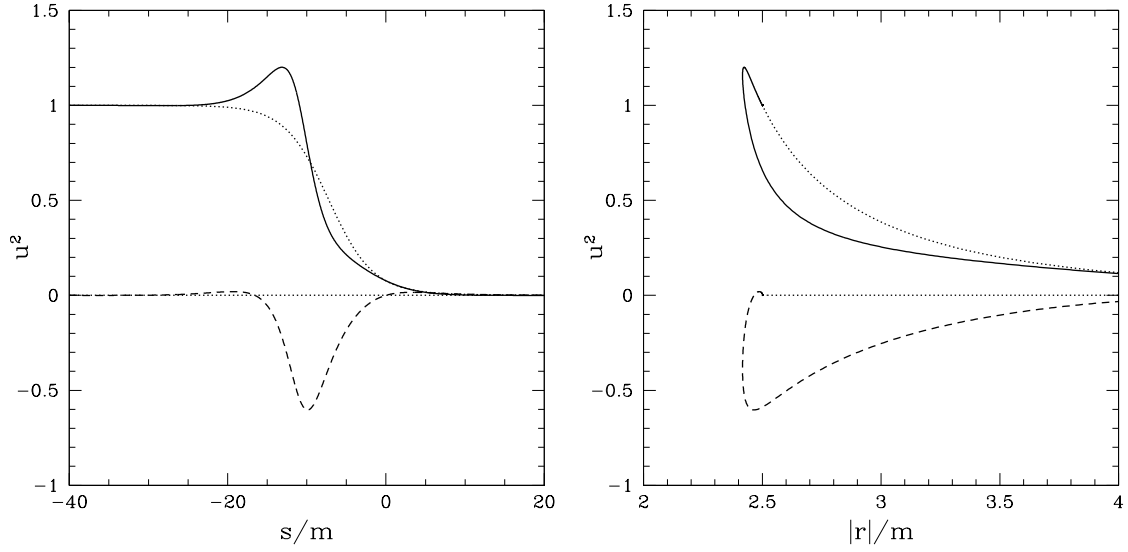
Figure 2.10: Real (solid) and imaginary (dashed) parts of u^2 for for $\gamma = 1.5$, $\theta = 32°$, and $r(s = 0) = r_c + 2m$. Dotted curves are u^2 for $\theta = 0°$.

then

$$1 + w = \xi q(r)w^{\gamma-1}. \tag{2.128}$$

The most straight-forward course of solution is Newton's method. Newton's method is a numerical technique to solve algebraic equations of the type $y(x) = 0$. Procedure is as follows:

(a). Guess x for which $y(x) \approx 0$;

(b). Compute $\Delta x = \dfrac{y(x)}{y'(x)}$;

(c). Set $x = x - \Delta x$;

(d). Go to (b).

After sufficient number of iterations, often determined by the magnitude of Δx, this algorithm converges onto a root of $y(x) = 0$.

Newton's method is fast and precise but, it will not work without a fair guess of w. While (2.128) cannot be solved exactly, an asymptotic solution can readily be

36
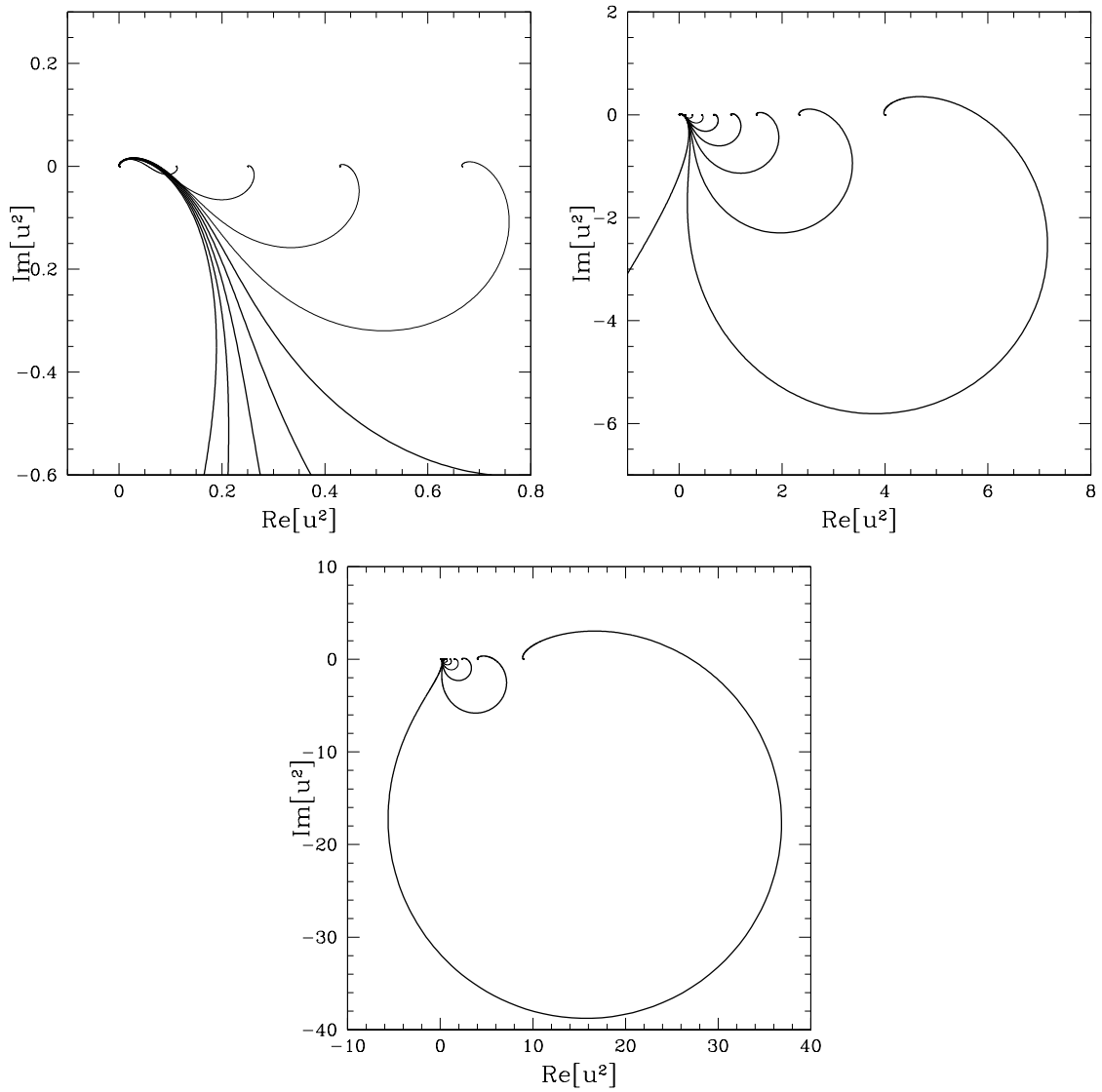
Figure 2.11: Complex parametric plots of u^2 for $\gamma = (1.1, 1.2, 1.3, 1.4, 1.5, 1.6, 1.7, 1.8, 1.9)$, $\theta = 32°$, and $r(s = 0) = r_c + 2m$; larger curves for larger γ.

obtained by assuming that away from the black hole the gas flows slowly, so w is small as compared to $\xi f(r) w^{\gamma-1}$. w is removed from the left side of the equation

$$1 \quad = \quad \xi f(r) w_0^{\gamma-1}, \tag{2.129}$$

$$w_0 \quad = \quad \frac{1}{r^4} \xi^{1/(1-\gamma)} f^{u_c^{-2}}. \tag{2.130}$$

Because of the sequential nature of integration[6], except for the end-points, any given w is very close to the one found previously. Due to this convenient fact, (2.130) only used once per integration, each subsequent guess is the value of w immediately preceding it.

Solution Branch

By virtue of the parameterization of the acoustic tortoise coordinate (2.120), r is a complex quantity, and so is 4-speed sqaured. Complex numbers raised to non-integer powers produce not one but, many solution branches. Blind root-seeking algorithms such as the Newton's method cannot distinguish between branches. If x somehow makes it to the neighboring solution branch, the algorithm will proceed to refine it and return a solution belonging to a different branch. Depending on the equation, solution branches can be spread apart or lie close together. It is therefore not uncommon for x to *hop* from one branch to another during successive refinement iterations. Branch-hopping of the solution $y(x) = 0$ causes discontinuities in $y(x)$ which, mathematically accurate as they may be, are undesirable in real life.

While the phenomenon can not be eliminated completely[7], tests have shown that separating the flow equation with polar coordinates ($u^2 = \delta e^{i\kappa}$), rather than cartesian

---

[6]as opposed to Monte Carlo simulations

[7]See subsections on Acoustic Event Horizon and Integration.
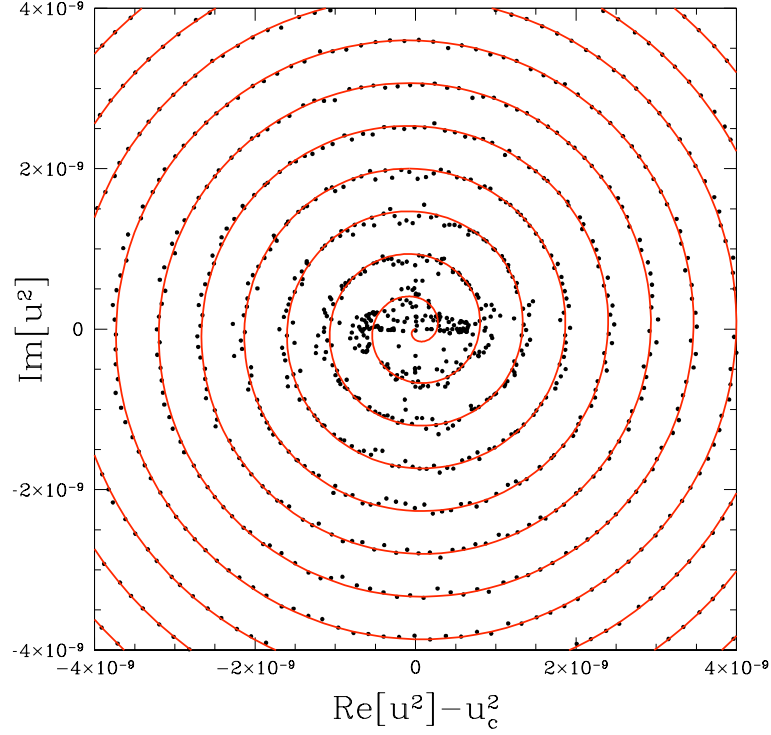
Figure 2.12: Spiral approach of the acoustic horizon. Dots are the numerical solutions of (2.57), solid line is (2.131).

($u^2 = \delta + i\kappa$), greatly curtails branch-hopping.

The Acoustic Event Horizon

It is no surprise that numerical problems are exacerbated by the proximity of the acoustic event horizon. All solution branches converge to the acoustic event horizon (r_c, u_c). Add to that proximity of the ram and breeze solutions, the roundoff error in the calculation of ξ, violent branch-hopping, solution-hopping, along with the good-old numerical instability and accuracy loss ensues as seen in Figure 2.12. To remedy this otherwise unavoidable chaos, in the immediate vicinity of the horizon, the flow is approximated by the Taylor series

$$u(r \to r_c) \to u_c - \frac{2}{m} \frac{u_c^3}{\sqrt{3\gamma - 2}} (r - r_c) + \xi \frac{(r - r_c)^2}{2} \tag{2.131}$$

This solution patch can be used instead of Newton's algorithm when $|r - r_c|$ drops below some desired tolerance.

2.6.2 The Acoustic Tortoise Coordinate

New acoustic tortoise coordinate s (2.120) is given by

$$\frac{dr}{ds} = e^{i\theta} f \sqrt{\gamma - 1} \left(1 - \frac{u^2}{u_c^2}\right). \tag{2.132}$$

$r(s)$ is used in (2.100) to compute $V(se^{i\theta})$. To avoid numerical error propagation, (2.132) is integrated from the origin outward:

(**a**). s is set to zero, r is set to some value[8] $r > r_c$;

(**b**). (2.132) is integrated using RK4 to the left, toward the acoustic horizon to obtain $r(s < 0)$;

(**c**). s is set to zero, r is set to the same value as in step (**a**)

(**d**). (2.132) is integrated using RK4 to the right, toward infinity to obtain $r(s > 0)$;

2.6.3 The Acoustic Scattering Potential

The potential is given by (2.100). Expanding the second tortoise derivative yields

$$
\begin{aligned}
r^2 V &= -u^2 \kappa + \frac{2 + \kappa \left[4 + 2\kappa + u^2 (6 + 5\kappa)\right]}{2 (1 + \kappa)} \left[\frac{2m}{r}\right] - \frac{(4 + 3\kappa)\left(4 + \left(5 + 8u^2\right)\kappa\right)}{16 (1 + \kappa)}\left[\frac{2m}{r}\right]^2 + \\
&+ l(l + 1)(1 + \kappa)\left(1 - \frac{u^2}{u_c^2}\right) f.
\end{aligned} \tag{2.133}
$$

---

[8]Differential equation is autonomous with respect to s. Value of r at $s = 0$ is therefore irrelevant so long as it is greater than the acoustic event horizon.
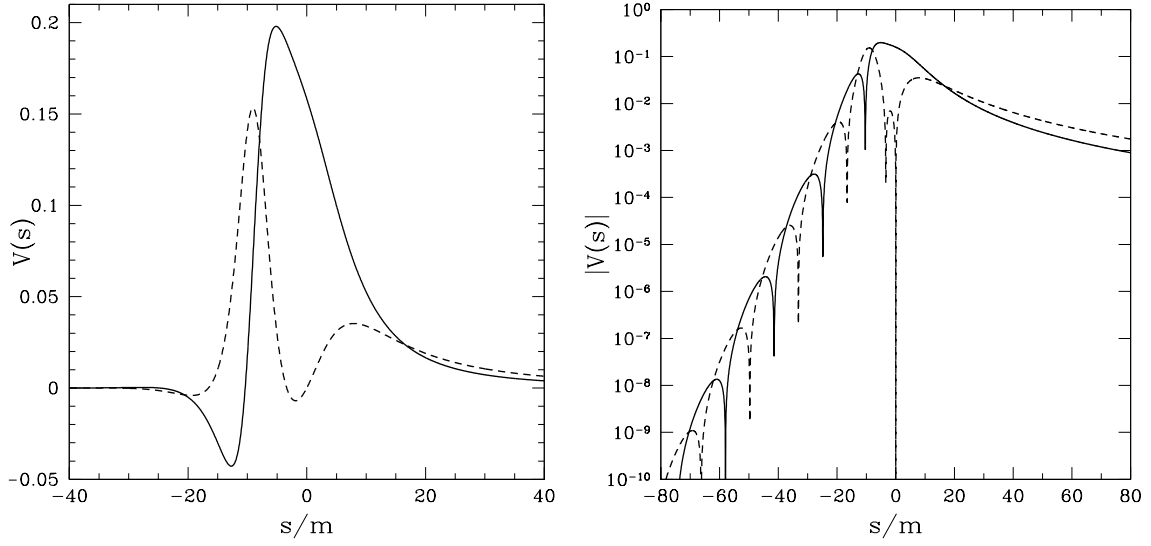
Figure 2.13: Real (solid) and imaginary (dashed) parts of the complex acoustic scattering potential (2.133) for $l = 3$, $\gamma = 1.5$, $\theta = 32°$, and $r(r_* = 0) = 4.5m$.

where

$$\kappa = \gamma - 2. \tag{2.134}$$

The potential is computed by substituting u^2 and r from Subsections (2.6.1) and (2.6.2) into (2.133). Figures 2.13 and 2.14.

2.6.4 Boundary Conditions

As seen in Figures 2.6 and 2.13, the potential decays exponentially toward the horizon (left). For sufficiently small negative values of r_*, V in (2.125) drops below the precision threshold[9] reducing the boundary conditions to $P(-\infty \leftarrow s) = -i\omega$.

Toward the spatial infinity, the potential does not drop off as quickly but, still close enough to zero to consider it *almost* a constant. Imposing the condition $\dfrac{V(s)}{\omega^2} \ll 1$, one can say

$$P(s \to \infty) \to i\sqrt{\omega^2 + V(s)}. \tag{2.135}$$

---

[9]i.e. barely distinguishable from zero by the FPU
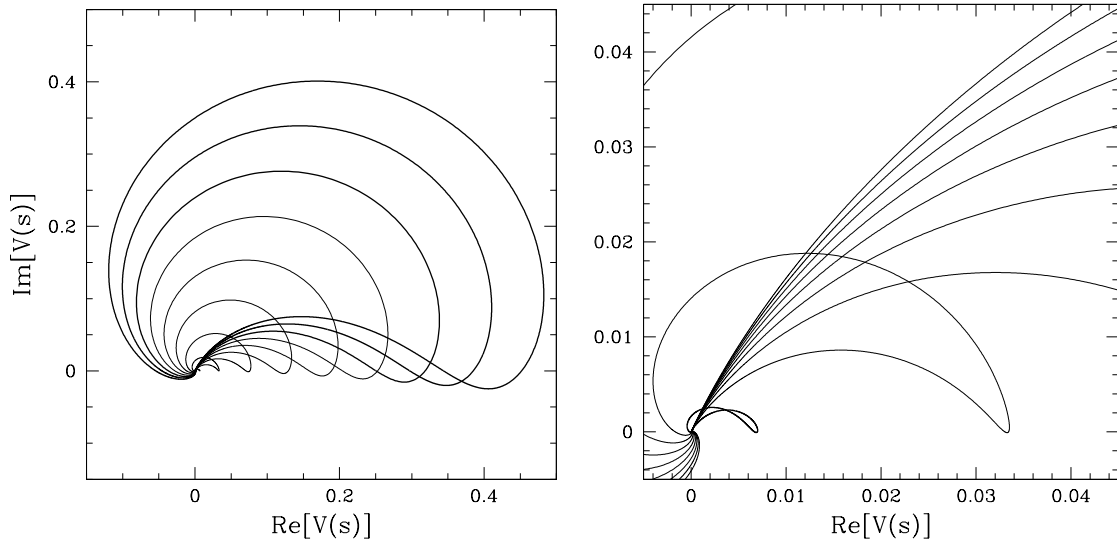
Figure 2.14: Complex acoustic scattering potential (2.133) for $\gamma = (1.1, 1.2, 1.3, 1.4, 1.5, 1.6, 1.7, 1.8, 1.9)$, $\theta = 32°$, $r(r_* = 0) = r_c + 2m$, and $l = 3$; larger curves for larger γ.

The WKB-like approximation for the boundary condition at spatial infinity, which becomes more accurate as s grows larger. Accuracy of (2.135) is determined as follows:

(a). (2.125) is integrated from some point numerically comparable to infinity s_∞ to a point still reasonably far from the origin $s_{\infty/2}$, thus obtaining $P(s_{\infty/2})$.

(b). $P(s_{\infty/2})$ is computed using (2.135).

(c). If both $P(s_{\infty/2})$ are within some desirable tolerance ϵ, s_∞ is used as *numerical infinity*; if not, s_∞ is increased and the process repeats.

s_∞ and $s_{\infty/2}$ used in this study conform to

$$\frac{s_{\infty/2}}{s_\infty} = \frac{4}{5}.$$ (2.136)

2.6.5 Integration

After the potential is computed and boundary conditions set, (2.125) is integrated with RK4 from the left (close to event horizon) to the origin; and then from the right (spatial infinity) to the origin.

2.6.6 Mode-seeking

Newton's algorithm is used to hone-in on guessed quasinormal modes.

(**a**). ω is guessed[10]

(**b**). Anti-stokes angle θ (2.119) and potential (2.133) (which is a function of θ) are computed.

(**c**). Integration yields two complex values for the Ricatti function P at the origin: one obtained via the integration from the left, and one via the integration from the right. The algorithms seeks ω for which the difference between wavefunctions approaches zero, i.e. they are one and same wavefunction, making ω a quasinormal mode.

$$P_- = \int_{-\infty}^{0} P \, ds; \tag{2.137}$$

$$P_+ = \int_{\infty}^{0} P \, ds; \tag{2.138}$$

$$\delta P = P_+ - P_-. \tag{2.139}$$

(**d**). The following two quantities are computed:

$$\Delta \omega = \omega_{current} - \omega_{previous}; \tag{2.140}$$

---

[10]First mode is approximated as discussed in (2.5.1), subsequent modes follow a known trend.

n	$m\omega$ $(l = 1)$	$m\omega$ $(l = 2)$	$m\omega$ $(l = 3)$
1	$0.122\,249 - 0.050\,329\,i$	$0.208\,363 - 0.050\,440\,i$	$0.293\,546 - 0.050\,477\,i$
2	$0.100\,331 - 0.162\,613\,i$	$0.193\,137 - 0.155\,877\,i$	$0.282\,282 - 0.153\,782\,i$
3	$0.078\,092 - 0.295\,930\,i$	$0.168\,470 - 0.274\,158\,i$	$0.261\,655 - 0.264\,154\,i$
4	$0.065\,970 - 0.435\,600\,i$	$0.145\,588 - 0.406\,279\,i$	$0.236\,423 - 0.385\,222\,i$
5	$0.058\,929 - 0.574\,859\,i$	$0.129\,854 - 0.544\,402\,i$	$0.213\,104 - 0.516\,423\,i$

n	$m\omega$ $(l = 4)$	$m\omega$ $(l = 5)$
1	$0.378\,400 - 0.050\,493\,i$	$0.463\,100 - 0.050\,502\,i$
2	$0.369\,520 - 0.152\,906\,i$	$0.455\,787 - 0.152\,461\,i$
3	$0.352\,586 - 0.259\,642\,i$	$0.441\,591 - 0.257\,316\,i$
4	$0.329\,645 - 0.373\,467\,i$	$0.421\,534 - 0.367\,016\,i$
5	$0.304\,303 - 0.496\,071\,i$	$0.397\,479 - 0.483\,252\,i$

Table 2.1: Quasinormal Modes for $\gamma = 4/3$

$$\Delta P \;=\; \delta P_{curent} - \delta P_{previous}. \tag{2.141}$$

(**e**). ω is incremented

$$\omega_{new} \;=\; \omega_{current} - \frac{\delta P_{current}}{\Delta P / \Delta \omega}. \tag{2.142}$$

(**f**). If $\Delta \omega$ is larger than some desired tolerance, go to (**b**).

2.7 Results

Given enough time and computing power, a multitude of quasinormal modes can be found. Table 2.1 displays a few computed as a conclusion of this study and demonstration of the first fully-relativistic quasinormal mode calculation of an acoustic black hole on Schwarzschild background.

Chapter 3

Metric $\mathcal{M}^2 \times \mathcal{S}^2$ Decomposition

3.1 Introduction

As already discussed in the introduction chapter, when working with forms and co-
variant derivatives thereof, compact notation proves useful beyond its ink-saving
tendencies, often yielding insight into the nature of equations, which otherwise re-
main hidden. On the other hand, excessively compact notation, however elegant, is
burdensome in practice. An example is the covariantly divergenceless stress-energy
tensor

$$T^{\mu\nu}{}_{|\mu} = 0, \tag{3.1}$$

an expression so condensed, it says everything and nothing. A healthy balance be-
tween elegance and utility is sought to cast the basic equations of tensor calculus
into a form that is neither excessively specific nor general. This chapter explores
one such device [27]. Presented here is a generalization of covariant operations on

spherically-symmetric backgrounds of the form

$$
g_{\mu\nu} = \begin{pmatrix} g_{00}(x^0, x^1) & g_{01}(x^0, x^1) & 0 & 0 \\ g_{10}(x^0, x^1) & g_{11}(x^0, x^1) & 0 & 0 \\ 0 & 0 & r^2 & 0 \\ 0 & 0 & 0 & r^2 \sin^2 \theta \end{pmatrix},
\tag{3.2}
$$

where the spatial-temporal quadrant[1] of the metric remains general while the rest is set. In other words: one is necessarily working in Schwarzschild spacetime but, not necessarily in Schwarzschild coordinates.

3.1.1 Formalism

It shall be the convention of this chapter to index the 0,1 components of forms with lower-case latin letters, and 2,3 (θ, ϕ) components with upper-case latin letters. Because the spatial-temporal and angular parts of the metric $g_{\mu\nu}$ are not mixed, one can write

$$
g_{ab} = \begin{pmatrix} g_{00} & g_{01} \\ g_{10} & g_{11} \end{pmatrix};
\tag{3.3}
$$

$$
g_{AB} = \begin{pmatrix} r^2 & 0 \\ 0 & r^2 \sin^2 \theta \end{pmatrix};
\tag{3.4}
$$

$$
g_{aB} = 0,
\tag{3.5}
$$

where r^2 can be factored in favor of the unit-sphere metric

$$
g_{AB} = r^2 \Omega_{AB},
\tag{3.6}
$$

---

[1] $g_{10}(x^0, x^1) = g_{01}(x^0, x^1)$

where

$$\Omega_{AB} = \begin{pmatrix} 1 & 0 \\ 0 & \sin^2\theta \end{pmatrix}.$$ (3.7)

Such separation creates two 2D manifolds: the $\mathcal{M}^2$ [spatial-temporal] manifold is spanned by the metric g_{ab}, and the $\mathcal{S}^2$ [angular] manifold shall be spanned by the metric g_{AB}.

3.2 The $\mathcal{M}^2$ One-Forms

To describe vectors/one-forms on $\mathcal{M}^2$, a basis set of vectors/one-forms is developed.

3.2.1 The Spatial One-Form

The following one-form is defined

$$\rho_a = \frac{\partial r}{\partial x^a} = r_{,a},$$ (3.8)

where r is the Schwarzschild r, and is better thought of *not* as a coordinate but, as a radius of a sphere whose surface area is $4\pi r^2$. In general, r can be a function of arbitrary coordinates ξ and ζ; x^a are those arbitrary coordinates.

To begin the illustration of the properties of ρ_a, the following inner product is computed

$$\rho^a \rho_a = g^{ab} \rho_a \rho_b.$$ (3.9)

A point to recognize is that (3.9) is a tensor expression. That is, if it is computed in one coordinate system, it is the same in all coordinate systems. In Schwarzschild

coordinates the metric is given by

$$g^{ab} = \begin{pmatrix} -1/f & 0 \\ 0 & f \end{pmatrix};$$ (3.10)

and

$$x^a = \{t, r\};$$ (3.11)

thus trivializing ρ_a to

$$\rho_a = \begin{pmatrix} 0 \\ 1 \end{pmatrix}.$$ (3.12)

Then the inner product becomes

$$\rho_a \rho^a = \rho_a g^{ab} \rho_b = \begin{pmatrix} 0 & 1 \end{pmatrix} \begin{pmatrix} -1/f & 0 \\ 0 & f \end{pmatrix} \begin{pmatrix} 0 \\ 1 \end{pmatrix} = \begin{pmatrix} 0 & 1 \end{pmatrix} \begin{pmatrix} 0 \\ f \end{pmatrix} = f.$$ (3.13)

As argued before, even though Schwarzschild coordinates are used in calculating this square, the result is coordinate-invariant, *e.g.* if one works in some (ξ, ζ) coordinates, the result does not change, provided that r is substituted with an appropriate function $r(\xi, \zeta)$

$$\rho_a \rho^a = f(\xi, \zeta) = 1 - \frac{2m}{r(\xi, \zeta)},$$ (3.14)

where, once more, r is a radius of a sphere whose surface area is $4\pi r^2$.

3.2.2   The Temporal One-Form

To describe any vector/one-form on $\mathcal{M}^2$, two orthogonal vectors/one-forms are necessary. Having found one (ρ_a) in the previous subsection, finding another is a simple matter of applying the orthogonality operator, also known as the Levi-Civita Tensor.

In general, Levi-Civita tensor is given by

$$\epsilon_{\alpha\beta\ldots\omega} = \sqrt{-g}[\alpha\beta\ldots\omega], \tag{3.15}$$

where [   ] is the permutation symbol or a Levi-Civita Tensor in flat spacetime. In the case of a two-dimensional manifold $\mathcal{M}^2$, Levi-Civita takes a simpler form

$$\epsilon_{ab} = \sqrt{-g}[a\,b]. \tag{3.16}$$

Second one-form can now be constructed

$$\tau_a = -\epsilon_a{}^b \rho_b. \tag{3.17}$$

Following a procedure outlined in (3.2.1) one obtains

$$\tau_a \tau^a \;=\; -f; \tag{3.18}$$

$$\tau_a \rho^a \;=\; 0. \tag{3.19}$$

ρ_a and τ_a constitute the basis for representing objects on $\mathcal{M}^2$.

3.2.3 Covariant Representation of The Metric

Consider the following combination of the spatial one-forms in Schwarzschild coordinates

$$\rho_a \rho_b = \begin{pmatrix} 0 \\ 1 \end{pmatrix} \begin{pmatrix} 0 & 1 \end{pmatrix} = \begin{pmatrix} 0 & 0 \\ 0 & 1 \end{pmatrix}, \tag{3.20}$$

and the combination of the temporal one-forms

$$\tau_a \tau_b = \begin{pmatrix} -f \\ 0 \end{pmatrix} \begin{pmatrix} -f & 0 \end{pmatrix} = \begin{pmatrix} f^2 & 0 \\ 0 & 0 \end{pmatrix}, \tag{3.21}$$

subtracting the two yields

$$\rho_a \rho_b - \tau_a \tau_b = \begin{pmatrix} -f^2 & 0 \\ 0 & 1 \end{pmatrix}. \tag{3.22}$$

One may recognize the expression to be f times the metric g_{ab}

$$g_{ab} = \frac{1}{f} (\rho_a \rho_b - \tau_a \tau_b), \tag{3.23}$$

which is a coordinate-independent representation of the temporal-spatial quadrant of the Schwarzschild metric. It is important to note that while the left side of (3.23) *matches* the right side in Schwarzschild coordinates, because the statement conforms to tensor analysis, it is a coordinate-invariant result and will *match* in any coordinates.

3.2.4   Covariant Representation of the Levi-Civita Tensor

Having explored the outer products of ρ_a and τ_a with themselves in (3.2.3), mixed outer products are a natural sequel

$$\rho_a \tau_b = \begin{pmatrix} 0 \\ 1 \end{pmatrix} \begin{pmatrix} -f & 0 \end{pmatrix} = \begin{pmatrix} 0 & 0 \\ -f & 0 \end{pmatrix}, \tag{3.24}$$

50

which implies that

$$\rho_b \tau_a = \begin{pmatrix} 0 & -f \\ 0 & 0 \end{pmatrix}, \tag{3.25}$$

allowing one to form the difference

$$\rho_a \tau_b - \rho_b \tau_a = \begin{pmatrix} 0 & f \\ -f & 0 \end{pmatrix}, \tag{3.26}$$

which is then recognized to be f times the Levi-Civita Tensor in Schwarzschild co-ordinates

$$\epsilon_{ab} = \frac{1}{f} \left(\rho_a \tau_b - \rho_b \tau_a \right), \tag{3.27}$$

which is a coordinate-invariant representation of the Levi-Civita Tensor on $\mathcal{M}^2$ of the Schwarzschild background.

3.2.5 Divergence

Covariant derivative on $\mathcal{M}^2$ compatible with the metric g_{ab} is defined in the usual way

$$\nabla_c g_{ab} = 0. \tag{3.28}$$

Consider its effect on r

$$\nabla_a r = \partial_a r = \rho_a. \tag{3.29}$$

Rather trivial. Consider the effect of the first covariant derivative on ρ_b

$$\nabla_a \rho_b = \partial_a \rho_b - \Gamma^c{}_{ab} \rho_c \tag{3.30}$$

$$= \partial_a \rho_b - \Gamma^0{}_{ab} \rho_0 - \Gamma^1{}_{ab} \rho_1. \tag{3.31}$$

51

To continue, Schwarzschild coordinates are used in hopes that the answer can some-how be generalized to a coordinateless expression. Recall that in Schwarzschild co-ordinates $\rho_0 = 0$ and $\rho_1 = 1$, simplifying (3.31)

$$\nabla_a \rho_b = -\Gamma^1{}_{ab}, \tag{3.32}$$

$$= -\frac{1}{2} g^{1c} \left(\partial_b g_{ca} + \partial_a g_{cb} - \partial_c g_{ab} \right), \tag{3.33}$$

which splits into four cases: $(a, b) = (0, 0)\,(0, 1)\,(1, 0)\,(1, 1)$. After some algebra, one finds

$$\nabla_0 \rho_0 = -f \frac{m}{r^2}; \tag{3.34}$$

$$\nabla_0 \rho_1 = 0; \tag{3.35}$$

$$\nabla_1 \rho_0 = 0; \tag{3.36}$$

$$\nabla_1 \rho_1 = \frac{1}{f} \frac{m}{r^2}. \tag{3.37}$$

Examined case by case, four cases can be compacted into one expression

$$\nabla_a \rho_b = \frac{m}{r^2} g_{ab}. \tag{3.38}$$

Once again, while the left side of (3.38) *matches* the right side in Schwarzschild coordinates, because the statement conforms to tensor analysis, it is a coordinate-invariant result and will *match* in any coordinates. Having a covariant derivative of ρ_a allows for an effortless calculation of $\nabla_a \tau_b$

$$\nabla_a \tau_b = \nabla_a \left(-\epsilon_{bc} \rho^c \right), \tag{3.39}$$

$$= -\epsilon_{bc} g^{cd} \nabla_a \rho_d, \tag{3.40}$$

$$= -\epsilon_{bc} g^{cd} \frac{m}{r^2} g_{ad}, \tag{3.41}$$

$$= \frac{m}{r^2} \epsilon_{ab}. \tag{3.42}$$

Divergence of both vectors can now be computed

$$\nabla_a \rho^a = g^{ab} \nabla_a \rho_b, \tag{3.43}$$

$$= \frac{m}{r^2} g^{ab} g_{ab}, \tag{3.44}$$

$$= \frac{2m}{r^2}. \tag{3.45}$$

$$\nabla_a \tau^a = g^{ab} \nabla_a \tau_b, \tag{3.46}$$

$$= \frac{m}{r^2} g^{ab} \epsilon_{ab}, \tag{3.47}$$

$$= 0. \tag{3.48}$$

$\nabla_a \tau^a = 0$ because g^{ab} is symmetric and ϵ_{ab} is anti-symmetric.

3.2.6 D'Alembertian

D'Alembertian, or the wave operator is given by

$$\Box = \nabla_\mu \nabla^\mu = g^{\mu\nu} \nabla_\mu \nabla_\nu. \tag{3.49}$$

On $\mathcal{M}^2$, it is given by no less than switching the greek indices with latin ones

$$\Box^{\mathcal{M}^2} = \nabla_a \nabla^a = g^{ab} \nabla_a \nabla_b. \tag{3.50}$$

D'Alembertian of ρ_a

$$\Box^{\mathcal{M}^2} \rho_c = g^{ab} \nabla_a \nabla_b \rho_c, \tag{3.51}$$

$$= g^{ab} \nabla_a \left(\frac{m}{r^2} g_{bc} \right), \tag{3.52}$$

53

$$= \nabla_c \frac{m}{r^2}, \tag{3.53}$$

$$= -\frac{2m}{r^3} \rho_c. \tag{3.54}$$

Following an identical procedure, D'Alembertian of τ_a is found

$$\Box^{M^{(2)}} \tau_a = -\frac{2m}{r^3} \tau_a. \tag{3.55}$$

From which one concludes that ρ_a and τ_a are eigenforms of the wave operator with eigenvalue $\left(-\frac{2m}{r^3} \right)$.

3.2.7 The Riemann Tensor

Function of the Riemann tensor is given by

$$\nabla_c \nabla_d X_a - \nabla_d \nabla_c X_a = R^{M^2}_{abcd} X^b. \tag{3.56}$$

To compute it, one can select the most general one-form X_a on M^2

$$X_a = p\rho_a + q\tau_a, \tag{3.57}$$

where p and q are some well-behaved functions. Substituting (3.57) into (3.56) gives

$$\nabla_c \nabla_d (p\rho_a + q\tau_a) - \nabla_d \nabla_c (p\rho_a + q\tau_a)$$

$$= \nabla_c \nabla_d (p\rho_a) - \nabla_d \nabla_c (p\rho_a) + \nabla_c \nabla_d (q\tau_a) - \nabla_d \nabla_c (q\tau_a), \tag{3.58}$$

$$= p \left(\nabla_c \nabla_d \rho_a - \nabla_d \nabla_c \rho_a \right) + q \left(\nabla_c \nabla_d \tau_a - \nabla_d \nabla_c \tau_a \right). \tag{3.59}$$

After some manipulation, one is able to obtain the following

$$R^{\mathcal{M}^2}_{abcd}X^b = \frac{2m}{r^3}\left(-\left[g_{da}g_{cb} - g_{ca}g_{db}\right]p\rho^b + \left[\epsilon_{da}\epsilon_{cb} - \epsilon_{ca}\epsilon_{db}\right]q\tau^b\right). \tag{3.60}$$

Using (3.23) and (3.27) it can be established that

$$-(g_{da}g_{cb} - g_{ca}g_{db}) = \epsilon_{da}\epsilon_{cb} - \epsilon_{ca}\epsilon_{db}. \tag{3.61}$$

Switching Levi-Civita tensors for metrics in (3.60) reveals the Riemann

$$R^{\mathcal{M}^2}_{abcd}X^b = \frac{2m}{r^3}(g_{ca}g_{db} - g_{da}g_{cb})\left(p\rho^b + q\tau^b\right) \tag{3.62}$$

$$= \frac{2m}{r^3}(g_{ca}g_{db} - g_{da}g_{cb})X^b, \tag{3.63}$$

$\Rightarrow$

$$R^{\mathcal{M}^2}_{abcd} = \frac{2m}{r^3}(g_{ca}g_{db} - g_{da}g_{cb}). \tag{3.64}$$

3.2.8 The Ricci Tensor

Ricci tensor is given by

$$R_{\mu\nu} = R^{\lambda}_{\ \mu\lambda\nu} = g^{\alpha\beta}R_{\alpha\mu\beta\nu}, \tag{3.65}$$

$\Rightarrow$

$$g^{ac}R^{\mathcal{M}^2}_{abcd} = g^{ac}\frac{2m}{r^3}(g_{ca}g_{db} - g_{da}g_{cb}), \tag{3.66}$$

$$R^{\mathcal{M}^2}_{ab} = \frac{2m}{r^3}g_{ab}. \tag{3.67}$$

3.3 The $\mathcal{M}^2$ Basis Tensors

To describe tensors on $\mathcal{M}^2$, a basis set of tensors/tensors is developed.

3.3.1 Definitions

Before constructing the basis tensors, few general rules are set forth:

(**a**). Any 2D rank n tensor can be completely represented by/decomposed to $(n+1)$ 2D rank n tensors, *e.g.* a 2D vector can be represented by two (1+1) 2D vectors;

(**b**). All $n+1$ basis tensors are mutually orthogonal, *e.g.* $\hat{x} \bullet \hat{y} = \hat{z} \bullet \hat{x} = \hat{z} \bullet \hat{y} = 0$;

(**c**). Resulting basis tensors are physically plausible, *i.e.* the basis tensors must be symmetrical: $z_{ab} = z_{ba}$.

The First $\mathcal{M}^2$ Tensor

To begin, one may take the metric tensor g_{ab} as the first basis tensor

$$y_{ab} = f g_{ab}, \tag{3.68}$$

where y_{ab} shall be the notation for the first $\mathcal{M}^2$ basis tensor, and a factor of f is arbitrary. It is symmetrical and so far has nothing to be orthogonal to.

The Second $\mathcal{M}^2$ Tensor

The next simplest tensor can be constructed from the two radial one-forms

$$u_{ab} = \rho_a \rho_b. \tag{3.69}$$

It is symmetric but, is it orthogonal to the first basis tensor y_{ab}? With aid from (3.14) one sees that it is not

$$y^{ab} u_{ab} = g^{ab} \rho_a \rho_b = \rho^a \rho_a = f. \tag{3.70}$$

The fact that $y^{ab} u_{ab}$ is non-zero disqualifies $\rho_a \rho_b$ from being one of the basis tensors. However, its simplicity prompts a desire to seek a correction to the original form of u_{ab} to *force* the inner product to zero.

$$u_{ab} = \rho_a \rho_b + x_{ab}, \tag{3.71}$$

where x_{ab} is an unknown, symmetric tensor. Contracting new u_{ab} on y_{ab} yields

$$y^{ab} u_{ab} = g^{ab} \rho_a \rho_b + g^{ab} x_{ab} = 0, \tag{3.72}$$

$$= f + g^{ab} x_{ab} = 0, \tag{3.73}$$

therefore

$$g^{ab} x_{ab} = -f. \tag{3.74}$$

After some fiddling, one discovers

$$x_{ab} = -\frac{1}{2} f g_{ab}. \tag{3.75}$$

Thus, the second $\mathcal{M}^2$ basis tensor is given by

$$u_{ab} = \rho_a \rho_b - \frac{1}{2} f g_{ab}; \tag{3.76}$$

$$u_{ab} = \rho_a \rho_b - \frac{1}{2} y_{ab}. \tag{3.77}$$

The Third $\mathcal{M}^2$ Tensor

Last basis tensor comes from the next simplest combination of the $\mathcal{M}^2$ one-forms

$$w_{ab} = \rho_a \tau_b. \tag{3.78}$$

Looks promising but, w_{ab} is not symmetric. Standard symmetry solution has always been to flip the indices, add the tensor to itself, and divide by two[2]

$$w_{ab} = \frac{1}{2} \left(\rho_a \tau_b + \rho_b \tau_a \right). \tag{3.79}$$

Checking orthogonality to the first two basis tensors

$$
\begin{aligned}
y^{ab} w_{ab} &= f g^{ab} \frac{1}{2} \left(\rho_a \tau_b + \rho_b \tau_a \right); & (3.80) \\
&= \frac{1}{2} f \left(g^{ab} \rho_a \tau_b + g^{ab} \rho_b \tau_a \right); & (3.81) \\
&= \frac{1}{2} \left(\rho^a \tau_a + \rho^a \tau_a \right); & (3.82) \\
&= 0, & (3.83)
\end{aligned}
$$

where (3.19) is used.

$$
\begin{aligned}
u^{ab} w_{ab} &= \left(\rho^a \rho^b - \frac{1}{2} y^{ab} \right) \frac{1}{2} \left(\rho_a \tau_b + \rho_b \tau_a \right); & (3.84) \\
&= \rho^a \rho^b \left(\rho_a \tau_b + \rho_b \tau_a \right) - \frac{1}{4} y^{ab} \left(\rho_a \tau_b + \rho_b \tau_a \right); & (3.85) \\
&= -\frac{1}{4} y^{ab} w_{ab}; & (3.86) \\
&= 0. & (3.87)
\end{aligned}
$$

---

[2]Division by two is arbitrary yet uniformly accepted as good form.

Summary

What we have before us is a [non-unique] set of $\mathcal{M}^2$ basis tensors fit to decompose any given $\mathcal{M}^2$ tensor.

$$y_{ab} = f g_{ab}; \tag{3.88}$$

$$u_{ab} = \rho_a \rho_b - \frac{1}{2} y_{ab}; \tag{3.89}$$

$$w_{ab} = \frac{1}{2} \left(\rho_a \tau_b + \rho_b \tau_a \right), \tag{3.90}$$

which can be alternatively expressed as

$$y_{ab} = \rho_a \rho_b - \tau_a \tau_b; \tag{3.91}$$

$$u_{ab} = \frac{1}{2} \left(\rho_a \rho_b + \tau_a \tau_b \right); \tag{3.92}$$

$$w_{ab} = \frac{1}{2} \left(\rho_a \tau_b + \rho_b \tau_a \right). \tag{3.93}$$

It should be noted that scaling of any basis system is arbitrary and hence left largely untouched.

3.3.2   Inner Product

Consistently scaling each member of the basis set is not crucial, knowing that scale is.

First Basis Tensor

$$y^{ab} y_{ab} = f g^{ab} f g_{ab} = 2 f^2. \tag{3.94}$$

Second Basis Tensor

Using (3.14),

$$u^{ab}u_{ab} = \left(\rho^a\rho^b - \frac{1}{2}fg^{ab}\right)\left(\rho_a\rho_b - \frac{1}{2}fg_{ab}\right); \tag{3.95}$$

$$= \rho^a\rho^b\rho_a\rho_b - \frac{1}{2}f\rho^a\rho^b g_{ab} - \frac{1}{2}fg^{ab}\rho_a\rho_b + \frac{1}{2}fg^{ab}\frac{1}{2}fg_{ab}; \tag{3.96}$$

$$= f^2 - \frac{1}{2}f^2 - \frac{1}{2}f^2 + \frac{1}{2}f\frac{1}{2}f2 = \frac{1}{2}f^2. \tag{3.97}$$

Third Basis Tensor

Using (3.14), (3.18), and (3.19)

$$w^{ab}w_{ab} = \frac{1}{2}\left(\rho^a\tau^b + \rho^b\tau^a\right)\frac{1}{2}\left(\rho_a\tau_b + \rho_b\tau_a\right); \tag{3.98}$$

$$= \frac{1}{4}\left(\rho^a\rho_a\tau^b\tau_b + \rho^a\tau_a\tau^b\rho_b + \rho^b\tau_b\tau^a\rho_a + \rho^b\rho_b\tau^a\tau_a\right); \tag{3.99}$$

$$= -\frac{1}{2}f^2. \tag{3.100}$$

Summary

Inner products, a.k.a. magnitudes, of the three $\mathcal{M}^2$ basis tensors are

$$y^{ab}y_{ab} = 2f^2; \tag{3.101}$$

$$u^{ab}u_{ab} = \frac{1}{2}f^2; \tag{3.102}$$

$$w^{ab}w_{ab} = -\frac{1}{2}f^2. \tag{3.103}$$

3.3.3   Covariant Derivative

Covariant differentiation of the basis tensors is not *as* trivial.

First Basis Tensor

$$\nabla_c y_{ab} = \nabla_c (f g_{ab}); \tag{3.104}$$

$$= g_{ab} \nabla_c f; \tag{3.105}$$

$$= \frac{2m}{r^2} g_{ab} \rho_c, \tag{3.106}$$

where (3.8) is used.

Second Basis Tensor

$$\nabla_c u_{ab} = \nabla_c \left(\rho_a \rho_b - \frac{1}{2} y_{ab} \right); \tag{3.107}$$

$$= \rho_b \nabla_c \rho_a + \rho_a \nabla_c \rho_b - \frac{1}{2} \nabla_c y_{ab}, \tag{3.108}$$

(3.38) and (3.106) allow the simplification

$$\nabla_c u_{ab} = \frac{m}{r^2} \left(\rho_b g_{ac} + \rho_a g_{cb} - \rho_c g_{ab} \right), \tag{3.109}$$

using (3.23) and (3.27), covariant derivative of the second basis tensor can be brought to

$$\nabla_c u_{ab} = \frac{m}{r^2} \left(g_{ca} \rho_b + \epsilon_{ca} \tau_b \right). \tag{3.110}$$

Third Basis Tensor

Following an identical procedure and using (3.48), it is straight-forward to show

$$\nabla_c w_{ab} = \frac{m}{r^2} \left(\epsilon_{cb} \rho_a + g_{cb} \tau_a \right). \tag{3.111}$$

Summary

Covariant derivatives of the basis tensors are given by

$$\nabla_c y_{ab} = \frac{2m}{r^2} g_{ab} \rho_c;$$

$$\tag{3.112}$$

$$\nabla_c u_{ab} = \frac{m}{r^2} (g_{ca} \rho_b + \epsilon_{ca} \tau_b);$$

$$\tag{3.113}$$

$$\nabla_c w_{ab} = \frac{m}{r^2} (\epsilon_{cb} \rho_a + g_{cb} \tau_a),$$

$$\tag{3.114}$$

or, for the sake of symmetry

$$\nabla_c y_{ab} = \frac{m}{r^2} (g_{ab} \rho_c + g_{ab} \rho_c);$$

$$\tag{3.115}$$

$$\nabla_c u_{ab} = \frac{m}{r^2} (g_{ca} \rho_b + \epsilon_{ca} \tau_b);$$

$$\tag{3.116}$$

$$\nabla_c w_{ab} = \frac{m}{r^2} (\epsilon_{cb} \rho_a + g_{cb} \tau_a).$$

$$\tag{3.117}$$

3.3.4 Divergence

Divergence of all three tensors is easily obtained by contracting the metric g^{ac} on (3.112) - (3.114) and recalling the orthogonality relationship of ρ_a and τ_a (3.17)

$$\nabla^a y_{ab} = \frac{2m}{r^2} \rho_b;$$

$$\tag{3.118}$$

$$\nabla^a u_{ab} = \frac{2m}{r^2} \rho_b;$$

$$\tag{3.119}$$

$$\nabla^a w_{ab} = \frac{2m}{r^2} \tau_b.$$

$$\tag{3.120}$$

3.3.5 D'Alembertian

First Basis Tensor

$$\nabla^c \nabla_c y_{ab} = \nabla^c \nabla_c (f g_{ab});$$

$$\tag{3.121}$$

$$= g_{ab} \nabla^c \nabla_c f; \tag{3.122}$$

$$= g_{ab} \nabla^c \left(\frac{2m}{r^2} \rho_c \right); \tag{3.123}$$

$$= g_{ab} \left(\rho^c \nabla_c \frac{2m}{r^2} + \frac{2m}{r^2} \nabla^c \rho_c \right). \tag{3.124}$$

(3.124) is expanded using (3.45), (3.14), and (3.8)

$$\nabla^c \nabla_c y_{ab} = -\frac{4m}{r^3} y_{ab} \left(1 - \frac{m}{rf} \right). \tag{3.125}$$

Second Basis Tensor

$$\nabla^c \nabla_c u_{ab} = \nabla^c \nabla_c \left(\rho_a \rho_b - \frac{1}{2} y_{ab} \right); \tag{3.126}$$

$$= \nabla^c \rho_b \nabla_c \rho_a + \rho_b \nabla^c \nabla_c \rho_a + \nabla^c \rho_a \nabla_c \rho_b + \rho_a \nabla^c \nabla_c \rho_b - \frac{1}{2} \nabla^c \nabla_c y_{ab}, \tag{3.127}$$

substituting (3.54) and (3.38) yields

$$\nabla^c \nabla_c u_{ab} = -\frac{4m}{r^3} u_{ab}. \tag{3.128}$$

Third Basis Tensor

$$\nabla^c \nabla_c w_{ab} = \nabla^c \nabla_c \frac{1}{2} \left(\rho_a \tau_b + \rho_b \tau_a \right); \tag{3.129}$$

$$= \frac{1}{2} \left(\nabla^c \tau_b \nabla_c \rho_a + \tau_b \nabla^c \nabla_c \rho_a + \nabla^c \rho_a \nabla_c \tau_b + \rho_a \nabla^c \nabla_c \tau_b + \nabla^c \tau_a \nabla_c \rho_b + \right.$$
$$\left. + \tau_a \nabla^c \nabla_c \rho_b + \nabla^c \rho_b \nabla_c \tau_a + \rho_b \nabla^c \nabla_c \tau_a \right), \tag{3.130}$$

substituting (3.54), (3.55), (3.38), and (3.42) yields

$$\nabla^c \nabla_c w_{ab} = -\frac{4m}{r^3} w_{ab}. \tag{3.131}$$

D'Alembertians of the three $\mathcal{M}^2$ basis tensors are given by

$$\nabla^c\nabla_c y_{ab} \quad = \quad -\frac{4m}{r^3}y_{ab}\left(1-\frac{m}{rf}\right); \tag{3.132}$$

$$\nabla^c\nabla_c u_{ab} \quad = \quad -\frac{4m}{r^3}u_{ab}; \tag{3.133}$$

$$\nabla^c\nabla_c w_{ab} \quad = \quad -\frac{4m}{r^3}w_{ab}. \tag{3.134}$$

3.3.6   Miscellaneous Contractions

Using techniques developed in this section, it is trivial to show the following useful

identities

$$\rho^c\nabla_c y_{ab} \quad = \quad \frac{2m}{r^2}y_{ab}; \tag{3.135}$$

$$\rho^c\nabla_c u_{ab} \quad = \quad \frac{2m}{r^2}u_{ab}; \tag{3.136}$$

$$\rho^c\nabla_c w_{ab} \quad = \quad \frac{2m}{r^2}w_{ab}. \tag{3.137}$$

$$\tau^c\nabla_c y_{ab} \quad = \quad 0; \tag{3.138}$$

$$\tau^c\nabla_c u_{ab} \quad = \quad \frac{2m}{r^2}w_{ab}; \tag{3.139}$$

$$\tau^c\nabla_c w_{ab} \quad = \quad \frac{2m}{r^2}u_{ab}. \tag{3.140}$$

3.4   Spherical Harmonics

Spherical harmonics have been an indispensable tool of science for centuries and are

thus not presented as novel or recent work. Reviewed here are their basic properties.

3.4.1 Definitions

It shall be the convention of this section to accept the covariant derivative ∇_A to be compatible with the metric g_{AB} (3.4), and the covariant derivative $\mathbf{D}_A$ to be compatible with the metric Ω_{AB} (3.7). Also, it is straight-forward to show

$$\nabla_A = \mathbf{D}_A; \tag{3.141}$$

$$\nabla^A = \frac{1}{r^2}\mathbf{D}^A; \tag{3.142}$$

$$\nabla_A\nabla^A = \frac{1}{r^2}\mathbf{D}_A\mathbf{D}^A. \tag{3.143}$$

Scalar spherical harmonics are the eigenfunctions of the D'Alembertian on a unit sphere, also known as the harmonic operator

$$\mathbf{D}_A\mathbf{D}^A\, Y^{lm} = -l(l+1)Y^{lm}. \tag{3.144}$$

By construction, scalar spherical harmonics are orthonormal

$$\left\langle Y^{lm}|Y^{l'm'}\right\rangle = \delta_{ll'}\delta_{mm'}, \tag{3.145}$$

where $\langle\,\rangle$ indicate integration over the solid angle.

3.5 Vector Spherical Harmonics

Also known as the $\mathcal{S}^2$ basis vectors.

3.5.1 Definitions

Similarly to basis vectors on $\mathcal{M}^2$, the first vector spherical harmonic is formed via differentiation of the scalar spherical harmonic

$$Y_A = \mathbf{D}_A Y, \tag{3.146}$$

where *lm* superscript has been dropped for brevity and Y_A shall be the notation for the first vector spherical harmonic[3]. To construct the second basis vector, Levi-Civita Tensor is used in the same manner as on $\mathcal{M}^2$

$$X_A = -\epsilon_A{}^B Y_B, \tag{3.147}$$

where $\epsilon_A{}^B$ is the orthogonality operator on a unit sphere and negative sign is a convention. Explicitly, Y_A and X_A are given by

$$Y_\theta = \partial_\theta Y; \tag{3.148}$$

$$Y_\phi = \partial_\phi Y; \tag{3.149}$$

$$X_\theta = -\frac{1}{\sin\theta}\partial_\phi Y; \tag{3.150}$$

$$X_\phi = \sin\theta\,\partial_\theta Y. \tag{3.151}$$

3.5.2 The Riemann Tensor

It can be shown[4] that the Riemann tensor on the unit sphere is given by

$$R^{\mathcal{S}^2}_{BDAC} = \Omega_{AB}\Omega_{CD} - \Omega_{CB}\Omega_{AD}. \tag{3.152}$$

---

[3]Even though it is a one-form.

[4]Tedious and uninteresting.

It is a similar expression to the Riemann on $\mathcal{M}^2$ (3.64). It should also be noted that only four components of the $\mathcal{S}^2$ Riemann endure, two unique and two reflections:

$$R^\theta{}_{\phi\theta\phi} = -R^\theta{}_{\phi\phi\theta} = \sin^2\theta; \tag{3.153}$$

$$R^\phi{}_{\theta\phi\theta} = -R^\phi{}_{\theta\theta\phi} = 1. \tag{3.154}$$

3.5.3 The Ricci Tensor

Contracting (3.152) on Ω^{AB} yields

$$R_{AB} = \Omega_{AB}. \tag{3.155}$$

3.5.4 Inner Product

For the sake of not repeating the title of this subsection once again, consider the following

$$\left\langle Y_A | Y^A \right\rangle = \int Y_A Y^A d\Omega, \tag{3.156}$$

$$= \int \mathbf{D}_A Y \, \mathbf{D}^A Y d\Omega, \tag{3.157}$$

using the product differentiation rule, integral can be written as

$$\left\langle Y_A | Y^A \right\rangle = Y \mathbf{D}_A Y|_{surface} - \int \left[\mathbf{D}_A \mathbf{D}^A Y \right] Y d\Omega, \tag{3.158}$$

$$= Y \mathbf{D}_A Y|_{surface} - \int \left[-l(l+1)Y \right] Y d\Omega, \tag{3.159}$$

surface term $Y \mathbf{D}_A Y$ is zero[5]

$$\langle Y_A | Y^A \rangle \quad = \quad l(l+1) \int Y Y d\Omega, \tag{3.160}$$

$$= \quad l(l+1) \langle Y | Y \rangle, \tag{3.161}$$

$$= \quad l(l+1), \tag{3.162}$$

where the Kronecker Delta factors $\delta_{ll'}\delta_{mm'}$, complex conjugation, and integration limits will henceforth be presumed but, dropped for brevity. A similar calculation reveals the inner product of the second vector harmonic

$$\langle X_A | X^A \rangle = l(l+1). \tag{3.163}$$

The two remain orthogonal by construction

$$\langle X_A | Y^A \rangle = 0. \tag{3.164}$$

3.5.5 Divergence

$$\mathbf{D}^A Y_A \quad = \quad \mathbf{D}^A \mathbf{D}_A Y, \tag{3.165}$$

$$= \quad -l(l+1)Y. \tag{3.166}$$

Not so for the X_A

$$\mathbf{D}^A X_A = \mathbf{D}^A \left(-\epsilon_A{}^B Y_B \right), \tag{3.167}$$

---

[5]Because it is evaluated at the boundaries.

Levi-Civita tensor $\left(\epsilon_A{}^B\right)$ is constant under covariant differentiation, it slips past the derivative

$$\mathbf{D}^A X_A \;=\; -\epsilon_A{}^B \mathbf{D}^A \mathbf{D}_B Y, \tag{3.168}$$

$$=\; 0, \tag{3.169}$$

zero because $\mathbf{D}^A \mathbf{D}_B$ is symmetric when acting on a scalar and $\epsilon_A{}^B$ is anti-symmetric.

3.5.6 D'Alembertian

Harmonic operator acting on a vector spherical harmonic is given by

$$\mathbf{D}_A \mathbf{D}^A Y_C = \Omega^{AB} \mathbf{D}_A \mathbf{D}_B \mathbf{D}_C Y, \tag{3.170}$$

covariant differentiation on a scalar commutes

$$\mathbf{D}_A \mathbf{D}^A Y_C \;=\; \Omega^{AB} \mathbf{D}_A \mathbf{D}_C \left(\mathbf{D}_B Y\right); \tag{3.171}$$

$$=\; \Omega^{AB} \mathbf{D}_A \mathbf{D}_C Y_B, \tag{3.172}$$

covariant differentiation on a vector doesn't

$$\mathbf{D}_A \mathbf{D}_C Y_B = \mathbf{D}_C \mathbf{D}_A Y_B + R_{BDAC} Y^D, \tag{3.173}$$

substituting (3.173) into (3.172) yields

$$\mathbf{D}_A \mathbf{D}^A Y_C = -l(l+1) Y_C + R_{DC} Y^D. \tag{3.174}$$

As mentioned previously

$$R_{AB} = \Omega_{AB}, \tag{3.175}$$

$\Rightarrow$

$$\mathbf{D}_A \mathbf{D}^A Y_C = [1 - l(l+1)] \, Y_C. \tag{3.176}$$

Effect of the harmonic operator on X_A is identical

$$\mathbf{D}_A \mathbf{D}^A X_C = [1 - l(l+1)] \, X_C. \tag{3.177}$$

Both vector spherical harmonics are eigenvectors of the harmonic operator with eigenvalue $[1 - l(l+1)]$.

3.6 Tensor Spherical Harmonics

One step up from vectors (one-forms) are tensors. Whereas vector spherical harmonics are used in decomposition of vectors on a unit sphere, tensor spherical harmonics are used in decomposition of tensors on a unit spehre. In this section, properties of tensor spherical harmonics are explored.

3.6.1 Definitions

Following the habits developed obtaining basis vectors via differentiation of [basis] scalars, one naturally attempts to obtain basis tensors by differentiating basis vectors. Rules discussed in (3.3.1) apply.

First Tensor Spherical Harmonic

To begin, one recognizes that the simplest basis tensor is given by

$$Y_{AB} = Y\,\Omega_{AB}, \tag{3.178}$$

where Y_{AB} shall be the notation for the first tensor spherical harmonic. It satisfies the first two conditions because it is the first in the sequence, (3.178) is symmetrical by construction.

Second Tensor Spherical Harmonic

To compute another basis tensor, one may differentiate vector spherical harmonic Y_A and call it U_{AB}

$$U_{AB} = \mathbf{D}_B Y_A = Y_{A|B}. \tag{3.179}$$

(3.179) is also symmetrical by construction[6] but, its orthogonality to the first basis tensor (3.179) must be established

$$\left\langle Y^{AB}|U_{AB}\right\rangle = \left\langle Y\,\Omega^{AB}|Y_{A|B}\right\rangle; \tag{3.180}$$

$$= \left\langle Y\,\Omega^{AB}|\mathbf{D}_A\mathbf{D}_B Y\right\rangle; \tag{3.181}$$

$$= \left\langle Y|\mathbf{D}_A\mathbf{D}^A Y\right\rangle; \tag{3.182}$$

$$= -l(l+1). \tag{3.183}$$

(3.178) and (3.179) are *not* orthogonal. To force the inner product to zero, one may add an unknown (symmetrical) tensor Z_{AB} to (3.179), which when contracted on Y^{AB}

---

[6] $Y_{A|B} = \mathbf{D}_B\mathbf{D}_A Y = \mathbf{D}_A\mathbf{D}_B Y = Y_{B|A}$

yields $l(l + 1)$.

$$\langle Y^{AB}|U_{AB} + Z_{AB}\rangle = \langle Y^{AB}|U_{AB}\rangle + \langle Y^{AB}|Z_{AB}\rangle = 0; \tag{3.184}$$

$$= -l(l + 1) + \langle Y\Omega^{AB}|Z_{AB}\rangle = 0. \tag{3.185}$$

After a few contractions one discovers one such Z_{AB}

$$Z_{AB} = \frac{1}{2}l(l + 1)Y\Omega_{AB}. \tag{3.186}$$

The second tensor spherical harmonic is therefore given by

$$U_{AB} = Y_{A|B} + \frac{1}{2}l(l + 1)Y\Omega_{AB}. \tag{3.187}$$

(3.187) is orthogonal to Y_{AB} and symmetrical. It can be alternatively expressed in terms of Y_{AB}

$$U_{AB} = Y_{A|B} + \frac{1}{2}l(l + 1)Y_{AB}. \tag{3.188}$$

Third Tensor Harmonic

Third basis tensor is found by differentiating the second vector spherical harmonic

$$W_{AB} = \mathbf{D}_B X_A = X_{A|B}, \tag{3.189}$$

where W_{AB} shall be the notation for the third basis tensor. Orthogonality to the two previously discovered basis tensors must be established.

$$\langle Y^{AB}|W_{AB}\rangle = \langle Y\Omega^{AB}|X_{A|B}\rangle; \tag{3.190}$$

$$= \langle Y\Omega^{AB}|\mathbf{D}_B X_A\rangle; \tag{3.191}$$

$$= \left\langle Y | \mathbf{D}^A X_A \right\rangle, \tag{3.192}$$

according to (3.169) $\mathbf{D}^A X_A = 0$,

$$\left\langle Y^{AB} | W_{AB} \right\rangle = 0. \tag{3.193}$$

W_{AB} is orthogonal to the first basis tensor Y_{AB}. Contracting W_{AB} onto U^{AB}

$$\left\langle U^{AB} | W_{AB} \right\rangle = \left\langle Y^{A|B} + \frac{1}{2} l(l+1) Y \, \Omega^{AB} | X_{A|B} \right\rangle; \tag{3.194}$$

$$= \left\langle Y^{A|B} | X_{A|B} \right\rangle + \frac{1}{2} l(l+1) \left\langle Y^{AB} | X_{A|B} \right\rangle, \tag{3.195}$$

last term is zero according to (3.193),

$$\left\langle U^{AB} | W_{AB} \right\rangle = \left\langle Y^{A|B} | X_{A|B} \right\rangle; \tag{3.196}$$

$$= \left\langle \mathbf{D}^B Y^A | \mathbf{D}_B X_A \right\rangle. \tag{3.197}$$

$$\tag{3.198}$$

using the product differentiation rule, $\mathbf{D}_B$ can be moved from operating on X_A to operating on Y^A

$$\left\langle U^{AB} | W_{AB} \right\rangle = X_A \mathbf{D}^B Y^A \big|_{surface} - \left\langle \mathbf{D}_B \mathbf{D}^B Y^A | X_A \right\rangle, \tag{3.199}$$

surface term is zero[7]. Using (3.176) and (3.164) it is trivial to show that

$$\left\langle U^{AB} | W_{AB} \right\rangle = 0. \tag{3.200}$$

---

[7]As always.

73

W_{AB} is declared orthogonal to Y_{AB} and U_{AB}. The last condition, which W_{AB} must satisfy to join Y_{AB} and U_{AB} as a basis tensor, is symmetricity.

$$X_{A|B} = \mathbf{D}_B X_A; \tag{3.201}$$

$$= \mathbf{D}_B \left(-\epsilon_A{}^C Y_C \right), \tag{3.202}$$

from which one can see that interchanging A and B has a profound effect on $X_{A|B}$ because differentiation and multiplication indices trade places: $W_{A|B}$ is not symmetrical. Since $W_{A|B}$ is orthogonal to the two other basis tensors, one would be wise to salvage it somehow. A common non-symmetricity remedy of index gymnastics yields a solution: if Z_{AB} is not symmetrical, $Z_{AB} + Z_{BA}$ is. One has therefore found the third basis tensor

$$W_{AB} = \frac{1}{2} \left(X_{A|B} + X_{B|A} \right), \tag{3.203}$$

where a factor of $1/2$ is arbitrary.

Summary

Three tensor spherical harmonics are defined as follows

$$Y_{AB} = Y \Omega_{AB}; \tag{3.204}$$

$$U_{AB} = Y_{B|A} + \frac{1}{2}l(l+1)Y_{AB}; \tag{3.205}$$

$$W_{AB} = \frac{1}{2} \left(X_{A|B} + X_{B|A} \right). \tag{3.206}$$

These are the basis tensors used by K. Martel [26], and much of the remaining GR community.

3.6.2   Inner Product

Normalization of the basis tensors is not of particular importance to most applications, their magnitudes are.

First Tensor Spherical Harmonic

$$\left\langle Y^{AB}|Y_{AB}\right\rangle \;=\; \left\langle Y\Omega^{AB}|Y\Omega_{AB}\right\rangle; \tag{3.207}$$

$$=\; 2. \tag{3.208}$$

Second Tensor Spherical Harmonic

$$\left\langle U^{AB}|U_{AB}\right\rangle \;=\; \left\langle Y^{B|A} + \frac{1}{2}l(l+1)Y^{AB}|Y_{B|A} + \frac{1}{2}l(l+1)Y_{AB}\right\rangle; \tag{3.209}$$

$$=\; \left\langle Y^{B|A}|Y_{B|A}\right\rangle + \frac{1}{2}l(l+1)\left\langle Y^{B|A}|Y_{AB}\right\rangle + \frac{1}{2}l(l+1)\left\langle Y^{AB}|Y_{B|A}\right\rangle +$$

$$\frac{1}{4}l^2(l+1)^2\left\langle Y^{AB}|Y_{AB}\right\rangle, \tag{3.210}$$

using (3.208) and some algebra yields

$$\left\langle U^{AB}|U_{AB}\right\rangle = \left\langle Y^{B|A}|Y_{B|A}\right\rangle + l(l+1)\left\langle Y^{B|A}|Y_{AB}\right\rangle + \frac{1}{2}l^2(l+1)^2, \tag{3.211}$$

(3.183) offers further reduction

$$\left\langle U^{AB}|U_{AB}\right\rangle = \left\langle Y^{B|A}|Y_{B|A}\right\rangle - \frac{1}{2}l^2(l+1)^2. \tag{3.212}$$

Remaining term is not as trivial.

$$\left\langle Y^{B|A}|Y_{B|A}\right\rangle = \left\langle \mathbf{D}^A Y^B|\mathbf{D}_A Y_B\right\rangle, \tag{3.213}$$

using the product differentiation rule[8], $\mathbf{D}_A$ can be moved from ket to bra

$$\left\langle Y^{B|A}|Y_{B|A}\right\rangle = -\left\langle \mathbf{D}_A\mathbf{D}^A Y^B|Y_B\right\rangle, \tag{3.214}$$

(3.176) allows one to compute the D'Alembertian of Y^B

$$\left\langle Y^{B|A}|Y_{B|A}\right\rangle = -\left[1 - l(l+1)\right]\left\langle Y^B|Y_B\right\rangle, \tag{3.215}$$

last step is to use the inner product computed previously (3.162)

$$\left\langle Y^{B|A}|Y_{B|A}\right\rangle = -l(l+1)\left[1 - l(l+1)\right]. \tag{3.216}$$

Substituting (3.216) into (3.212) yields the coveted inner product

$$\left\langle U^{AB}|U_{AB}\right\rangle = l(l+1)\left[\frac{1}{2}l(l+1) - 1\right]. \tag{3.217}$$

Or, if one wishes to trade efficiency for elegancy

$$\begin{aligned}
\left\langle U^{AB}|U_{AB}\right\rangle &= \frac{1}{2}(l-1)l(l+1)(l+2); & \text{(3.218)} \\
&= \frac{1}{2}\frac{(l+2)!}{(l-2)!}. & \text{(3.219)}
\end{aligned}$$

Third Tensor Spherical Harmonic

$$\left\langle W^{AB}|W_{AB}\right\rangle = \frac{1}{2}\left\langle X_{A|B}|X^{A|B}\right\rangle + \frac{1}{2}\left\langle X_{A|B}|X^{B|A}\right\rangle. \tag{3.220}$$

---

[8]surface term not shown for brevity

Via the procedure identical to the one used in obtaining (3.216), one can show

$$\left\langle X_{A|B}|X^{A|B}\right\rangle = l(l+1)\left[l(l+1)-1\right]. \tag{3.221}$$

Second term in (3.220) is not *as* trivial.

$$\left\langle X_{A|B}|X^{B|A}\right\rangle = \left\langle \mathbf{D}_B X_A|\mathbf{D}^A X^B\right\rangle, \tag{3.222}$$

using the product differentiation rule, $\mathbf{D}^A$ is shifted from ket to bra

$$\left\langle X_{A|B}|X^{B|A}\right\rangle = -\left\langle \mathbf{D}^A \mathbf{D}_B X_A|X^B\right\rangle. \tag{3.223}$$

(3.223) is a dead end unless $\mathbf{D}^A \mathbf{D}_B$ are flipped. To that end, one may employ the Riemann

$$\mathbf{D}^A \mathbf{D}_B X_A = \mathbf{D}_B \mathbf{D}^A X_A + R^A{}_{EAB} X^E. \tag{3.224}$$

Substituting (3.224) into (3.223) and using (3.152), (3.169), (3.163), yields

$$\left\langle X_{A|B}|X^{B|A}\right\rangle = -l(l+1). \tag{3.225}$$

Inserting (3.225) and (3.221) into (3.220) produces the inner product

$$\left\langle W^{AB}|W_{AB}\right\rangle = l(l+1)\left[\frac{1}{2}l(l+1)-1\right], \tag{3.226}$$

which is the same for $\left\langle U^{AB}|U_{AB}\right\rangle$, (3.217).

3.6.3 Divergence

First Tensor Spherical Harmonic

$$\mathbf{D}^A Y_{AB} = \mathbf{D}^A \left(Y \Omega_{AB} \right), \tag{3.227}$$

Ω_{AB} is covariantly divergenceless, thus unaffected by differentiation

$$\mathbf{D}^A Y_{AB} = \Omega_{AB} Y^A = Y_B. \tag{3.228}$$

Second Tensor Spherical Harmonic

$$\mathbf{D}^A U_{AB} = \mathbf{D}^A Y_{B|A} + \frac{1}{2} l(l+1) \mathbf{D}^A Y_{AB}. \tag{3.229}$$

Utilizing (3.228) and (3.176) it can be shown

$$\mathbf{D}^A U_{AB} = \left[1 - \frac{1}{2} l(l+1) \right] Y_B. \tag{3.230}$$

Third Tensor Spherical Harmonic

$$\mathbf{D}^A W_{AB} = \frac{1}{2} \left(\mathbf{D}^A X_{A|B} + \mathbf{D}^A X_{B|A} \right), \tag{3.231}$$

(3.177) simplifies the expression somewhat

$$\mathbf{D}^A W_{AB} = \frac{1}{2} \left(\mathbf{D}^A \mathbf{D}_B X_A + [1 - l(l+1)] X_B \right). \tag{3.232}$$

Riemann assists in calculation of the remaining term

$$\mathbf{D}^A \mathbf{D}_B X_A = R^A{}_{EAB} X^E + \mathbf{D}_B \mathbf{D}^A X_A. \tag{3.233}$$

Including (3.233) into (3.232) and utilizing (3.152) and (3.169) yields the sought divergence

$$\mathbf{D}^A W_{AB} = \left[1 - \frac{1}{2}l(l+1)\right] X_B. \tag{3.234}$$

3.6.4 D'Alembertian

First Tensor Spherical Harmonic

$$\begin{align}
\mathbf{D}^C \mathbf{D}_C Y_{AB} &= \mathbf{D}^C \mathbf{D}_C Y \Omega_{AB}; \tag{3.235} \\
&= \Omega_{AB} \mathbf{D}^C \mathbf{D}_C Y; \tag{3.236} \\
&= -Y \Omega_{AB} l(l+1); \tag{3.237} \\
&= -l(l+1) Y_{AB}, \tag{3.238}
\end{align}$$

where (3.144) is used. Y_{AB} is an eigentensor of the harmonic operator with an eigenvalue of $[-l(l+1)]$.

Second Tensor Spherical Harmonic

$$\begin{align}
\mathbf{D}^C \mathbf{D}_C U_{AB} &= \mathbf{D}^C \mathbf{D}_C Y_{B|A} + \frac{1}{2}l(l+1)\mathbf{D}^C \mathbf{D}_C Y_{AB}; \tag{3.239} \\
&= \mathbf{D}^C \mathbf{D}_C Y_{B|A} - \frac{1}{2}l^2(l+1)^2 Y_{AB}, \tag{3.240}
\end{align}$$

where (3.238) simplifies the second term. To continue, the non-commuting covariant differentiation of Y_B must be reworked to yield a previously computed quantity, namely

$$\mathbf{D}^C \mathbf{D}_C \mathbf{D}_A Y_B \rightarrow \mathbf{D}^C \mathbf{D}_A \mathbf{D}_C Y_B \rightarrow \mathbf{D}_A \mathbf{D}^C \mathbf{D}_C Y_B. \tag{3.241}$$

$\mathbf{D}_A$ has to be extracted from beneath the harmonic operator $\mathbf{D}^C\mathbf{D}_C$. First interchange is achieved through the usual method

$$\mathbf{D}^C\mathbf{D}_C\mathbf{D}_A Y_B = \mathbf{D}^C\left(R_{BECA}Y^E\right) + \mathbf{D}^C\mathbf{D}_A\mathbf{D}_C Y_B. \tag{3.242}$$

Second interchange is more complicated because it acts on a tensor, rather than a vector

$$\mathbf{D}^C\mathbf{D}_A Y_{B|C} = \mathbf{D}_A\mathbf{D}^C Y_{B|C} + R^C{}_{ECA}Y_B{}^{|E} + R_{BECA}Y^{E|C}. \tag{3.243}$$

Aftrer inserting (3.243) into (3.242), (3.242) into (3.240), using the definition of Riemann (3.152), and performing some calculations it can be shown that U_{AB} is an eigenform (eigentensor) of the harmonic operator

$$\mathbf{D}^C\mathbf{D}_C U_{AB} = [4 - l(l+1)]\, U_{AB}. \tag{3.244}$$

Third Tensor Spherical Harmonic

$$\mathbf{D}^C\mathbf{D}_C W_{AB} = \frac{1}{2}\left(\mathbf{D}^C\mathbf{D}_C X_{A|B} + \mathbf{D}^C\mathbf{D}_C X_{B|A}\right). \tag{3.245}$$

Intimidating expression, however one notices that it can be cast into a familiar form

$$\mathbf{D}^C\mathbf{D}_C W_{AB} = -\frac{1}{2}\left(\epsilon_A{}^E\mathbf{D}^C\mathbf{D}_C Y_{A|B} + \epsilon_B{}^E\mathbf{D}^C\mathbf{D}_C Y_{B|A}\right). \tag{3.246}$$

Action of the harmonic operator on the derivatives of the first vector spherical harmonic has already been computed: (3.242) and (3.243). Exploiting said result one can show that W_{AB} is also an eigentensor of the harmonic operator, with the same exact eigenvalue as U_{AB}

$$\mathbf{D}^C\mathbf{D}_C W_{AB} = [4 - l(l+1)]\, W_{AB}. \tag{3.247}$$

3.7 Reconstruction: 4-space Operators

Elaborate machinery developed in this chapter has so far been on two-dimensional manifolds, it must now be recombined to act on four-dimensional spacetime.

3.7.1 The Connection

Due to the unmixed nature of the metric (*i.e.* $g_{aB} = 0$), the four-space connection of the spatial-temporal region is equal to the $\mathcal{M}^2$ connection

$$\Gamma^a{}_{bc} = {}^{\mathcal{M}^2}\Gamma^a{}_{bc}, \tag{3.248}$$

same can be said about the angular region

$$\Gamma^A{}_{BC} = {}^{\mathcal{S}^2}\Gamma^A{}_{BC}. \tag{3.249}$$

Mixed connection coefficients must be computed.

$$\Gamma^a{}_{bC} = \frac{1}{2}g^{a\mu}\left(g_{\mu b,C} + g_{\mu C,b} - g_{bC,\mu}\right). \tag{3.250}$$

$g_{bC,\mu}$ is zero because the metric is unmixed; $g_{\mu C,b}$ is zero because no part of the angular metric depends on any of the spatial-temporal coordinates, vice-versa for $g_{\mu b,C}$. Therefore, this particular connection coefficient is zero

$$\Gamma^a{}_{bC} = \Gamma^a{}_{Cb} = 0. \tag{3.251}$$

Continuing on in this fashion, one is able to obtain the remaining mixed connection coefficients

$$\Gamma^A_{\ bc} = 0; \tag{3.252}$$

$$\Gamma^A_{\ Bc} = \frac{1}{r}\rho_c\delta^A_{\ B}; \tag{3.253}$$

$$\Gamma^a_{\ BC} = -\frac{1}{r}\rho^a g_{BC}; \tag{3.254}$$

$$= -r\rho^a\Omega_{BC}. \tag{3.255}$$

3.7.2 Divergence of a Vector/One-Form

In 2×2 formalism, every indexed operation is specialized to spatial-temporal and angular regions. For example

$$F_{\beta|\alpha}, \tag{3.256}$$

is split into four cases

$$F_{b|a} = F_{b,a} - \Gamma^\mu_{\ ab}F_\mu; \tag{3.257}$$

$$F_{B|a} = F_{B,a} - \Gamma^\mu_{\ aB}F_\mu; \tag{3.258}$$

$$F_{b|A} = F_{b,A} - \Gamma^\mu_{\ Ab}F_\mu; \tag{3.259}$$

$$F_{B|A} = F_{B,A} - \Gamma^\mu_{\ AB}F_\mu. \tag{3.260}$$

The μ summation is separated into the summation over spatial-temporal and angular indices

$$F_{b|a} = F_{b,a} - \Gamma^m_{\ ab}F_m - \Gamma^M_{\ ab}F_M; \tag{3.261}$$

$$F_{B|a} = F_{B,a} - \Gamma^m_{\ aB}F_m - \Gamma^M_{\ aB}F_M; \tag{3.262}$$

$$F_{b|A} = F_{b,A} - \Gamma^m_{\ Ab}F_m - \Gamma^M_{\ Ab}F_M; \tag{3.263}$$

$$F_{B|A} = F_{B,A} - \Gamma^m{}_{AB}F_m - \Gamma^M{}_{AB}F_M. \tag{3.264}$$

Equations (3.251)-(3.255) are used in place of the connection coefficients.

$$F_{b|a} = F_{b,a} - \Gamma^m{}_{ab}F_m; \tag{3.265}$$

$$F_{B|a} = F_{B,a} - \frac{1}{r}\rho_a\delta^M{}_B F_M; \tag{3.266}$$

$$F_{b|A} = F_{b,A} - \frac{1}{r}\rho_b\delta^M{}_A F_M; \tag{3.267}$$

$$F_{B|A} = F_{B,A} + \frac{1}{r}\rho^m g_{AB}F_m - \Gamma^M{}_{AB}F_M, \tag{3.268}$$

using (3.248) and (3.249), contracting the Kronecker Delta functions, and rearranging

$$F_{b|a} = \left[F_{b,a} - {}^{M^2}\Gamma^m{}_{ab}F_m\right]; \tag{3.269}$$

$$F_{B|a} = F_{B,a} - \frac{1}{r}\rho_a F_B; \tag{3.270}$$

$$F_{b|A} = F_{b,A} - \frac{1}{r}\rho_b F_A; \tag{3.271}$$

$$F_{B|A} = \left[F_{B,A} - {}^{S^2}\Gamma^M{}_{AB}F_M\right] + \frac{1}{r}\rho^m F_m g_{AB}, \tag{3.272}$$

terms in brackets are recognized to be the expanded covariant derivatives on their respective manifolds

$$F_{b|a} = \nabla_a F_b; \tag{3.273}$$

$$F_{B|a} = F_{B,a} - \frac{1}{r}\rho_a F_B; \tag{3.274}$$

$$F_{b|A} = F_{b,A} - \frac{1}{r}\rho_b F_A; \tag{3.275}$$

$$F_{B|A} = \nabla_A F_B + \frac{1}{r}\rho^m F_m g_{AB}. \tag{3.276}$$

Divergence of F^μ can now be computed

$$
\begin{aligned}
F^\mu{}_{|\mu} &= F^a{}_{|a} + F^A{}_{|A}, & (3.277) \\
&= g^{ab} F_{b|a} + g^{AB} F_{B|A}, & (3.278)
\end{aligned}
$$

substituting (3.273) and (3.276)

$$
\begin{aligned}
F^\mu{}_{|\mu} &= g^{ab} \nabla_a F_b + g^{AB} \left[\nabla_A F_B + \frac{1}{r} \rho^m F_m g_{AB} \right], & (3.279) \\
&= \nabla_a F^a + \nabla_A F^A + \frac{2}{r} \rho_m F^m. & (3.280)
\end{aligned}
$$

Thus, four-divergence of a four-vector is the sum of the spatial-temporal and the angular divergences of its two-vector components, plus a *cross term*[9] $\frac{2}{r} \rho_m F^m$.

3.7.3 D'Alembertian of a Vector/One-Form

Wave operator acting on a one-form

$$
F_{\alpha|\nu}{}^\nu = g^{\mu\nu} F_{\alpha|\mu\nu}. \tag{3.281}
$$

As before, free index α is specialized to two sub-manifolds

$$
\begin{aligned}
F_{a|\nu}{}^\nu &= g^{\mu\nu} F_{a|\mu\nu}; & (3.282) \\
F_{A|\nu}{}^\nu &= g^{\mu\nu} F_{A|\mu\nu}, & (3.283)
\end{aligned}
$$

---

[9]Which is a misnomer because the term involves only $\mathcal{M}^2$ components.

so are the summations over μ and ν

$$F_{a|\nu}{}^{\nu} = g^{mn}F_{a|mn} + g^{mN}F_{a|mN} + g^{Mn}F_{a|Mn} + g^{MN}F_{a|MN}; \tag{3.284}$$

$$F_{A|\nu}{}^{\nu} = g^{mn}F_{A|mn} + g^{mN}F_{A|mN} + g^{Mn}F_{A|Mn} + g^{MN}F_{A|MN}, \tag{3.285}$$

two middle terms in each summation vanish because $g^{aB} = 0$

$$F_{a|\nu}{}^{\nu} = g^{mn}F_{a|mn} + g^{MN}F_{a|MN}; \tag{3.286}$$

$$F_{A|\nu}{}^{\nu} = g^{mn}F_{A|mn} + g^{MN}F_{A|MN}. \tag{3.287}$$

Second derivatives of a one-form have not been computed, (3.273) - (3.276) are used as a starting point

$$F_{a|mn} = (F_{a|m})_{|n}; \tag{3.288}$$

$$= (\nabla_m F_a)_{|n}; \tag{3.289}$$

$$= (\nabla_m F_a)_{,n} - \Gamma^{\sigma}{}_{nm}(\nabla_{\sigma}F_a) - \Gamma^{\sigma}{}_{na}(\nabla_m F_{\sigma}); \tag{3.290}$$

$$= (\nabla_m F_a)_{,n} - \Gamma^s{}_{nm}(\nabla_s F_a) - \Gamma^s{}_{nm}(\nabla_s F_a) +$$

$$\quad -\Gamma^S{}_{na}(\nabla_m F_S) - \Gamma^S{}_{na}(\nabla_m F_S), \tag{3.291}$$

substituting (3.248) - (3.255), gives

$$F_{a|mn} = (\nabla_m F_a)_{,n} - {}^{M^2}\Gamma^s{}_{nm}(\nabla_s F_a) - {}^{M^2}\Gamma^s{}_{nm}(\nabla_s F_a); \tag{3.292}$$

$$= \nabla_m \nabla_n F_a. \tag{3.293}$$

The angular part

$$F_{A|MN} = (F_{A|M})_{|N}; \tag{3.294}$$

$$= (F_{A|M})_{,N} - \Gamma^{\sigma}{}_{NA}(F_{\sigma|M}) - \Gamma^{\sigma}{}_{NM}(F_{A|\sigma}); \tag{3.295}$$

$$= (F_{A|M})_{,N} - \Gamma^{s}{}_{NA}(F_{s|M}) - \Gamma^{S}{}_{NA}(F_{S|M}) +$$
$$-\Gamma^{s}{}_{NM}(F_{A|s}) - \Gamma^{S}{}_{NM}(F_{A|S}); \tag{3.296}$$

$$= \left[(F_{A|M})_{,N} - \Gamma^{S}{}_{NM}(F_{A|S}) - \Gamma^{S}{}_{NA}(F_{S|M})\right] +$$
$$+\frac{1}{r}\rho^{s}g_{NM}\left(F_{A,s} - \frac{1}{r}\rho_{s}F_{A}\right) + \frac{1}{r}\rho^{s}g_{NA}\left(F_{s,M} - \frac{1}{r}\rho_{s}F_{M}\right), \tag{3.297}$$

quantity in brackets is the expanded covariant derivative of $F_{A|M}$ on $\mathcal{S}^2$ manifold,

$$F_{A|MN} = \nabla_{N}F_{A|M} +$$
$$+\frac{1}{r}g_{NM}\left(\rho^{s}F_{A,s} - \frac{f}{r}F_{A}\right) + \frac{1}{r}g_{NA}\left(\rho^{s}F_{s,M} - \frac{f}{r}F_{M}\right), \tag{3.298}$$

substituting (3.276)

$$F_{A|MN} = \nabla_{N}\nabla_{M}F_{A} + \frac{1}{r}\rho^{s}F_{s,N}g_{AM} +$$
$$+\frac{1}{r}g_{NM}\left(\rho^{s}F_{A,s} - \frac{f}{r}F_{A}\right) + \frac{1}{r}g_{NA}\left(\rho^{s}F_{s,M} - \frac{f}{r}F_{M}\right), \tag{3.299}$$

where $\nabla_{N}F_{s} = F_{s,N}$ because as far as $\mathcal{S}^2$ manifold is concerned, any $\mathcal{M}^2$ object is a scalar. After computing the remaining two terms, $F_{A|mn}$ and $F_{a|MN}$, in much the same manner one finds

$$F_{a|\nu}{}^{\nu} = \nabla_{m}\nabla^{m}F_{a} + \nabla_{M}\nabla^{M}F_{a} + \frac{2}{r}\rho^{m}\nabla_{m}F_{a} - \frac{2}{r}\rho_{a}\nabla^{M}F_{M} - \frac{2}{r^{2}}\rho_{a}\rho^{m}F_{m}; \tag{3.300}$$

$$F_{A|\nu}{}^{\nu} = \nabla_{m}\nabla^{m}F_{A} + \nabla_{M}\nabla^{M}F_{A} + \frac{2}{r}\rho^{m}F_{m,A} - \frac{1}{r^{2}}F_{A}. \tag{3.301}$$

3.7.4 Divergence of a Tensor

Consider a familiar expression

$$T_{\mu\nu|}{}^{\nu} = g^{\nu\sigma} T_{\mu\nu|\sigma}, \tag{3.302}$$

which is split into two cases for the free index μ

$$T_{m\nu|}{}^{\nu} = g^{\nu\sigma} T_{m\nu|\sigma}; \tag{3.303}$$

$$T_{M\nu|}{}^{\nu} = g^{\nu\sigma} T_{M\nu|\sigma}. \tag{3.304}$$

$$\tag{3.305}$$

The summations over ν and σ are further specialized to sub-manifolds

$$T_{m\nu|}{}^{\nu} = g^{ns} T_{mn|s} + g^{NS} T_{mN|S}; \tag{3.306}$$

$$T_{M\nu|}{}^{\nu} = g^{ns} T_{Mn|s} + g^{NS} T_{MN|S}. \tag{3.307}$$

Following the techniques described in the previous subsections, it is possible[10] to derive all of the following:

$$T_{ab|n} = \nabla_n T_{ab}; \tag{3.308}$$

$$T_{aB|n} = \nabla_n T_{aB} - \frac{1}{r} \rho_n T_{aB}; \tag{3.309}$$

$$T_{Ab|n} = \nabla_n T_{Ab} - \frac{1}{r} \rho_n T_{Ab}; \tag{3.310}$$

$$T_{AB|n} = \nabla_n T_{AB} - \frac{2}{r} \rho_n T_{AB}; \tag{3.311}$$

$$T_{ab|N} = \nabla_N T_{ab} - \frac{1}{r} \rho_a T_{Nb} - \frac{1}{r} \rho_b T_{aN}; \tag{3.312}$$

---

[10] After many pages.

$$T_{aB|N} = \nabla_N T_{aB} + \frac{1}{r}\rho^g g_{NB}T_{ag} - \frac{1}{r}\rho_a T_{NB}; \tag{3.313}$$

$$T_{Ab|N} = \nabla_N T_{Ab} + \frac{1}{r}\rho^g g_{NA}T_{gb} - \frac{1}{r}\rho_b T_{AN}; \tag{3.314}$$

$$T_{AB|N} = \nabla_N T_{AB} + \frac{1}{r}\rho^g g_{NA}T_{gB} + \frac{1}{r}\rho^g g_{NB}T_{Ag}. \tag{3.315}$$

Using some of those above, divergence of a tensor is expressed as

$$T_{m\nu|}{}^{\nu} = \nabla^N T_{mN} + \nabla^n T_{mn} + \frac{2}{r}\rho^n T_{mn} - \frac{1}{r}\rho_m g^{MN} T_{MN}; \tag{3.316}$$

$$T_{M\nu|}{}^{\nu} = \nabla^N T_{MN} + \nabla^n T_{Mn} + \frac{2}{r}\rho^n T_{Mn}. \tag{3.317}$$

Note that (3.317) is identical to (3.280), only difference is the free index M. (3.316) is not that dissimilar from (3.280) either.

3.7.5 D'Alembertian of a Tensor

Second Covariant Derivatives of a Tensor

Another, similarly lengthy derivation produces the following:

$$T_{ab|nm} = \nabla_m \nabla_n T_{ab}; \tag{3.318}$$

$$T_{aB|nm} = \left[\nabla_m \nabla_n + \frac{2}{r^2}\rho_m\rho_n - \frac{m}{r^3}g_{mn} - \frac{2}{r}\rho_{(n}\nabla_{m)}\right]T_{aB}; \tag{3.319}$$

$$T_{AB|nm} = \left[\nabla_m \nabla_n + \frac{6}{r^2}\rho_m\rho_n - \frac{2m}{r^3}g_{mn} - \frac{4}{r}\rho_{(m}\nabla_{n)}\right]T_{AB}; \tag{3.320}$$

$$T_{ab|Nm} = \nabla_n \nabla_N T_{ab} - \frac{1}{r}\rho_m \nabla_N T_{ab} - \left[\frac{m}{r^3}g_{am} + \frac{1}{r}\rho_a\nabla_m - \frac{2}{r^2}\rho_a\rho_m\right]T_{Nb}$$
$$- \left[\frac{m}{r^3}g_{bm} + \frac{1}{r}\rho_b\nabla_m - \frac{2}{r^2}\rho_b\rho_m\right]T_{aN}; \tag{3.321}$$

$$T_{aB|Nm} = \nabla_m \nabla_N T_{aB} - \frac{2}{r}\rho_m \nabla_N T_{aB} + \frac{m}{r}\Omega_{NB}T_{am} + r\rho^g\Omega_{NB}\nabla_m T_{ag}$$
$$- \rho_m\rho^g\Omega_{NB}T_{ag} - \frac{m}{r^3}g_{ma}T_{NB} + \frac{3}{r^2}\rho_m\rho_a T_{NB} - \frac{1}{r}\rho_a\nabla_m T_{NB}; \tag{3.322}$$

$$T_{AB|Nm} = \nabla_m \nabla_N T_{AB} - \frac{3}{r}\rho_m \nabla_N T_{AB} + \frac{m}{r}\Omega_{NA}T_{mB} + r\rho^g\Omega_{NA}\nabla_m T_{gB}$$

$$-2\rho_m\rho^g\Omega_{NA}T_{gB} + \frac{m}{r}\Omega_{NB}T_{Am} + r\rho^g\Omega_{NB}\nabla_m T_{Ag}$$

$$-2\rho_m\rho^g\Omega_{NB}T_{Ag}; \tag{3.323}$$

$$
\begin{aligned}
T_{ab|nM} =\ & \nabla_M\nabla_n T_{ab} - \frac{1}{r}\rho_a\nabla_n T_{Mb} - \frac{1}{r}\rho_b\nabla_n T_{aM} - \frac{1}{r}\rho_n\nabla_M T_{ab} \\
& + \frac{2}{r^2}\rho_n\rho_a T_{Mb} + \frac{2}{r^2}\rho_b\rho_n T_{aM};
\end{aligned}
\tag{3.324}
$$

$$
\begin{aligned}
T_{aB|nM} =\ & \nabla_M\nabla_n T_{aB} - \frac{1}{r}\rho_a\nabla_n T_{MB} + r\rho^g\Omega_{MB}\nabla_n T_{ag} - \frac{2}{r}\rho_n\nabla_M T_{aB} \\
& - \rho_n\rho^g\Omega_{MB}T_{ag} + \frac{3}{r^2}\rho_n\rho_a T_{MB};
\end{aligned}
\tag{3.325}
$$

$$
\begin{aligned}
T_{AB|nM} =\ & \nabla_M\nabla_n T_{AB} + r\rho^g\Omega_{MA}\nabla_n T_{gB} + r\rho^g\Omega_{MB}\nabla_n T_{Ag} - \frac{3}{r}\rho_n\nabla_M T_{AB} \\
& - 2\rho^g\rho_n\Omega_{MA}T_{gB} - 2\rho^g\rho_n\Omega_{MB}T_{Ag};
\end{aligned}
\tag{3.326}
$$

$$
\begin{aligned}
T_{ab|NM} =\ & \nabla_M\nabla_N T_{ab} - \frac{1}{r}\rho_a\nabla_M T_{Nb} - \frac{1}{r}\rho_b\nabla_M T_{aN} - \frac{1}{r}\rho_a\nabla_N T_{Mb} \\
& - \rho_a\rho^g\Omega_{NM}T_{gb} - \frac{1}{r}\rho_b\nabla_N T_{aM} - \rho_b\rho^g\Omega_{NM}T_{ag} + \frac{2}{r^2}\rho_b\rho_a T_{MN} \\
& + r\rho^g\Omega_{MN}\nabla_g T_{ab};
\end{aligned}
\tag{3.327}
$$

$$
\begin{aligned}
T_{aB|NM} =\ & \nabla_M\nabla_N T_{aB} - \frac{1}{r}\rho_a\nabla_N T_{MB} + r\rho^g\Omega_{MB}\nabla_N T_{ag} + r\rho^g\Omega_{NB}\nabla_M T_{ag} \\
& - \rho_a\rho^g\Omega_{NB}T_{Mg} - f\Omega_{MB}T_{aN} - \frac{1}{r}\rho_a\nabla_M T_{BN} - \rho_a\rho^g\Omega_{NM}T_{gB} \\
& - \rho_a\rho^g\Omega_{MB}T_{Ng} + r\rho^g\Omega_{MN}\nabla_g T_{aB} - f\Omega_{MN}T_{aB};
\end{aligned}
\tag{3.328}
$$

$$
\begin{aligned}
T_{AB|NM} =\ & \nabla_M\nabla_N T_{AB} + r\rho^g\Omega_{NA}\nabla_M T_{gB} + r\rho^g\Omega_{NB}\nabla_M T_{Ag} + r\rho^g\Omega_{MA}\nabla_N T_{gB} \\
& + r^2\rho^c\rho^g\Omega_{MA}\Omega_{NB}T_{gc} - f\Omega_{MA}T_{NB} + r\rho^g\Omega_{MB}\nabla_N T_{Ag} \\
& + r^2\rho^g\rho^c\Omega_{MB}\Omega_{NA}T_{cg} - f\Omega_{MB}T_{AN} + r\rho^g\Omega_{MN}\nabla_g T_{AB} \\
& - 2f\Omega_{MN}T_{AB}.
\end{aligned}
\tag{3.329}
$$

Contracted Second Covariant Derivatives of a Tensor

$$g^{mn}T_{ab|nm} = \nabla_m\nabla^m T_{ab}; \tag{3.330}$$

$$g^{mn}T_{aB|nm} = \left[\nabla_m\nabla^m + \frac{2}{r^2}\left(1 - \frac{3m}{r}\right) - \frac{2}{r}\rho^m\nabla_m\right]T_{aB}; \tag{3.331}$$

$$g^{mn}T_{AB|nm} = \left[\nabla_m \nabla^m + \frac{2}{r^2}\left(3 - \frac{8m}{r}\right) - \frac{4}{r}\rho^m \nabla_m \right] T_{AB}; \tag{3.332}$$

$$g^{NM}T_{ab|NM} = \nabla^N \nabla_N T_{ab} - \frac{2}{r}\left(\rho_a \nabla^N T_{Nb} + \rho_b \nabla^N T_{Na}\right)$$
$$- \frac{2}{r^2}\left(\rho_a \rho^g T_{gb} + \rho_b \rho^g T_{ag}\right) + \frac{2}{r^2}\rho_b \rho_a g^{NM} T_{MN}$$
$$+ \frac{2}{r}\rho^g \nabla_g T_{ab}; \tag{3.333}$$

$$g^{NM}T_{aB|NM} = \nabla^N \nabla_N T_{aB} - \frac{2}{r}\rho_a \nabla^N T_{NB} + \frac{2}{r}\rho^g \nabla_B T_{ag} - \frac{4}{r^2}\rho_a \rho^g T_{gB}$$
$$+ \frac{2}{r}\rho^g \nabla_g T_{aB} - \frac{3f}{r^2}T_{aB}; \tag{3.334}$$

$$g^{NM}T_{AB|NM} = \nabla^N \nabla_N T_{AB} + \frac{2}{r}\rho^g \nabla_A T_{gB} + \frac{2}{r}\rho^g \nabla_B T_{Ag} + 2\rho^c \rho^g \Omega_{AB} T_{gc}$$
$$- \frac{6f}{r^2}T_{AB} + \frac{2}{r}\rho^g \nabla_g T_{AB} \tag{3.335}$$

D'Alembertian of a Tensor

$$T_{\mu\nu|\alpha}{}^{\alpha} = g^{ab}T_{\mu\nu|ab} + g^{aB}T_{\mu\nu|aB} + g^{Ab}T_{\mu\nu|Ab} + g^{AB}T_{\mu\nu|AB}, \tag{3.336}$$

$$= g^{ab}T_{\mu\nu|ab} + g^{AB}T_{\mu\nu|AB}, \tag{3.337}$$

$$= g^{ab}T_{\mu\nu|ab} + \frac{1}{r^2}\Omega^{AB}T_{\mu\nu|AB}. \tag{3.338}$$

which expands into three cases

$$\mu\nu = ab, aB, AB. \tag{3.339}$$

Using (3.330) - (3.335) it can be shown

$$T_{ab|\mu}{}^{\mu} = \nabla_m \nabla^m T_{ab} + \nabla_N \nabla^N T_{ab}$$
$$- \frac{2}{r}\left(\rho_a \nabla^N T_{Nb} + \rho_b \nabla^N T_{Na}\right) - \frac{2}{r^2}\rho^g \left(\rho_a T_{gb} + \rho_b T_{ag}\right)$$
$$+ \frac{2}{r^2}\rho_b \rho_a g^{NM} T_{MN} + \frac{2}{r}\rho^g \nabla_g T_{ab}; \tag{3.340}$$

$$T_{aB|\mu}{}^{\mu} = \nabla_m \nabla^m T_{aB} + \nabla^N \nabla_N T_{aB} - \frac{1}{r^2} T_{aB} - \frac{2}{r} \rho_a \nabla^N T_{NB}$$

$$+ \frac{2}{r} \rho^g \nabla_B T_{ag} - \frac{4}{r^2} \rho_a \rho^g T_{gB}; \tag{3.341}$$

$$T_{AB|\mu}{}^{\mu} = \nabla_m \nabla^m T_{AB} + \nabla^N \nabla_N T_{AB} - \left[\frac{4m}{r^3} + \frac{2}{r} \rho^m \nabla_m \right] T_{AB}$$

$$+ \frac{2}{r} \rho^g \nabla_A T_{gB} + \frac{2}{r} \rho^g \nabla_B T_{Ag} + 2\rho^c \rho^g \Omega_{AB} T_{gc}. \tag{3.342}$$

3.7.6 The Riemann Tensor

After writing the Riemann in terms of Christoffel symbols (connection coefficients) it takes a few pages to discover its simplified form

$$R_{abcd} = \frac{2m}{r^3} \left(g_{ac} g_{bd} - g_{ad} g_{bc} \right); \tag{3.343}$$

$$R_{AbCd} = -R_{AbdC} = -R_{bACd} = R_{bAdC} = -\frac{m}{r^3} g_{AC} g_{bd}; \tag{3.344}$$

$$R_{ABCD} = \frac{2m}{r^3} \left(g_{AC} g_{DB} - g_{AD} g_{BC} \right), \tag{3.345}$$

all other components vanish.

3.8 Sample Application

A simple case of a scalar perturbation on Schwarzschild background is investigated as an example. Corresponding wave equation is given by

$$\Psi_{|\nu}{}^{\nu} = \Psi_{,\nu}{}^{|\nu} = 0, \tag{3.346}$$

where Ψ is some scalar function. To proceed, the wavefunction Ψ is decomposed using scalar spherical harmonics

$$\Psi = \psi\, Y^{lm}; \tag{3.347}$$

$$\Psi_{,v} = \left(\psi\, Y^{lm}\right)_{,v}, \tag{3.348}$$

$$\tag{3.349}$$

where all angular dependence is carried by Y^{lm}. According to (3.280), divergence of a vector, or a D'Alembertian of a scalar is given by

$$
\begin{aligned}
\Psi_{|v}{}^{v} &= \nabla^a \left(\psi\, Y\right)_{,a} + \nabla^A \left(\psi\, Y\right)_{,A} + \frac{2}{r}\rho^a \left(\psi\, Y\right)_{,a}, & (3.350)\\
&= \nabla^a \nabla_a \left(\psi\, Y\right) + \nabla^A \nabla_A \left(\psi\, Y\right) + \frac{2}{r}\rho^a \nabla_a \left(\psi\, Y\right), & (3.351)
\end{aligned}
$$

because all angular dependence is retained by Y^{lm}, it slips past the spatial-temporal derivatives, and vice-versa for ψ,

$$\Psi_{|v}{}^{v} = Y\nabla^a\nabla_a\psi + \psi\nabla^A\nabla_A Y + Y\frac{2}{r}\rho^a\nabla_a\psi, \tag{3.352}$$

recall the action of the harmonic operator on Y^{lm} (3.144)

$$\Psi_{|v}{}^{v} = Y^{lm}\left[\nabla^a\nabla_a\psi - \frac{l(l+1)}{r^2}\psi + \frac{2}{r}\rho^a\nabla_a\psi\right] = 0, \tag{3.353}$$

which after some algebra can be expressed as

$$\Psi_{|v}{}^{v} = \frac{1}{r}Y^{lm}\left[\nabla^a\nabla_a\varphi - \left(\frac{l(l+1)}{r^2} + \frac{2m}{r^3}\right)\varphi\right] = 0, \tag{3.354}$$

where $\varphi = r\psi$, or simply

$$\nabla^a\nabla_a\varphi - \left[\frac{l(l+1)}{r^2} + \frac{2m}{r^3}\right]\varphi = 0. \tag{3.355}$$

(3.355) is an $\mathcal{M}^2$-covariant scalar wave equation on Schwarzschild background; even so, one can undoubtedly recognize the Regge-Wheeler-like [38] scalar potential.

3.8.1 Specialization to Schwarzschild coordinates

In Schwarzschild coordinates, D'Alembertian becomes

$$\nabla^c \nabla_c \varphi \quad = \quad \frac{1}{\sqrt{-g}} \partial_c \left(\sqrt{-g} g^{bc} \partial_b \varphi \right), \tag{3.356}$$

$$= \quad -\frac{1}{f} \partial_t^2 \varphi + \partial_r \left(f \partial_r \varphi \right). \tag{3.357}$$

Recall the tortoise coordinate

$$\frac{dr}{dr_*} = f, \tag{3.358}$$

in terms of the tortoise coordinate, (3.357) is given by

$$\nabla^c \nabla_c \varphi = \frac{1}{f} \left(-\partial_t^2 + \partial_{r_*}^2 \right) \varphi, \tag{3.359}$$

$\Rightarrow$

$$\left(-\partial_t^2 + \partial_{r_*}^2 \right) \varphi - f \left(\frac{l(l+1)}{r^2} + \frac{2m}{r^3} \right) \varphi = 0, \tag{3.360}$$

which is the Regge-Wheeler scattering equation for a scalar wave on Schwarzschild background.

3.9   Conclusion

While this chapter does not represent novel work, because the technique is relatively new, relations of the $\mathcal{M}^2 \times \mathcal{S}^2$ methodology are not tabulated in literature or publications. In other words: an idea can be easily acquired, implementing it becomes the

sole responsibility of the researcher. This chapter shall serve as the $\mathcal{M}^2 \times \mathcal{S}^2$ encyclopedia for the remainder of the thesis.

Chapter 4

Electromagnetic Waves on Schwarzschild Background

4.1 Introduction

Having developed a strong footing in scalar perturbations, next on the difficulty scale are perturbations of vectors fields. This chapter employs the $\mathcal{M}^2 \times \mathcal{S}^2$ manifold splitting technique to study the scattering of electromagnetic radiation on Schwarzschild background. Such scattering has been studied in the past however, this study offers a novel method of approaching the calculations.

4.2 The Field Equations

Electromagnetic field conforms to the differential equations given by[29]

$$A_{\alpha|\mu}{}^{\mu} - A^{\mu}{}_{|\mu\alpha} - R_{\alpha\mu}A^{\mu} = -4\pi J_{\alpha}. \qquad (4.1)$$

where A_{μ} is the electromagnetic 4-vector potential[20].

4.2.1 Field Equations in Vacuum

Ricci Tensor is zero on Schwarzschild background[1] (5.8),

$$A_{\alpha|\mu}{}^{\mu} - A^{\mu}{}_{|\mu\alpha} = -4\pi J_{\alpha}. \tag{4.2}$$

(4.2) is the compact form of the most general electromagnetic field equations on Schwarzschild background. Vacuum usually implies lack of current J_{α} but, for generality's sake J_{α} is not set to zero just yet.

4.2.2 The Lorenz Gauge

(4.4) can be simplified further upon application of the gauge attributed to L. Lorenz[22]

$$A^{\mu}{}_{|\mu} = 0, \tag{4.3}$$

therefore

$$A_{\alpha|\mu}{}^{\mu} = -4\pi J_{\alpha}. \tag{4.4}$$

4.3 $\mathcal{M}^2 \times \mathcal{S}^2$ Decomposition of the System

4.3.1 Decomposition of the Wave Equation

(4.4) is to be split: one equation on $\mathcal{M}^2$ manifold, and one on $\mathcal{S}^2$ manifold

$$A_{b|\mu}{}^{\mu} = -4\pi J_b; \tag{4.5}$$

$$A_{B|\mu}{}^{\mu} = -4\pi J_B. \tag{4.6}$$

---

[1]All Schwarzschild spaces are vacua but, not all vacua are Schwarzschild spaces.

Using (3.300) and (3.301) one obtains

$$- 4\pi J_b \;=\; \nabla_m \nabla^m A_b + \nabla_M \nabla^M A_b + \frac{2}{r} \rho^m \nabla_m A_b - \frac{2}{r} \rho_b \nabla^M A_M - \frac{2}{r^2} \rho_b \rho^m A_m; \qquad (4.7)$$

$$-4\pi J_B \;=\; \nabla_m \nabla^m A_B + \nabla_M \nabla^M A_B + \frac{2}{r} \rho^m \nabla_B A_m - \frac{1}{r^2} A_B. \qquad (4.8)$$

4.3.2 Decomposition of the Wave

Electromagnetic vector potential is written in terms of $\mathcal{M}^2$ basis vectors

$$A_b = (a_0 \tau_b + a_1 \rho_b)\, Y, \qquad (4.9)$$

where the scalar spherical harmonic Y is present because A_b is not only decomposed for $\mathcal{M}^2$ manifold, but also for $\mathcal{S}^2$. Recall that from $\mathcal{S}^2$ stand-point, any object on $\mathcal{M}^2$ is a scalar (and vice-versa), thus a scalar spherical harmonic is used to carry all angular dependence. Same for the current vector J

$$J_b = (j_0 \tau_b + j_1 \rho_b)\, Y. \qquad (4.10)$$

Angular components get a slightly different treatment

$$A_B \;=\; a_2 Y_B + a_3 X_B; \qquad (4.11)$$

$$J_B \;=\; j_2 Y_B + j_3 X_B, \qquad (4.12)$$

where a_μ and j_μ are functions of the spatial-temporal coordinates, allowing the Scalar and vector spherical harmonics to retain all of the angular dependence. With aid from (4.9) - (4.12), (3.45), (3.48), (3.54), (3.55), (3.142), (3.143), (3.166), (3.169), (3.176),

and (3.177), (4.8) becomes

$$Y_B\nabla_m\nabla^m a_2 + X_B\nabla_m\nabla^m a_3 - \frac{l(l+1)}{r^2}a_2 Y_B - \frac{l(l+1)}{r^2}a_3 X_B + \frac{2}{r}fa_1 Y_B = -4\pi\left(j_2 Y_B + j_3 X_B\right), \quad (4.13)$$

One may notice that no term is *not* multiplied by Y_B or X_B. Collecting like terms and dividing out the vector spherical harmonics[2] yields the first two field equations

$$-4\pi j_2 = \nabla_m\nabla^m a_2 - \frac{l(l+1)}{r^2}a_2 + \frac{2}{r}fa_1; \qquad (4.14)$$

$$-4\pi j_3 = \nabla_m\nabla^m a_3 - \frac{l(l+1)}{r^2}a_3. \qquad (4.15)$$

Following a similar derivation for (4.8) yields

$$-4\pi\left(j_0\tau_b + j_1\rho_b\right) =$$

$$\tau_b\nabla_m\nabla^m a_0 + \rho_b\nabla_m\nabla^m a_1 + \frac{2}{r}\left(\frac{m}{r}\epsilon^m{}_b + \tau_b\rho^m\right)\nabla_m a_0 + \frac{2}{r}\left(\frac{m}{r}g^m{}_b + \rho_b\rho^m\right)\nabla_m a_1 +$$

$$-\tau_b\frac{l(l+1)}{r^2}a_0 - \rho_b\frac{1}{r^2}\left[2f + l(l+1)\right]a_1 + \rho_b\frac{2l(l+1)}{r^3}a_2. \qquad (4.16)$$

Although not as explicit as the angular case, every term in (4.16) is either along (multiplied by) ρ_b or τ_b. An unambiguous method to discern ρ_b and τ_b components is to contract/project/multiply left and right sides of (4.16) on/by ρ^b and τ^b: (3.14), (3.18), (3.19). Projecting (4.16) on τ^b

$$-4\pi j_0 = \nabla_m\nabla^m a_0 + \frac{2}{rf}\left(1 - \frac{m}{r}\right)\rho^m\nabla_m a_0 - \frac{2m}{r^2 f}\tau^m\nabla_m a_1 - \frac{l(l+1)}{r^2}a_0. \qquad (4.17)$$

---

[2]"Dividing out" is a loose term for that fact Y_B and X_B are linearly independent, which means that expression $\xi Y_B + \zeta X_B = 0$ can only be true in general *iff* $\xi = \zeta = 0$.

Projecting (4.16) on ρ^b

$$-4\pi j_1 = \nabla_m \nabla^m a_1 + \frac{2}{rf}\left(1 - \frac{m}{r}\right)\rho^m \nabla_m a_1 - \frac{2m}{r^2 f}\tau^m \nabla_m a_0 +$$
$$-\frac{1}{r^2}\left[2f + l(l+1)\right] a_1 + 2\frac{l(l+1)}{r^3}a_2. \tag{4.18}$$

In summary, the four field equations of the electromagnetic perturbations (waves) on Schwarzschild background in Lorenz gauge are

$$-4\pi j_0 = \nabla_m \nabla^m a_0 + \frac{2}{rf}\left(1 - \frac{m}{r}\right)\rho^m \nabla_m a_0 - \frac{2m}{r^2 f}\tau^m \nabla_m a_1 - \frac{l(l+1)}{r^2}a_0; \tag{4.19}$$

$$-4\pi j_1 = \nabla_m \nabla^m a_1 + \frac{2}{rf}\left(1 - \frac{m}{r}\right)\rho^m \nabla_m a_1 - \frac{2m}{r^2 f}\tau^m \nabla_m a_0 +$$
$$-\frac{1}{r^2}\left[2f + l(l+1)\right] a_1 + 2\frac{l(l+1)}{r^3}a_2; \tag{4.20}$$

$$-4\pi j_2 = \nabla_m \nabla^m a_2 - \frac{l(l+1)}{r^2}a_2 + \frac{2}{r}fa_1; \tag{4.21}$$

$$-4\pi j_3 = \nabla_m \nabla^m a_3 - \frac{l(l+1)}{r^2}a_3, \tag{4.22}$$

with a_μ and j_μ given by (4.9) - (4.12)

4.3.3 Specialization to Schwarzschild Coordinates

In Schwarzschild (t, r) coordinates, ρ_a and τ_a are given by (3.12) and (3.21)

$$\tau^0 = \rho_1 = 1; \tag{4.23}$$

$$\tau_0 = -\rho^1 = -f; \tag{4.24}$$

$$\tau^1 = \tau_1 = 0; \tag{4.25}$$

$$\rho^0 = \rho_0 = 0. \tag{4.26}$$

Also, when acting on a scalar

$$\tau^b \nabla_b = \partial_t; \tag{4.27}$$

$$\rho^b \nabla_b = \partial_{r_*}, \tag{4.28}$$

where r_* is the tortoise coordinate. From (3.359) is it known that the D'Alembertian is given by

$$\nabla^c \nabla_c = \frac{1}{f}\left(-\partial_t^2 + \partial_{r_*}^2\right). \tag{4.29}$$

Rewriting (4.19) - (4.22) in Schwarzschild coordinates

$$-4\pi f j_0 = \left(-\partial_t^2 + \partial_{r_*}^2\right)a_0 + \frac{2}{r}\left(1 - \frac{m}{r}\right)\partial_{r_*}a_0 - \frac{2m}{r^2}\partial_t a_1 - f\frac{l(l+1)}{r^2}a_0; \tag{4.30}$$

$$-4\pi f j_1 = \left(-\partial_t^2 + \partial_{r_*}^2\right)a_1 + \frac{2}{r}\left(1 - \frac{m}{r}\right)\partial_{r_*}a_1 - \frac{2m}{r^2}\partial_t a_0 + $$
$$-\frac{f}{r^2}\left[2f + l(l+1)\right]a_1 + 2f\frac{l(l+1)}{r^3}a_2; \tag{4.31}$$

$$-4\pi f j_2 = \left(-\partial_t^2 + \partial_{r_*}^2\right)a_2 - f\frac{l(l+1)}{r^2}a_2 + \frac{2}{r}f^2 a_1; \tag{4.32}$$

$$-4\pi f j_3 = \left(-\partial_t^2 + \partial_{r_*}^2\right)a_3 - f\frac{l(l+1)}{r^2}a_3, \tag{4.33}$$

with the 4-vector potential and current given by

$$A_t = a_0 Y; \tag{4.34}$$

$$A_r = a_1 Y; \tag{4.35}$$

$$J_t = j_0 Y; \tag{4.36}$$

$$J_r = j_1 Y. \tag{4.37}$$

Angular components are unchanged (4.11), (4.12). One may note that (4.33) is a Regge-Wheeler [38] (*odd* parity) field equation for a vector (spin 1) wave. Remaining equations represent the so-called *even* parity field.

4.3.4 Specialization to Frequency Domain

In instances when it is necessary to study monochromatic waves, it stands a reason to write equations (4.30) - (4.33) in frequency domain via a Fourier transformation

$$a_\mu(t, r) = a_\mu(r)e^{-i\omega t}. \tag{4.38}$$

Substituting (4.38) into (4.30) - (4.33) reduces them to linear, second order, coupled differential equations

$$-4\pi f j_0 = \left(\omega^2 + \partial_{r_*}^2\right) a_0 + \frac{2}{r}\left(1 - \frac{m}{r}\right)\partial_{r_*} a_0 + i\frac{2m\omega}{r^2} a_1 - f\frac{l(l+1)}{r^2} a_0; \tag{4.39}$$

$$-4\pi f j_1 = \left(\omega^2 + \partial_{r_*}^2\right) a_1 + \frac{2}{r}\left(1 - \frac{m}{r}\right)\partial_{r_*} a_1 + i\frac{2m\omega}{r^2} a_0 +$$

$$-\frac{f}{r^2}\left[2f + l(l+1)\right] a_1 + 2f\frac{l(l+1)}{r^3} a_2; \tag{4.40}$$

$$-4\pi f j_2 = \left(\omega^2 + \partial_{r_*}^2\right) a_2 - f\frac{l(l+1)}{r^2} a_2 + \frac{2}{r}f^2 a_1; \tag{4.41}$$

$$-4\pi f j_3 = \left(\omega^2 + \partial_{r_*}^2\right) a_3 - f\frac{l(l+1)}{r^2} a_3. \tag{4.42}$$

4.4 Scattering

In this section reflection from, and transmission through, Schwarzschild background is investigated. The goal is to produce a reflection vs. frequency plot for the electromagnetic waves on Schwarzschild background. To that end, source terms j_μ are set to zero.

4.4.1 Reflection and Transmission

The notions of reflection and transmission are typically reserved for waves crossing a medium boundary. In the case of Schwarzschild black hole, the only conceivable

boundary is the event horizon ($r = 2m$), from which a wave cannot reflect for it will forever disappear into the black hole. However, a *hard* boundary is not a requirement for reflection. The phrase *scattering off the curvature* is sometimes used to describe the phenomenon of gradual reflection from smeared interfaces. While such scattering remains largely intractable analytically, it is quite straight-forward to solve numerically. Consider a flat-space, 1D wave equation

$$\partial_t^2 \varphi - \partial_x^2 \varphi = 0, \tag{4.43}$$

converted to frequency domain

$$\partial_x^2 \varphi + \omega^2 \varphi = 0, \tag{4.44}$$

solutions to which are simple waves

$$\varphi = e^{\pm i\omega x}, \tag{4.45}$$

and/or linear combinations thereof. Such waves travel unperturbed through all space and are of little interest. For a wave to reflect, a barrier, either *soft* or *hard*, has to be introduced; such barrier is typically referred to as the *potential*

$$\partial_x^2 \varphi + \left[\omega^2 - V(x)\right]\varphi = 0, \tag{4.46}$$

where $V(x)$ is the potential, consider Figure (4.1). Where the derivative of the potential $V(x)$ is close to zero[3], the waves behave like simple sinusoids (4.45) and can therefore be approximately separated into incoming, reflecting, and transmitting. In

---

[3]Which would imply that $V(x)$ is a constant and as such only modifies the effective frequency of the oscillation: $\omega^2 \rightarrow \omega^2 - V$.
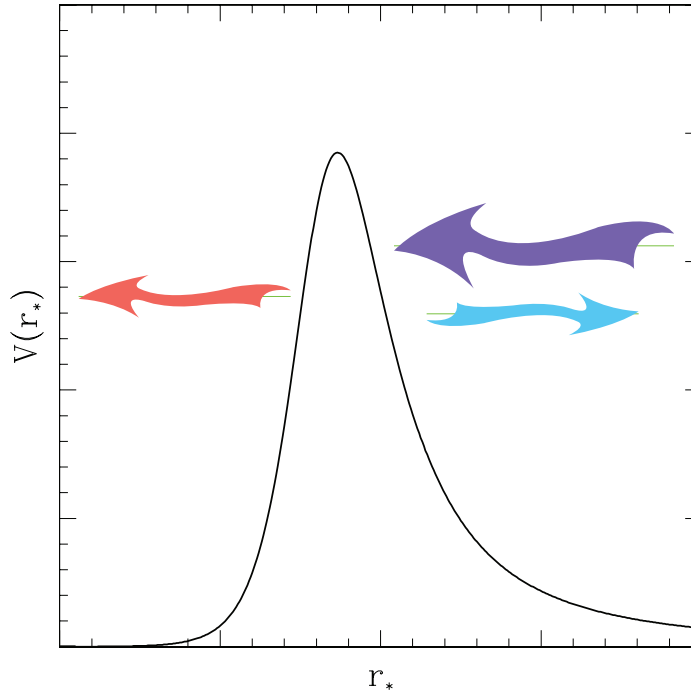
Figure 4.1: A wave approaching from the right partially transmits through the barrier and partially reflects from it.

the regions where $V(x)$ varies, the separation of waves is ambiguous.

Computing Reflection/Transmission

One way to compute the reflection/transmission is to start with a left-traveling (transmitted) wave far on the left

$$\varphi(-\infty \leftarrow x) \rightarrow e^{-i\omega x}, \tag{4.47}$$

and integrate the equation forward until $V'(x)$ approaches zero on the *other side* of the potential barrier. At that point, due to unique initial condition of a single transmitted wave, a superposition of the incoming and the reflected waves emerges

$$\varphi(x \rightarrow \infty) \rightarrow \mathcal{I}e^{-i\omega x} + \mathcal{R}e^{i\omega x}, \tag{4.48}$$

where $\mathcal{I}$ and $\mathcal{R}$ are the incident and reflected amplitudes. Reflection is then given by

$$R = \left|\frac{\mathcal{R}}{\mathcal{I}}\right|^2, \tag{4.49}$$

because the reflected power is the square of the amplitude; the transmission is then

$$T = \left|\frac{1}{\mathcal{I}}\right|^2, \tag{4.50}$$

unity in the numerator is due to [arbitrary] unit amplitude of the transmitted wave (4.47).

Wave Separation

Looking at (4.48) one may wonder how to extract $\mathcal{I}$ and $\mathcal{R}$ from φ: because the two waves are superimposed, only their sum is known. After some algebraic gymnastics, the obvious solution is elucidated

$$\frac{1}{2}\left(\varphi_\infty + \frac{1}{i\omega}\varphi'_\infty\right) = \mathcal{R}e^{i\omega x}; \tag{4.51}$$

$$\frac{1}{2}\left(\varphi_\infty - \frac{1}{i\omega}\varphi'_\infty\right) = \mathcal{I}e^{-i\omega x}, \tag{4.52}$$

where shorthand $\varphi_\infty \equiv \varphi(x \to \infty)$ is adopted.

4.4.2 Stress-Energy Tensor

Method for computing the radiant reflection, *i.e.* the energy, outlined in (4.4.1) is only partly applicable because it deals with one field, whereas the electromagnetic field comprise four field functions. One is still able to separate the left- and right-moving parts of a_λ but, $|a_\lambda|^2$ has no physical meaning in E&M case.

The electromagnetic stress-energy tensor is the equivalent of the $|\varphi|^2$ from (4.4.1).

More specifically, the *tr* component is the energy flux. As such, the reflection and transmission will have the form

$$R = \frac{T_{\rightarrow}^{tr}}{T_{\leftarrow}^{tr}};$$

(4.53)

$$T = \frac{T_{\twoheadleftarrow}^{tr}}{T_{\leftarrow}^{tr}},$$

(4.54)

where the arrows illustrate the direction of the flow: $\leftarrow$ incident, $\rightarrow$ reflected, $\twoheadleftarrow$ transmitted. Electromagnetic stress-energy tensor is given by [29]

$$T^{\alpha\beta} = \frac{1}{4\pi}\left(g^{\alpha\mu}F_{\mu\lambda}F^{\beta\lambda} - \frac{1}{4}g^{\alpha\beta}F_{\mu\nu}F^{\mu\nu}\right).$$

(4.55)

In Schwarzschild coordinates, the *tr* component is

$$T^{tr} = -\frac{1}{4\pi}\frac{1}{f}F_{t\lambda}F^{\lambda r}.$$

(4.56)

Field strength tensor $F^{\mu\nu}$ is given by[20]

$$F^{\mu\nu} = \partial^\mu A^\nu - \partial^\nu A^\mu.$$

(4.57)

Inserting (4.9), (4.11), and (4.57) into (4.56) yields

$$T^{tr} = \frac{1}{4\pi r^2}\left(\epsilon X_A X^A + \kappa Y_A Y^A + \delta X_A Y^A\right),$$

(4.58)

where

$$\epsilon = -i\omega a_3 \partial_r a_3;$$

(4.59)

$$\kappa = (a_0 f - i\omega a_2)(\partial_r a_2 - a_1);$$

(4.60)

$$\delta = (a_0 f - i\omega a_2)\partial_r a_3 - i\omega a_3(\partial_r a_2 - a_1).$$

(4.61)

(4.58) is still a function of θ and ϕ, it is an energy flux: energy per unit time per unit area. An integral (3.156) over the surface of a sphere[4] of radius r is carried out to compute the total power at r,

$$P = \frac{l(l+1)}{4\pi}\left[(a_0 f - i\omega a_2)(\partial_r a_2 - a_1) - i\omega a_3 \partial_r a_3\right]. \tag{4.62}$$

Just like the field equations, the energy flux separates into two orthogonal (independent) parts

$$P_{even} = \frac{1}{4\pi}l(l+1)\left[(a_0 f - i\omega a_2)(\partial_r a_2 - a_1)\right]; \tag{4.63}$$

$$P_{odd} = \frac{1}{4\pi}l(l+1)\left[-i\omega a_3 \partial_r a_3\right]; \tag{4.64}$$

$$P = P_{even} + P_{odd}, \tag{4.65}$$

converting to tortoise coordinate and taking the modulus[5]

$$P_{even} = \frac{1}{4\pi}l(l+1)\left|(a_0 f - i\omega a_2)\left(f^{-1}a_2' - a_1\right)\right|; \tag{4.66}$$

$$P_{odd} = \frac{1}{4\pi}l(l+1)\left|f^{-1}\omega a_3 a_3'\right|; \tag{4.67}$$

$$P = P_{even} + P_{odd}, \tag{4.68}$$

where prime indicates a derivative with respect to the tortoise coordinate. Note,

$$R = \frac{P^{\rightarrow}}{P^{\leftarrow}} = \frac{P_{even}^{\rightarrow}}{P_{even}^{\leftarrow}} = \frac{P_{odd}^{\rightarrow}}{P_{odd}^{\leftarrow}}, \tag{4.69}$$

---

[4] $r^2 \sin\theta dr d\theta d\phi$

[5] While mathematically (4.62) is valid, imaginary components of power are ordinarily not tolerated.

where the arrows indicate the direction of the energy flow, more precisely

$$\vec{P}_{odd} = \frac{1}{4\pi} l(l+1) \left| f^{-1} \omega \vec{a_3} \vec{a'_3} \right|, \tag{4.70}$$

in which a_3 was separated into incoming and reflecting waves as in (4.51) and (4.52); same for P_{even}.

4.4.3 Initial/Boundary Conditions

Boundary conditions are simplest close to event horizon because, in r_* coordinate, f, the quantity that appears in the field equations (4.39) - (4.42) so often, decays exponentially to zero[6] for relatively small negative values of r_*. Taking the $r_* \to -\infty$ limit yields the following:

$$f(-\infty \leftarrow r_*) \quad \to \quad 0; \tag{4.71}$$

$$r(-\infty \leftarrow r_*) \quad \to \quad 2m, \tag{4.72}$$

substituting these limits into the field equations reveals the field behavior close to the event horizon

$$0 = \left(\omega^2 + \partial^2_{r_*}\right) a_0 + \frac{1}{2m} i\omega a_1 + \frac{1}{2m} \partial_{r_*} a_0; \tag{4.73}$$

$$0 = \left(\omega^2 + \partial^2_{r_*}\right) a_1 + \frac{1}{2m} i\omega a_0 + \frac{1}{2m} \partial_{r_*} a_1; \tag{4.74}$$

$$0 = \left(\omega^2 + \partial^2_{r_*}\right) a_2; \tag{4.75}$$

$$0 = \left(\omega^2 + \partial^2_{r_*}\right) a_3. \tag{4.76}$$

---

[6]r also exponentially decays to/approaches $2m$, which is the reason f decays to zero.

Just as in (4.4.1), a_2 and a_3 are obviously pure left-going (toward the horizon) waves with [arbitrary] unit amplitude

$$a_{2,3}(-\infty \leftarrow r_*) \rightarrow e^{-i\omega r_*}. \tag{4.77}$$

Assuming down-going waves for a_0 and a_1

$$a_0(-\infty \leftarrow r_*) \quad \rightarrow \quad Ae^{-i\omega r_*}; \tag{4.78}$$

$$a_1(-\infty \leftarrow r_*) \quad \rightarrow \quad Be^{-i\omega r_*}, \tag{4.79}$$

and substituting these assumptions into the near-horizon field equations (4.73) and (4.74) yields a restriction on A and B

$$A = B. \tag{4.80}$$

A choice of these simple waves (4.78, 4.79, 4.77) satisfies the field equations but, these field equations are derived with Lorenz gauge (4.3) built in, thus the initial conditions must also satisfy the gauge. Using (4.3), (3.280), (4.9), and (4.11) one can show that in Schwarzschild coordinates Lorenz gauge has the form

$$\partial_t a_0 + \partial_{r_*} a_1 - a_2 \frac{l(l+1)}{r^2} + \frac{2}{r}\left(1 - \frac{m}{r}\right)a_1 = 0, \tag{4.81}$$

near the horizon, it becomes

$$\partial_t a_0 + \partial_{r_*} a_1 - a_2 \frac{l(l+1)}{4m^2} + \frac{1}{2m}a_1 = 0. \tag{4.82}$$
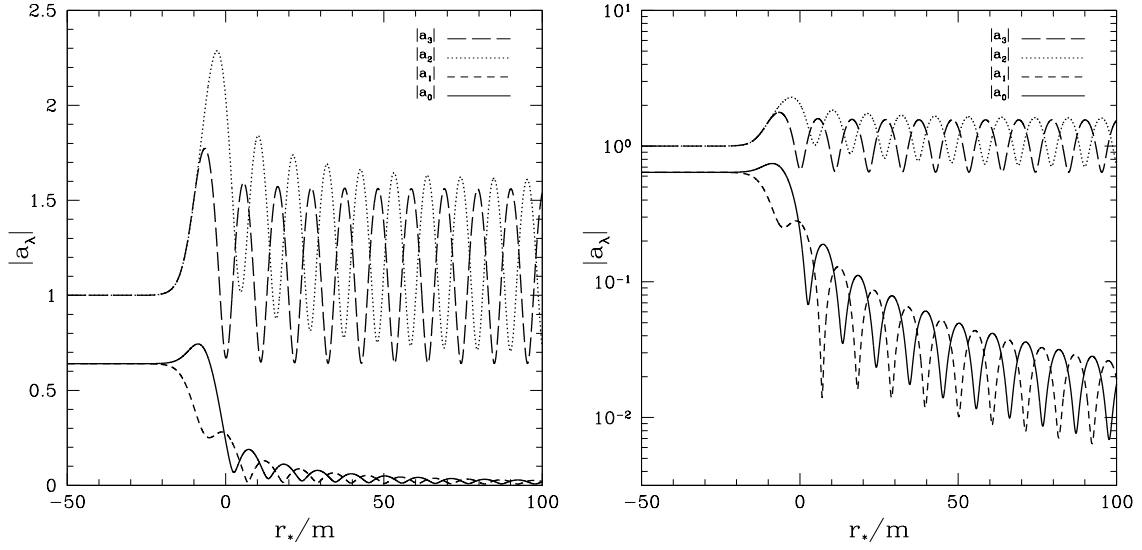
Figure 4.2: Electromagnetic field functions a_λ for $l = 1$ and $m\omega = 0.3$. Field functions begin as plane waves near the horizon, hence the stable magnitude/amplitude, then become a superposition of incident and reflected waves, as evident from an oscillating (beating) magnitude/amplitude.

Inserting (4.77)-(4.79) into (4.82) leads to the boundary conditions for a down-going electromagnetic wave

$$a_0(r_* \to -\infty) \quad \to \quad \frac{1}{2m}\frac{l(l+1)}{1-4mi\omega}e^{-i\omega r_*}; \tag{4.83}$$

$$a_1(r_* \to -\infty) \quad \to \quad \frac{1}{2m}\frac{l(l+1)}{1-4mi\omega}e^{-i\omega r_*}; \tag{4.84}$$

$$a_2(r_* \to -\infty) \quad \to \quad e^{-i\omega r_*}; \tag{4.85}$$

$$a_3(r_* \to -\infty) \quad \to \quad e^{-i\omega r_*}. \tag{4.86}$$

4.5 Numerical Implementation

4.5.1 The Field Equations

After integrating (4.39) - (4.42) one necessarily notices that a_b decay as $\frac{1}{r}$ with $r_* \to r \to \infty$, while a_B approach a constant amplitude, Figure (4.2). This situation compli-

cates wave separation[7] (4.4.1) and, above all, contributes to the loss of accuracy due to increased roundoff error; as far as numerical analysis is concerned: best quantities undergo as little (amplitude) change as possible, if change[8] is inevitable – conservation of the order of magnitude is next on the list. Hence, the following substitution is made

$$\alpha_b = r a_b, \tag{4.87}$$

where α_b is to have a constant amplitude as $r_* \to r \to \infty$. Rewriting (4.39), (4.40), and (4.41) in terms of α_b yields

$$0 = \left(\omega^2 + \partial^2_{r_*}\right)\alpha_0 - \frac{f}{r^2}\left[l(l+1) + \frac{4m}{r}\right]\alpha_0 + \frac{2mi\omega}{r^2}\alpha_1 + \frac{2m}{r^2}\alpha_0'; \tag{4.88}$$

$$0 = \left(\omega^2 + \partial^2_{r_*}\right)\alpha_1 - \frac{f}{r^2}\left[l(l+1) + 2\right]\alpha_1 + \frac{2l(l+1)f}{r^2}a_2 + \frac{2mi\omega}{r^2}\alpha_0 + \frac{2m}{r^2}\alpha_1'; \tag{4.89}$$

$$0 = \left(\omega^2 + \partial^2_{r_*}\right)a_2 - f\frac{l(l+1)}{r^2}a_2 + \frac{2}{r^2}f^2\alpha_1, \tag{4.90}$$

(4.42) remains unchanged. Lorenz gauge (4.81) is also rewritten in terms of the new field functions α_b

$$\dot{\alpha}_0 + \alpha_1' - a_2\frac{l(l+1)}{r} + \frac{1}{r}\alpha_1 = 0, \tag{4.91}$$

followed by the initial conditions

$$\alpha_0(r_* \to -\infty) = \alpha_1(r_* \to -\infty) \to \frac{l(l+1)}{1 - 4mi\omega}e^{-i\omega r_*}; \tag{4.92}$$

followed by the radiated power

$$P_{even} = \frac{1}{4\pi}l(l+1)\left|\left(\frac{\alpha_0}{r}f - i\omega a_2\right)\left(f^{-1}a_2' - \frac{\alpha_1}{r}\right)\right|, \tag{4.93}$$

---

[7]Simple multiplication by r and subsequent division by r after separation solves that problem.

[8]Oscillation is known to literally *shake away* the accuracy of numerical analysis.

110
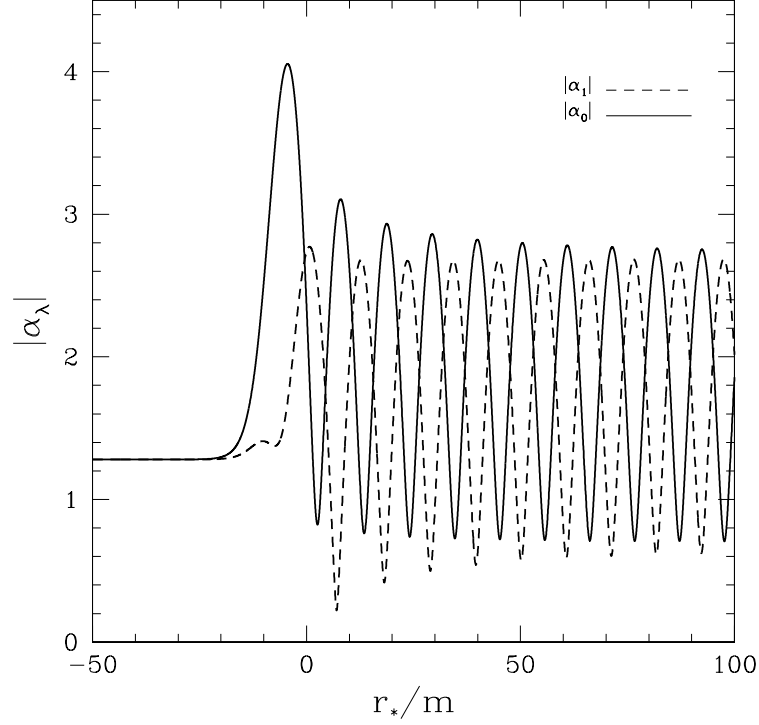
Figure 4.3: Electromagnetic field functions α_λ for $l = 1$ and $\omega = 0.3$.

P_{odd} remains unchanged. Resulting $\alpha_{0,1}$ are plotted in Figure (4.3).

4.5.2   Integration

$r(r_*)$ is found by integrating $\dfrac{dr}{dr_*} = f$ with RK4 in the same style as in (2.6.2) setting[9] $r_* = 0$ at $r = 10m$. r is then used in (4.88) - (4.90) and (4.42), which are also integrated with RK4 setting initial conditions according to (4.92) and (4.77). Integration step/length is decreased/increased until the desired tolerance of the reflection/transmission is achieved.

---

[9]Initial condition in this case is not essential because r_* is not explicitly present in the differential equation.
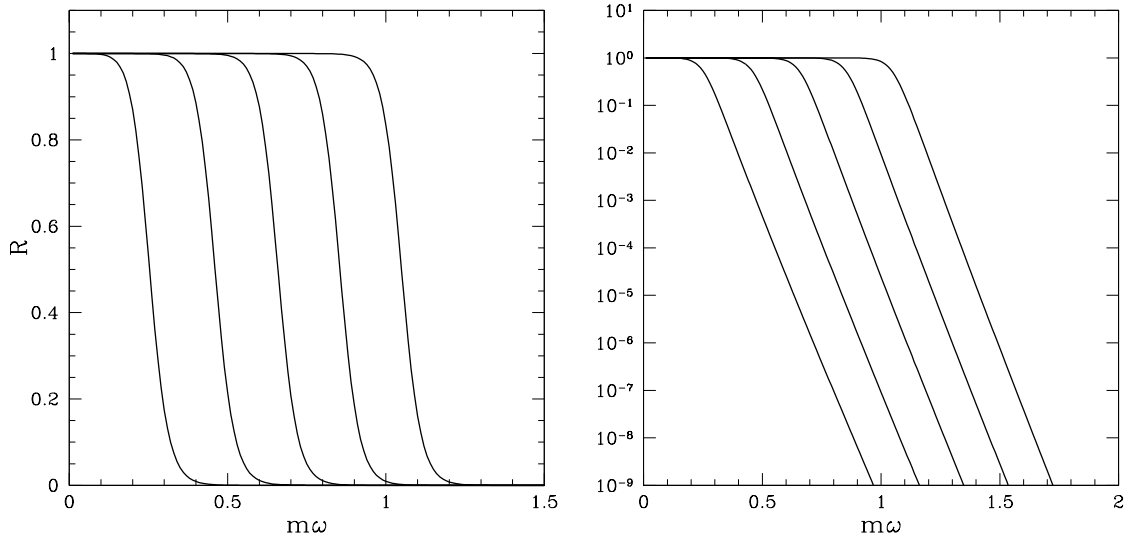
Figure 4.4: Reflection of electromagnetic radiation from a Schwarzschild black hole for (left to right) $l = 1, 2, 3, 4, 5$.

4.6 Results

Plotted in Figure (4.4) and displayed in Table (4.1) are the results. Obtained reflections are in agreement with universally accepted values to at least seven (7) digits significant figures.

4.7 Conclusion

While computing reflection of electromagnetic waves from a Schwarzschild black hole is a trivial goal, that which has already been accomplished some time ago, this study shows that the direct perturbation of the electromagnetic 4-vector potential is a mathematically valid, physically sound, and computationally feasible method of working with electromagnetic waves in curved spacetime. The method does not reduce the field functions to mathematical constructs[10] (as done by Regge-Wheeler

---

[10]Which must later undergo non-trivial operations to elucidate the physical field.

$m\omega$	$l = 1$	2	3	4
0.1	1.97585×10^{-3} †	1.88325×10^{-7} †	1.07004×10^{-11} †	3.74342×10^{-16} †
0.2	8.70026×10^{-1}	5.24149×10^{-5} †	1.14552×10^{-8} †	1.56404×10^{-12} †
0.3	1.74142×10^{-1}	3.41939×10^{-3} †	1.61156×10^{-6} †	4.80427×10^{-10} †
0.4	9.01744×10^{-3}	8.85300×10^{-1}	1.03050×10^{-4} †	5.28535×10^{-8} †
0.5	4.61934×10^{-4}	2.14491×10^{-1}	4.31392×10^{-3} †	3.35454×10^{-6} †
0.6	2.59173×10^{-5}	1.14064×10^{-2}	8.76764×10^{-1}	1.51296×10^{-4} †
0.7	1.55311×10^{-6}	5.48974×10^{-4}	2.07126×10^{-1}	5.38594×10^{-3} †
0.8	9.75649×10^{-8}	2.84705×10^{-5}	1.07570×10^{-2}	8.59067×10^{-1}
0.9	6.34815×10^{-9}	1.57249×10^{-6}	4.96956×10^{-4}	1.85679×10^{-1}
1.0	4.24398×10^{-10}	9.12092×10^{-8}	2.44479×10^{-5}	9.31182×10^{-3}

Table 4.1: Reflection of electromagnetic radiation from a Schwarzschild black hole; † signifies transmission. Integration parameters: $r_* \in [-200, 100\,000]$, $\Delta r_* = 0.01$, $r(r_* = 0) = 10m$.

[38] and Zerilli [48]) and equations (4.9) and (4.11) unambiguously reconstruct A_μ.

Possible future applications of this method include, but are not limited to: adiabatic and full self-force trajectory/orbit calculations of charged particles in Schwarzschild spacetimes.

Chapter 5

Gravitational Waves on Schwarzschild Background

5.1 Introduction

The previous chapter demonstrates the efficacy of perturbing A_μ, rather than traditional scalars, to study the propagation of electromagnetic radiation in curved spacetime. Investigated in this chapter is the feasibility of an equivalent technique as it is implemented in studying gravitational waves, *i.e.* directly perturbing the metric.

5.2 The Field Equations

Albert Einstein's gift to the world:

$$G_{\mu\nu} = 8\pi T_{\mu\nu}, \tag{5.1}$$

where $G_{\mu\nu}$ is the Einstein tensor and $T_{\mu\nu}$ is the stress-energy tensor [29]. The expression is quite general hence useless without pages of calculus to describe it. That said, the pages follow.

5.2.1 Field Equations in Vacuum

The Einstein tensor is the trace-trversed[1] Ricci Tensor

$$G_{\mu\nu} = R_{\mu\nu} - \frac{1}{2}Rg_{\mu\nu}, \tag{5.2}$$

where R is the Ricci Scalar

$$R = R_\mu{}^\mu, \tag{5.3}$$

and $R_{\mu\nu}$ is the Ricci Tensor, which is formed by contracting first and third indices of the Riemann

$$R_{\mu\nu} = R^\sigma{}_{\mu\sigma\nu}. \tag{5.4}$$

Because one is to study the perturbations in free space[2], $T_{\mu\nu} = 0$, (5.1) reduces to

$$G_{\mu\nu} = 0; \tag{5.5}$$

$$R_{\mu\nu} - \frac{1}{2}Rg_{\mu\nu} = 0, \tag{5.6}$$

contraction of $g^{\mu\nu}$ on (5.6) is revealing

$$g^{\mu\nu}\left(R_{\mu\nu} - \frac{1}{2}Rg_{\mu\nu}\right) = -R = 0, \tag{5.7}$$

$\Rightarrow$

$$R_{\mu\nu} = 0. \tag{5.8}$$

(5.8) are Einstein's field equations in vacuum.

---

[1] $g^{\mu\nu}G_{\mu\nu} = -g^{\mu\nu}R_{\mu\nu}$ or $G = -R$

[2] As opposed to plasma inside a star.

5.2.2 The Perturbed Metric

When one speaks of gravitational waves, one typically implies an arbitrary space-time spanned by metric $g_{\mu\nu}$ upon which a metric disturbance $h_{\mu\nu}$ propagates

$$\mathbf{g}_{\mu\nu} = g_{\mu\nu} + h_{\mu\nu}, \tag{5.9}$$

where $h_{\mu\nu}$ is the aforementioned "wave," $g_{\mu\nu}$ is the background (static) metric, and $\mathbf{g}_{\mu\nu}$ is the total metric. The following is generally required of the perturbation

$$|h_{\mu\nu}| < |g_{\mu\nu}|, \tag{5.10}$$

where the comparison refers to typical local maximum values. Before any significant calculations commence, an inverse metric $\mathbf{g}^{\mu\nu}$ must be found. Taking a perturbative[3] approach one assumes

$$\mathbf{g}^{\mu\nu} = g^{\mu\nu} + s^{\mu\nu}, \tag{5.11}$$

where $s^{\mu\nu}$ is an undetermined correction to the inverse perturbation metric. Further calculation relies on the self-consistency of any matrix and its inverse

$$\mathbf{g}^{\mu\gamma}\mathbf{g}_{\gamma\nu} = \delta^{\mu}{}_{\nu}, \tag{5.12}$$

in other words

$$\mathbf{g}^{-1}\mathbf{g} = \mathbf{1}. \tag{5.13}$$

Using (5.9) and (5.11) in (5.12) yields

$$\delta^{\mu}{}_{\nu} = (g^{\mu\gamma} + s^{\mu\gamma})\left(g_{\gamma\nu} + h_{\gamma\nu}\right); \tag{5.14}$$

---

[3]In the sense of mathematical perturbation theory.

$$0 \;=\; g^{\mu\gamma}h_{\gamma\nu} + s^{\mu\gamma}g_{\gamma\nu} + s^{\mu\gamma}h_{\gamma\nu}. \tag{5.15}$$

At this point, mathematical perturbation theory directs one to keep only the linear order terms:[4]

- $g^{\mu\gamma}h_{\gamma\nu}$ - linear;

- $g_{\gamma\nu}s^{\mu\gamma}$ - linear;

- $s^{\mu\gamma}h_{\gamma\nu}$ - quadratic,

$s^{\mu\gamma}h_{\gamma\nu}$, is of order h^2 and is therefore neglected for the first order iteration.

$$0 \;=\; g^{\mu\gamma}h_{\gamma\nu} + p^{\mu\gamma}g_{\gamma\nu}; \tag{5.16}$$

$$p^{\mu\nu} \;=\; -h^{\mu\nu}. \tag{5.17}$$

First order inverse perturbed metric is given by

$$\mathbf{g}^{\mu\nu} \approx g^{\mu\nu} - h^{\mu\nu}. \tag{5.18}$$

Repeating this procedure while adding subsequent perturbation orders to (5.11) yields an infinite series for $\mathbf{g}^{\mu\nu}$

$$\mathbf{g}^{\mu\nu} = g^{\mu\nu} - h^{\mu\nu} + h^{\mu\gamma}h_{\gamma}{}^{\nu} - h^{\mu\beta}h_{\beta}{}^{\gamma}h_{\gamma}{}^{\nu} + h^{\mu\beta}h_{\beta}{}^{\gamma}h_{\gamma}{}^{\delta}h_{\delta}{}^{\nu} - h^{\mu\beta}h_{\beta}{}^{\gamma}h_{\gamma}{}^{\delta}h_{\delta}{}^{\epsilon}h_{\epsilon}{}^{\nu} + \ldots. \tag{5.19}$$

where the background metric is used in raising/lowering of the indices of $h_{\mu\nu}$. It is of course assumed that $h_{\mu\nu}$ is sufficiently small for the series to converge.

Analysis of this subsection shows that either the perturbed metric (matrix) or its inverse is known exactly, the other is forced to be an infinite series.

----

[4] $s^{\mu\nu}$ is expected to be of order $h^{\mu\nu}$ due to (5.9)

5.2.3 The Perturbed Christoffel Symbol

A circuitous yet effective technique to derive perturbed Christoffel Symbols, Riemann, and Ricci is suggested[5] by Misner *et. al.* [29]. The perturbed connection coefficients have the form

$$\mathbf{\Gamma}^{\alpha}{}_{\beta\gamma} = \Gamma^{\alpha}{}_{\beta\gamma} + S^{\alpha}{}_{\beta\gamma}, \tag{5.20}$$

where from this point forth **bold** symbols shall represent the quantities derived from the total metric $\mathbf{g}_{\mu\nu}$, and regular symbols shall represent the quantities derived from the background metric $g_{\mu\nu}$; $S^{\alpha}{}_{\beta\gamma}$ is the undetermined correction term to the background connection coefficients,

$$S^{\alpha}{}_{\beta\gamma} = \mathbf{\Gamma}^{\alpha}{}_{\beta\gamma} - \Gamma^{\alpha}{}_{\beta\gamma}, \tag{5.21}$$

where

$$\mathbf{\Gamma}^{\alpha}{}_{\beta\gamma} = \frac{1}{2}\mathbf{g}^{\alpha\mu}\left(\mathbf{g}_{\beta\mu,\gamma} + \mathbf{g}_{\gamma\mu,\beta} - \mathbf{g}_{\beta\gamma,\mu}\right); \tag{5.22}$$

$$\Gamma^{\alpha}{}_{\beta\gamma} = \frac{1}{2}g^{\alpha\mu}\left(g_{\beta\mu,\gamma} + g_{\gamma\mu,\beta} - g_{\beta\gamma,\mu}\right). \tag{5.23}$$

Inserting (5.22) and (5.23) into (5.21) yields

$$S^{\alpha}{}_{\beta\gamma} = \frac{1}{2}\mathbf{g}^{\alpha\mu}\left(h_{\beta\mu,\gamma} + h_{\gamma\mu,\beta} - h_{\beta\gamma,\mu}\right) + \frac{1}{2}s^{\alpha\mu}\left(g_{\beta\mu,\gamma} + g_{\gamma\mu,\beta} - g_{\beta\gamma,\mu}\right), \tag{5.24}$$

where

$$s^{\alpha\mu} = \mathbf{g}^{\alpha\mu} - g^{\alpha\mu}, \tag{5.25}$$

---

[5]Yet left for the reader to explore and derive.

which is given by (5.19). To beautify (5.24) one can show the following

$$h_{\beta\mu|\gamma} + h_{\gamma\mu|\beta} - h_{\beta\gamma|\mu} = h_{\beta\mu,\gamma} + h_{\gamma\mu,\beta} - h_{\beta\gamma,\mu} - 2h_{\epsilon\mu}\Gamma^{\epsilon}{}_{\beta\gamma}, \tag{5.26}$$

where | (pipe) signifies a covariant derivative with respect to the background metric $g_{\mu\nu}$. Substituting (5.26) into (5.24) yields

$$S^{\alpha}{}_{\beta\gamma} = \frac{1}{2}\mathbf{g}^{\alpha\mu}\left(h_{\beta\mu|\gamma} + h_{\gamma\mu|\beta} - h_{\beta\gamma|\mu}\right) + \frac{1}{2}\left(g_{\beta\sigma,\gamma} + g_{\gamma\sigma,\beta} - g_{\beta\gamma,\sigma}\right)\left(\mathbf{g}^{\alpha\mu}h_{\epsilon\mu}g^{\epsilon\sigma} + s^{\alpha\sigma}\right), \tag{5.27}$$

from (5.15) one can see that the last term in (5.27) vanishes

$$S^{\alpha}{}_{\beta\gamma} = \mathbf{\Gamma}^{\alpha}{}_{\beta\gamma} - \Gamma^{\alpha}{}_{\beta\gamma} = \frac{1}{2}\mathbf{g}^{\alpha\mu}\left(h_{\beta\mu|\gamma} + h_{\gamma\mu|\beta} - h_{\beta\gamma|\mu}\right). \tag{5.28}$$

5.2.4 The Perturbed Riemann Tensor

Riemann tensor is given by

$$R^{\alpha}{}_{\beta\gamma\delta} = \Gamma^{\alpha}{}_{\beta\delta,\gamma} - \Gamma^{\alpha}{}_{\beta\gamma,\delta} + \Gamma^{\alpha}{}_{\mu\gamma}\Gamma^{\mu}{}_{\beta\delta} - \Gamma^{\alpha}{}_{\mu\delta}\Gamma^{\mu}{}_{\beta\gamma}, \tag{5.29}$$

for the background metric, and

$$\mathbf{R}^{\alpha}{}_{\beta\gamma\delta} = \mathbf{\Gamma}^{\alpha}{}_{\beta\delta,\gamma} - \mathbf{\Gamma}^{\alpha}{}_{\beta\gamma,\delta} + \mathbf{\Gamma}^{\alpha}{}_{\mu\gamma}\mathbf{\Gamma}^{\mu}{}_{\beta\delta} - \mathbf{\Gamma}^{\alpha}{}_{\mu\delta}\mathbf{\Gamma}^{\mu}{}_{\beta\gamma}, \tag{5.30}$$

for the perturbed, full metric. Difference of the two is

$$\begin{aligned} \mathbf{R}^{\alpha}{}_{\beta\gamma\delta} - R^{\alpha}{}_{\beta\gamma\delta} \;=\; & \left(\mathbf{\Gamma}^{\alpha}{}_{\beta\delta,\gamma} - \Gamma^{\alpha}{}_{\beta\delta,\gamma}\right) - \left(\mathbf{\Gamma}^{\alpha}{}_{\beta\gamma,\delta} - \Gamma^{\alpha}{}_{\beta\gamma,\delta}\right) \\ & + \left(\mathbf{\Gamma}^{\alpha}{}_{\mu\gamma}\mathbf{\Gamma}^{\mu}{}_{\beta\delta} - \Gamma^{\alpha}{}_{\mu\gamma}\Gamma^{\mu}{}_{\beta\delta}\right) - \left(\mathbf{\Gamma}^{\alpha}{}_{\mu\delta}\mathbf{\Gamma}^{\mu}{}_{\beta\gamma} - \Gamma^{\alpha}{}_{\mu\delta}\Gamma^{\mu}{}_{\beta\gamma}\right), \end{aligned} \tag{5.31}$$

using (5.21) to substitute $\mathbf{\Gamma}$ in favor of S yields

$$
\begin{aligned}
\mathbf{R}^{\alpha}{}_{\beta\gamma\delta} - R^{\alpha}{}_{\beta\gamma\delta} &= \left(S^{\alpha}{}_{\beta\delta,\gamma} + S^{\mu}{}_{\beta\delta}\Gamma^{\alpha}{}_{\mu\gamma} - S^{\alpha}{}_{\mu\delta}\Gamma^{\mu}{}_{\beta\gamma} \right) \\
&\quad - \left(S^{\alpha}{}_{\beta\gamma,\delta} + S^{\mu}{}_{\beta\gamma}\Gamma^{\alpha}{}_{\mu\delta} - S^{\alpha}{}_{\mu\gamma}\Gamma^{\mu}{}_{\beta\delta} \right) \\
&\quad + S^{\alpha}{}_{\mu\gamma}S^{\mu}{}_{\beta\delta} - S^{\alpha}{}_{\mu\delta}S^{\mu}{}_{\beta\gamma},
\end{aligned}
\tag{5.32}
$$

while it may not be immediately obvious why one would go down that route, the following sheds some light on the subject

$$
\begin{aligned}
\mathbf{R}^{\alpha}{}_{\beta\gamma\delta} - R^{\alpha}{}_{\beta\gamma\delta} &= \left(S^{\alpha}{}_{\beta\delta,\gamma} + S^{\mu}{}_{\beta\delta}\Gamma^{\alpha}{}_{\mu\gamma} - S^{\alpha}{}_{\mu\delta}\Gamma^{\mu}{}_{\beta\gamma} - \underline{S^{\alpha}{}_{\beta\mu}\Gamma^{\mu}{}_{\delta\gamma}} \right) \\
&\quad - \left(S^{\alpha}{}_{\beta\gamma,\delta} + S^{\mu}{}_{\beta\gamma}\Gamma^{\alpha}{}_{\mu\delta} - S^{\alpha}{}_{\mu\gamma}\Gamma^{\mu}{}_{\beta\delta} - \underline{S^{\alpha}{}_{\beta\mu}\Gamma^{\mu}{}_{\gamma\delta}} \right) \\
&\quad + S^{\alpha}{}_{\mu\gamma}S^{\mu}{}_{\beta\delta} - S^{\alpha}{}_{\mu\delta}S^{\mu}{}_{\beta\gamma}.
\end{aligned}
\tag{5.33}
$$

The sum of underlined terms in (5.33) is zero, their addition does nothing to the expression save for allowing one to recognize the terms in parentheses as covariant derivatives (with respect to the background metric) of S

$$
\mathbf{R}^{\alpha}{}_{\beta\gamma\delta} - R^{\alpha}{}_{\beta\gamma\delta} = S^{\alpha}{}_{\beta\delta|\gamma} - S^{\alpha}{}_{\beta\gamma|\delta} + S^{\alpha}{}_{\mu\gamma}S^{\mu}{}_{\beta\delta} - S^{\alpha}{}_{\mu\delta}S^{\mu}{}_{\beta\gamma};
\tag{5.34}
$$

$$
\mathbf{R}_{\beta\delta} - R_{\beta\delta} = S^{\gamma}{}_{\beta\delta|\gamma} - S^{\gamma}{}_{\beta\gamma|\delta} + S^{\gamma}{}_{\mu\gamma}S^{\mu}{}_{\beta\delta} - S^{\gamma}{}_{\mu\delta}S^{\mu}{}_{\beta\gamma}.
\tag{5.35}
$$

5.2.5 Interlude

While it has not been stated explicitly, one must note that everything derived in this section thus far is *exact*. No approximations and/or assumptions have been made save for the convergence of $\mathbf{g}^{\mu\nu}$.

Development of wave equations shuns exact expressions in favor of less accurate yet more manageable quantities often retaining only first perturbative order, hence

the term *linear* differential equation. In the following subsections, gravitational wave equation is derived with an assumption

$$|h_{\mu\nu}| \ll |g_{\mu\nu}|. \tag{5.36}$$

Such assumption justifies the removal of perturbative orders higher than first/linear.

5.2.6 Development of The Wave Equation

Starting point are the field equations in vacuum (5.8), in the absence of matter Ricci tensor vanishes

$$\mathbf{R}_{\mu\nu} = 0. \tag{5.37}$$

One can conceive of $\mathbf{R}_{\mu\nu}$ is an infinite series in orders of $h_{\mu\nu}$

$$\mathbf{R}_{\mu\nu} = R_{\mu\nu}^{(0)} + R_{\mu\nu}^{(1)} + R_{\mu\nu}^{(2)} + \ldots = 0 \tag{5.38}$$

$R_{\mu\nu}^{(0)}$ is the background Ricci[6] according to (5.35), and remaining orders are given by

$$R_{\mu\nu}^{(1)} + R_{\mu\nu}^{(2)} + R_{\mu\nu}^{(3)} + \ldots + R_{\mu\nu}^{(n)} = S^{\gamma}{}_{\mu\nu|\gamma} - S^{\gamma}{}_{\mu\gamma|\nu} + S^{\gamma}{}_{\lambda\gamma}S^{\lambda}{}_{\mu\nu} - S^{\gamma}{}_{\lambda\nu}S^{\lambda}{}_{\mu\gamma}, \tag{5.39}$$

and can be computed by expanding the right side of (5.39) and retaining orders of $h_{\mu\nu}$ less than or equal to n. For the sought wave equation, $n = 1$. Looking at (5.28) it is clear that $S^{\alpha}{}_{\beta\gamma}$ is of order h, the SS terms in (5.35) are therefore of order h^2 and are negligible

$$R_{\beta\delta}^{(1)} = S^{\gamma}{}_{\beta\delta|\gamma} - S^{\gamma}{}_{\beta\gamma|\delta} = 0. \tag{5.40}$$

---

[6]Ricci Tensor of order zero, *i.e.* $h_{\mu\nu} = 0$.

Via the same reasoning, (5.28) is simplified

$$S^{\alpha(1)}_{\ \beta\gamma} = \frac{1}{2}g^{\alpha\mu}\left(h_{\beta\mu|\gamma} + h_{\gamma\mu|\beta} - h_{\beta\gamma|\mu}\right). \tag{5.41}$$

Using (5.41) in (5.40) gives

$$R^{(1)}_{\beta\delta} = \frac{1}{2}\left(h_{\delta\gamma|\beta}{}^{\gamma} + h_{\beta\gamma|}{}^{\gamma}{}_{\delta} - h_{\beta\delta|\gamma}{}^{\gamma} - h_{|\beta\delta}\right) + \frac{1}{2}g^{\gamma\mu}\left(h_{\beta\mu|\delta\gamma} - h_{\beta\mu|\gamma\delta}\right), \tag{5.42}$$

where $h = g^{\mu\nu}h_{\mu\nu}$. Last term in (5.42) is commutator of $h_{\beta\mu}$, albeit contracted but, that is another matter

$$\frac{1}{2}g^{\gamma\mu}\left(h_{\beta\mu|\delta\gamma} - h_{\beta\mu|\gamma\delta}\right) \quad = \quad \frac{1}{2}g^{\gamma\mu}\left(R_{\beta\lambda\gamma\delta}h^{\lambda}{}_{\mu} + R_{\mu\lambda\gamma\delta}h_{\beta}{}^{\lambda}\right); \tag{5.43}$$

$$= \quad \frac{1}{2}\left(R_{\beta\lambda\gamma\delta}h^{\lambda\gamma} + R_{\lambda\delta}h_{\beta}{}^{\lambda}\right), \tag{5.44}$$

$R_{\lambda\delta} = 0$ as established in (5.8)

$$\frac{1}{2}g^{\gamma\mu}\left(h_{\beta\mu|\delta\gamma} - h_{\beta\mu|\gamma\delta}\right) = \frac{1}{2}R_{\beta\lambda\gamma\delta}h^{\lambda\gamma}. \tag{5.45}$$

This is certainly not a simplification one hopes for. An awkward term in (5.42) becomes useful

$$\frac{1}{2}h_{\beta\gamma|}{}^{\gamma}{}_{\delta} \quad = \quad \frac{1}{2}g^{\gamma\lambda}h_{\beta\gamma|\lambda\delta}; \tag{5.46}$$

$$= \quad \frac{1}{2}g^{\gamma\lambda}\left(h_{\beta\gamma|\delta\lambda} + R_{\beta\sigma\delta\lambda}h^{\sigma}{}_{\gamma} + R_{\gamma\sigma\delta\lambda}h_{\beta}{}^{\sigma}\right), \tag{5.47}$$

using the symmetries of the Riemann and (5.8)

$$\frac{1}{2}h_{\beta\gamma|}{}^{\gamma}{}_{\delta} \quad = \quad \frac{1}{2}g^{\gamma\lambda}\left(h_{\beta\gamma|\delta\lambda} - R_{\beta\sigma\lambda\delta}h^{\sigma}{}_{\gamma} - R_{\gamma\sigma\lambda\delta}h_{\beta}{}^{\sigma}\right); \tag{5.48}$$

$$= \quad \frac{1}{2}\left(h_{\beta\gamma|\delta}{}^{\gamma} - R_{\beta\sigma\lambda\delta}h^{\sigma\gamma} - R_{\sigma\delta}h_{\beta}{}^{\sigma}\right), \tag{5.49}$$

122

$$= \frac{1}{2}\left(h_{\beta\gamma|\delta}{}^{\gamma} - R_{\beta\sigma\lambda\delta}h^{\sigma\gamma}\right), \tag{5.50}$$

substituting (5.45) and (5.50) into (5.42) results in a much-coveted first order correction to the Ricci Tensor

$$R^{(1)}_{\beta\delta} = \frac{1}{2}\left(h_{\delta\gamma|\beta}{}^{\gamma} + h_{\beta\gamma|\delta}{}^{\gamma} - h_{\beta\delta|\gamma}{}^{\gamma} - h_{|\beta\delta}\right). \tag{5.51}$$

Recalling the vacuum field equations (5.38)

$$\mathbf{R}_{\mu\nu} = R^{(0)}_{\mu\nu} + R^{(1)}_{\mu\nu} + R^{(2)}_{\mu\nu} + \ldots = 0, \tag{5.52}$$

$R^{(0)}$, background Ricci, is zero because there is no matter; $R^{(2)}$ and higher are ignored in this first-order investigation; what remains is a gravitational wave equation

$$0 = R^{(1)}_{\mu\nu}; \tag{5.53}$$

$$0 = h_{\nu\gamma|\mu}{}^{\gamma} + h_{\mu\gamma|\nu}{}^{\gamma} - h_{\mu\nu|\gamma}{}^{\gamma} - h_{|\mu\nu}. \tag{5.54}$$

The Lorentz Gauge

Equation (5.54) can be simplified upon selection of a proper gauge. Gauge selected for this study was originally proposed by H. A. Lorentz

$$\bar{h}_{\mu\nu|}{}^{\nu} = 0, \tag{5.55}$$

where $\bar{h}_{\mu\nu}$ is the trace-reversed[7] $h_{\mu\nu}$

$$\bar{h}_{\mu\nu} = h_{\mu\nu} - \frac{1}{2}g_{\mu\nu}h; \tag{5.56}$$

---

[7] $h = -\bar{h}$

123

$$h_{\mu\nu} = \bar{h}_{\mu\nu} - \frac{1}{2}g_{\mu\nu}\bar{h}. \tag{5.57}$$

Substituting (5.57) into (5.54) yields

$$\bar{h}_{\mu\gamma|\nu}{}^{\gamma} + \bar{h}_{\nu\gamma|\mu}{}^{\gamma} - \bar{h}_{\mu\nu|\gamma}{}^{\gamma} + \frac{1}{2}g_{\mu\nu}\bar{h}_{|\gamma}{}^{\gamma} = 0. \tag{5.58}$$

The gauge can not be implemented immediately, (5.58) is re-formed such that terms akin to $\bar{h}_{\mu\nu|}{}^{\gamma}$ surface. One may use the identity derived earlier (5.50)

$$\bar{h}_{\mu\gamma|\nu}{}^{\gamma} = \bar{h}_{\mu\gamma|}{}^{\gamma}{}_{\nu} - R_{\mu\lambda\nu\sigma}\bar{h}^{\lambda\sigma}; \tag{5.59}$$

$$\bar{h}_{\nu\gamma|\mu}{}^{\gamma} = \bar{h}_{\nu\gamma|}{}^{\gamma}{}_{\mu} - R_{\nu\lambda\mu\sigma}\bar{h}^{\lambda\sigma}. \tag{5.60}$$

Applying Lorentz gauge together with symmetries of the Riemann[8] and the perturbation metric[9] to (5.59) and (5.60) yields

$$\bar{h}_{\mu\gamma|\nu}{}^{\gamma} = \bar{h}_{\nu\gamma|\mu}{}^{\gamma} = -R_{\mu\lambda\nu\sigma}\bar{h}^{\lambda\sigma}, \tag{5.61}$$

inserting (5.61) into (5.58) yields

$$\bar{h}_{\mu\nu|\gamma}{}^{\gamma} + 2R_{\mu\lambda\nu\sigma}\bar{h}^{\lambda\sigma} + \frac{1}{2}g_{\mu\nu}\bar{h}_{|\gamma}{}^{\gamma} = 0, \tag{5.62}$$

contracting (5.62) on $g^{\mu\nu}$

$$g^{\mu\nu}\left(\bar{h}_{\mu\nu|\gamma}{}^{\gamma} + 2R_{\mu\lambda\nu\sigma}\bar{h}^{\lambda\sigma} + \frac{1}{2}g_{\mu\nu}\bar{h}_{|\gamma}{}^{\gamma}\right) = 3\bar{h}_{|\gamma}{}^{\gamma} = 0, \tag{5.63}$$

---

[8] $R_{\alpha\beta\gamma\delta} = R_{\gamma\delta\alpha\beta}$

[9] $\bar{h}^{\mu\nu} = \bar{h}^{\nu\mu}$

$$\Rightarrow \qquad \bar{h}_{|\gamma}{}^{\gamma} = 0. \tag{5.64}$$

(5.62) become the field equations governing the linear perturbations on a given vacuous background in Lorentz gauge

$$\bar{h}_{\mu\nu|\gamma}{}^{\gamma} + 2R_{\mu\lambda\nu\sigma}\bar{h}^{\lambda\sigma} = 0. \tag{5.65}$$

5.3 $\mathcal{M}^2 \times \mathcal{S}^2$ Decomposition of the System

5.3.1 Decomposition of the Wave Equation

Using (3.340)-(3.342) and (3.343)-(3.345), (5.65) can be cast into three equations in terms of $\mathcal{M}^2 \times \mathcal{S}^2$ differential operators and metrics

$$
\begin{aligned}
0 \;=\;& \nabla_m \nabla^m h_{ab} + \nabla^N \nabla_N h_{ab} - \frac{2}{r}\left(\rho_a \nabla^N h_{Nb} + \rho_b \nabla^N h_{Na}\right) - \frac{2}{r^2}\rho^g\left(\rho_a h_{gb} + \rho_b h_{ag}\right) + \\
&+ \frac{2}{r^2}\left(\rho_b \rho_a - \frac{m}{r}g_{ab}\right)g^{NM}h_{MN} + \frac{2}{r}\rho^g \nabla_g h_{ab} + \frac{4m}{r^3}\left(g_{ab}g^{MN}h_{MN} - h_{ab}\right); \tag{5.66}
\end{aligned}
$$

$$
\begin{aligned}
0 \;=\;& \nabla_m \nabla^m h_{AB} + \nabla^N \nabla_N h_{AB} - \frac{8m}{r^3}h_{AB} + \frac{2}{r}\rho^g\left(\nabla_A h_{gB} + \nabla_B h_{Ag} - \nabla_g h_{AB}\right) + \\
&+ \frac{2}{r^2}\rho^c \rho^g g_{AB} h_{gc} + \frac{2m}{r^3}g_{AB}\left(2g^{MN}h_{MN} - g^{mn}h_{mn}\right); \tag{5.67}
\end{aligned}
$$

$$
0 \;=\; \nabla_m \nabla^m h_{aB} + \nabla^N \nabla_N h_{aB} - \frac{f}{r^2}h_{aB} - \frac{2}{r}\rho_a \nabla^N h_{NB} + \frac{2}{r}\rho^g \nabla_B h_{ag} - \frac{4}{r^2}\rho_a \rho^g h_{gB}. \tag{5.68}
$$

These equations are covariant on $\mathcal{M}^2$.

5.3.2 Decomposition of the Perturbation

(5.65) is the gravitational counterpart of (4.4); and A_μ is the electromagnetic counterpart of $\bar{h}_{\mu\nu}$. Similarly to A_μ, $\bar{h}_{\mu\nu}$ is decomposed in terms of $\mathcal{M}^2$ and $\mathcal{S}^2$ objects described

in the chapter on Metric $\mathcal{M}^2 \times \mathcal{S}^2$ Decomposition

$$\bar{h}_{ab} = (P_{00}y_{ab} + P_{01}u_{ab} + P_{11}w_{ab}) Y; \tag{5.69}$$

$$\bar{h}_{aB} = (Q_0\tau_a + Q_1\rho_a) Y_B + (R_0\tau_a + R_1\rho_a) X_B; \tag{5.70}$$

$$\bar{h}_{AB} = HY_{AB} + JU_{AB} + KW_{AB}, \tag{5.71}$$

where $P_{00}, P_{01}, P_{11}, Q_0, Q_1, R_0, R_1, H, J$, and K are functions of the temporal-spatial coordinates. Inserting (5.69)-(5.71) into (5.66)-(5.68) and using the entire chapter on $\mathcal{M}^2 \times \mathcal{S}^2$ decomposition, one obtains ten perturbation field equations

$$0 = f\nabla_m\nabla^m R_0 + \frac{2m}{r^2}\rho^m\nabla_m R_0 - \frac{2m}{r^2}\tau^m\nabla_m R_1 - \frac{f\beta}{r^2}R_0; \tag{5.72}$$

$$0 = f\nabla_m\nabla^m R_1 + \frac{2m}{r^2}\rho^m\nabla_m R_1 - \frac{2m}{r^2}\tau^m\nabla_m R_0 - \frac{f}{r^2}(4f+\beta)R_1 - \frac{f}{r^3}(2-\beta)K; \tag{5.73}$$

$$0 = f\nabla_m\nabla^m K - \frac{2f}{r}\rho^m\nabla_m K + \frac{f}{r^2}(4f-\beta)K + \frac{4f^2}{r}R_1; \tag{5.74}$$

$$0 = f\nabla_m\nabla^m P_{00} + \frac{2}{r}\rho^m\nabla_m P_{00} + \frac{1}{r^2}\left[\frac{4m^2}{r^2} - 2f\left(1 - \frac{4m}{r}\right) - \beta f\right]P_{00} - \frac{f^2}{r^2}P_{01} +$$

$$+\frac{2f\beta}{r^3}Q_1 + \frac{2}{r^4}\left(1 - \frac{4m}{r}\right)H; \tag{5.75}$$

$$0 = f\nabla_m\nabla^m P_{01} + \frac{2}{r}\rho^m\nabla_m P_{01} - \frac{4m}{r^2}\tau^m\nabla_m P_{11} - \frac{f}{r^2}(\beta+2)P_{01} + \frac{4f\beta}{r^3}Q_1 +$$

$$-\frac{4f^2}{r^2}P_{00} + \frac{4f}{r^4}H; \tag{5.76}$$

$$0 = f\nabla_m\nabla^m P_{11} + \frac{2}{r}\rho^m\nabla_m P_{11} - \frac{4m}{r^2}\tau^m\nabla_m P_{01} - \frac{f}{r^2}(\beta+2)P_{11} + \frac{4f\beta}{r^3}Q_0; \tag{5.77}$$

$$0 = f\nabla_m\nabla^m Q_0 + \frac{2m}{r^2}\rho^m\nabla_m Q_0 - \frac{2m}{r^2}\tau^m\nabla_m Q_1 - \frac{f\beta}{r^2}Q_0 + \frac{f^2}{r}P_{11}; \tag{5.78}$$

$$0 = f\nabla_m\nabla^m Q_1 + \frac{2m}{r^2}\rho^m\nabla_m Q_1 - \frac{2m}{r^2}\tau^m\nabla_m Q_0 - \frac{f}{r^2}(\beta+4f)Q_1 +$$

$$-\frac{2f}{r^3}\left[H + J\left(1 - \frac{1}{2}\beta\right)\right] + \frac{f^2}{r}(2P_{00} + P_{01}); \tag{5.79}$$

$$0 = f\nabla_m\nabla^m H - \frac{2f}{r}\rho^m\nabla_m H - \frac{\beta f}{r^2}H - \frac{2f^2\beta}{r}Q_1 + 2f^2\left(1 - \frac{4m}{r}\right)P_{00} + f^3 P_{01}; \tag{5.80}$$

$$0 = f\nabla_m\nabla^m J - \frac{2f}{r}\rho^m\nabla_m J + \frac{f}{r^2}(4f-\beta)J + \frac{4f^2}{r}Q_1. \tag{5.81}$$

where $\beta = l(l + 1)$. One may readily notice that the first three equations are not coupled to the remaining seven; they are the *odd* parity perturbations to the metric, and are completely independent of[10] the *even* parity perturbations represented by the other seven. These equations are still covariant on $\mathcal{M}^2$.

5.3.3 Specialization to Schwarzschild Coordinates

Following identical substitutions from the electromagnetic section (4.3.3), one is able to obtain the gravitational field perturbation equations on Schwarzschild background in Schwarzschild coordinates[11]

$$0 = \left(-\partial_t^2 + \partial_{r_*}^2\right) R_0 + \frac{2m}{r^2}\partial_{r_*} R_0 - \frac{2m}{r^2}\partial_t R_1 - \frac{f\beta}{r^2} R_0; \tag{5.82}$$

$$0 = \left(-\partial_t^2 + \partial_{r_*}^2\right) R_1 + \frac{2m}{r^2}\partial_{r_*} R_1 - \frac{2m}{r^2}\partial_t R_0 - \frac{f}{r^2}(4f + \beta) R_1 - \frac{f}{r^3}(2 - \beta) K; \tag{5.83}$$

$$0 = \left(-\partial_t^2 + \partial_{r_*}^2\right) K - \frac{2f}{r}\partial_{r_*} K + \frac{f}{r^2}(4f - \beta) K + \frac{4f^2}{r} R_1; \tag{5.84}$$

$$0 = \left(-\partial_t^2 + \partial_{r_*}^2\right) P_{00} + \frac{2}{r}\partial_{r_*} P_{00} + \frac{1}{r^2}\left[\frac{4m^2}{r^2} - 2f\left(1 - \frac{4m}{r}\right) - \beta f\right] P_{00} - \frac{f^2}{r^2} P_{01} +$$
$$+ \frac{2f\beta}{r^3} Q_1 + \frac{2}{r^4}\left(1 - \frac{4m}{r}\right) H; \tag{5.85}$$

$$0 = \left(-\partial_t^2 + \partial_{r_*}^2\right) P_{01} + \frac{2}{r}\partial_{r_*} P_{01} - \frac{4m}{r^2}\partial_t P_{11} - \frac{f}{r^2}(\beta + 2) P_{01} + \frac{4f\beta}{r^3} Q_1 +$$
$$- \frac{4f^2}{r^2} P_{00} + \frac{4f}{r^4} H; \tag{5.86}$$

$$0 = \left(-\partial_t^2 + \partial_{r_*}^2\right) P_{11} + \frac{2}{r}\partial_{r_*} P_{11} - \frac{4m}{r^2}\partial_t P_{01} - \frac{f}{r^2}(\beta + 2) P_{11} + \frac{4f\beta}{r^3} Q_0; \tag{5.87}$$

$$0 = \left(-\partial_t^2 + \partial_{r_*}^2\right) Q_0 + \frac{2m}{r^2}\partial_{r_*} Q_0 - \frac{2m}{r^2}\partial_t Q_1 - \frac{f\beta}{r^2} Q_0 + \frac{f^2}{r} P_{11}; \tag{5.88}$$

$$0 = \left(-\partial_t^2 + \partial_{r_*}^2\right) Q_1 + \frac{2m}{r^2}\partial_{r_*} Q_1 - \frac{2m}{r^2}\partial_t Q_0 - \frac{f}{r^2}(\beta + 4f) Q_1 +$$

---

[10]Orthogonal to.

[11]Changing the radial coordinate from r to r_* has nothing to do with Schwarzschild coordinates *per se* but, might as well take care of the tortoise coordinate while one's at it.

$$-\frac{2f}{r^3}\left[H + J\left(1 - \frac{1}{2}\beta\right)\right] + \frac{f^2}{r}\left(2P_{00} + P_{01}\right); \tag{5.89}$$

$$0 = \left(-\partial_t^2 + \partial_{r_*}^2\right)H - \frac{2f}{r}\partial_{r_*}H - \frac{\beta f}{r^2}H - \frac{2f^2\beta}{r}Q_1 + 2f^2\left(1 - \frac{4m}{r}\right)P_{00} + f^3P_{01}; \tag{5.90}$$

$$0 = \left(-\partial_t^2 + \partial_{r_*}^2\right)J - \frac{2f}{r}\partial_{r_*}J + \frac{f}{r^2}(4f - \beta)J + \frac{4f^2}{r}Q_1. \tag{5.91}$$

5.3.4 Specialization to Frequency Domain

Borrowing the procedure form the electromagnetic counterpart of this subsection $(4.3.4)$[12],

$$X \rightarrow Xe^{-i\omega t}; \tag{5.92}$$

$$\tau^m\nabla_m \rightarrow \partial_t \rightarrow -i\omega, \tag{5.93}$$

gravitational perturbation field equations are cast into second order, coupled, linear differential equations

$$0 = \left(\omega^2 + \partial_{r_*}^2\right)R_0 + \frac{2m}{r^2}\partial_{r_*}R_0 + i\frac{2m\omega}{r^2}R_1 - \frac{f\beta}{r^2}R_0; \tag{5.94}$$

$$0 = \left(\omega^2 + \partial_{r_*}^2\right)R_1 + \frac{2m}{r^2}\partial_{r_*}R_1 + i\frac{2m\omega}{r^2}R_0 - \frac{f}{r^2}(4f + \beta)R_1 - \frac{f}{r^3}(2 - \beta)K; \tag{5.95}$$

$$0 = \left(\omega^2 + \partial_{r_*}^2\right)K - \frac{2f}{r}\partial_{r_*}K + \frac{f}{r^2}(4f - \beta)K + \frac{4f^2}{r}R_1; \tag{5.96}$$

$$0 = \left(\omega^2 + \partial_{r_*}^2\right)P_{00} + \frac{2}{r}\partial_{r_*}P_{00} + \frac{1}{r^2}\left[\frac{4m^2}{r^2} - 2f\left(1 - \frac{4m}{r}\right) - \beta f\right]P_{00} - \frac{f^2}{r^2}P_{01} +$$

$$+\frac{2f\beta}{r^3}Q_1 + \frac{2}{r^4}\left(1 - \frac{4m}{r}\right)H; \tag{5.97}$$

$$0 = \left(\omega^2 + \partial_{r_*}^2\right)P_{01} + \frac{2}{r}\partial_{r_*}P_{01} + i\frac{4m\omega}{r^2}P_{11} - \frac{f}{r^2}(\beta + 2)P_{01} + \frac{4f\beta}{r^3}Q_1 +$$

$$-\frac{4f^2}{r^2}P_{00} + \frac{4f}{r^4}H; \tag{5.98}$$

$$0 = \left(\omega^2 + \partial_{r_*}^2\right)P_{11} + \frac{2}{r}\partial_{r_*}P_{11} + i\frac{4m\omega}{r^2}P_{01} - \frac{f}{r^2}(\beta + 2)P_{11} + \frac{4f\beta}{r^3}Q_0; \tag{5.99}$$

---

[12]Fourier-transforming the field equations.

128

$$0 = \left(\omega^2 + \partial^2_{r_*}\right) Q_0 + \frac{2m}{r^2}\partial_{r_*}Q_0 + i\frac{2m\omega}{r^2}Q_1 - \frac{f\beta}{r^2}Q_0 + \frac{f^2}{r}P_{11}; \tag{5.100}$$

$$0 = \left(\omega^2 + \partial^2_{r_*}\right) Q_1 + \frac{2m}{r^2}\partial_{r_*}Q_1 + i\frac{2m\omega}{r^2}Q_0 - \frac{f}{r^2}(\beta + 4f)Q_1 +$$
$$- \frac{2f}{r^3}\left[H + J\left(1 - \frac{1}{2}\beta\right)\right] + \frac{f^2}{r}\left(2P_{00} + P_{01}\right); \tag{5.101}$$

$$0 = \left(\omega^2 + \partial^2_{r_*}\right) H - \frac{2f}{r}\partial_{r_*}H - \frac{\beta f}{r^2}H - \frac{2f^2\beta}{r}Q_1 + 2f^2\left(1 - \frac{4m}{r}\right)P_{00} +$$
$$+ f^3 P_{01}; \tag{5.102}$$

$$0 = \left(\omega^2 + \partial^2_{r_*}\right) J - \frac{2f}{r}\partial_{r_*}J + \frac{f}{r^2}(4f - \beta)J + \frac{4f^2}{r}Q_1. \tag{5.103}$$

Derived here are the frequency-decomposed wave equations describing first-order perturbations, the trace-reversed metric $\bar{h}_{\mu\nu}$ (5.69)-(5.71), of the Schwarzschild background in Schwarzschild coordinates.

5.4   Scattering

5.4.1   Gravitational Energy Flux

Groundwork for scattering has already been laid in (4.4). All that remains is to compute the Stress-Energy Tensor of the gravitational field, which is given by [29]

$$T^{(gw)}_{\mu\nu} = \frac{1}{32\pi}\left\langle \bar{h}_{\alpha\beta|\mu}\bar{h}^{\alpha\beta}{}_{|\nu} - \frac{1}{2}\bar{h}_{|\mu}\bar{h}_{|\nu} - 2\bar{h}^{\alpha\beta}{}_{|\beta}\bar{h}_{\alpha(\mu|\nu)}\right\rangle. \tag{5.104}$$

In Lorentz gauge $\left(\bar{h}^{\alpha\beta}{}_{|\beta} = 0\right)$ this expression simplifies to

$$T^{(gw)}_{\mu\nu} = \frac{1}{32\pi}\left\langle \bar{h}_{\alpha\beta|\mu}\bar{h}^{\alpha\beta}{}_{|\nu} - \frac{1}{2}\bar{h}_{|\mu}\bar{h}_{|\nu}\right\rangle, \tag{5.105}$$

where superscript (gw) signifies the Stress-Energy Tensor of a gravitational wave, as opposed to matter. The energy flux is given by $T^{(gw)}_{01}$.

5.4.2 Odd Parity Energy Flux

A priori knowledge of the fact that, just like the wave equations and $\dot{E}$ in E&M case, the energy flux will separate into *odd* and *even* parts, somewhat simplifies the calculation of the 01 component of (5.105). Even so, the simplest method is using a *Mathematica* routine to perform the inner summations and integrate over all angles to obtain the total energy impinging on a spherical shell of radius r

$$\dot{E} = \frac{1}{32\pi} \int_0^{2\pi} \int_0^{\pi} \left\langle \bar{h}_{\alpha\beta|t} \bar{h}^{\alpha\beta}{}_{|r} - \frac{1}{2} \bar{h}_{,t} \bar{h}_{,r} \right\rangle \sin\theta \, d\theta d\phi; \tag{5.106}$$

$$= \frac{1}{32\pi} \int_0^{2\pi} \int_0^{\pi} \left\langle \sum_\alpha \sum_\beta \sum_\delta \sum_\gamma g^{\alpha\delta} g^{\beta\gamma} \left(\bar{h}_{\alpha\beta,t} - \sum_\lambda \Gamma^\lambda{}_{\alpha t} \bar{h}_{\lambda\beta} - \sum_\lambda \Gamma^\lambda{}_{\beta t} \bar{h}_{\alpha\lambda} \right) \times \right.$$

$$\times \left(\bar{h}_{\delta\gamma,r} - \sum_\lambda \Gamma^\lambda{}_{\delta r} \bar{h}_{\lambda\gamma} - \sum_\lambda \Gamma^\lambda{}_{\gamma r} \bar{h}_{\delta\lambda} \right) +$$

$$\left. - \frac{1}{2} \partial_t \left(\sum_\alpha \sum_\beta g^{\alpha\beta} \bar{h}_{\alpha\beta} \right) \partial_r \left(\sum_\alpha \sum_\beta g^{\alpha\beta} \bar{h}_{\alpha\beta} \right) \right\rangle \sin\theta \, d\theta d\phi, \tag{5.107}$$

where Christoffel symbols and metric are those of Schwarzschild spacetime in Schwarzschild coordinates. Inserting the odd perturbation metric $\bar{h}^{(odd)}_{\mu\nu}$ given by

$$\bar{h}^{(odd)}_{ab} = 0; \tag{5.108}$$

$$\bar{h}^{(odd)}_{aB} = (R_0 \tau_a + R_1 \rho_a) X_B; \tag{5.109}$$

$$\bar{h}^{(odd)}_{AB} = K W_{AB}. \tag{5.110}$$

into (5.107) yields the odd-parity energy flux

$$P_{odd} = \frac{l(l+1)}{32\pi r^2} \left[\frac{1}{2r^2}(l-1)(l+2) \left(\partial_r K - \frac{2}{r} K \right) \partial_t K + \right. \tag{5.111}$$

$$\left. + 2 \left(\partial_r R_1 - \frac{1}{r} R_1 \right) \partial_t R_1 - 2 \left(\partial_r R_0 - \frac{1}{r} R_0 \right) \partial_t R_0 \right].$$

In frequency domain ($\partial_t = -i\omega$) and tortoise coordinate $\left(\partial_r = \frac{1}{f}\partial_{r_*}\right)$ it looks like this

$$P_{odd} = -i\omega\frac{l(l+1)}{32\pi r^2}\left[\frac{1}{2r^2}(l-1)(l+2)\left(\frac{1}{f}\partial_{r_*}K - \frac{2}{r}K\right)K+\right.\tag{5.112}$$
$$\left. + 2\left(\frac{1}{f}\partial_{r_*}R_1 - \frac{1}{r}R_1\right)R_1 - 2\left(\frac{1}{f}\partial_{r_*}R_0 - \frac{1}{r}R_0\right)R_0\right].$$

$-i$ can be ignored because only $|P_{odd}|$ is physically meaningful[13].

5.4.3   Even Parity Energy Flux

Using (5.107) together with the even parity metric perturbation

$$\bar{h}_{ab}^{(even)} = (P_{00}y_{ab} + P_{01}u_{ab} + P_{11}w_{ab})\,Y;\tag{5.113}$$

$$\bar{h}_{aB}^{(even)} = (Q_0\tau_a + Q_1\rho_a)\,Y_B;\tag{5.114}$$

$$\bar{h}_{AB}^{(even)} = HY_{AB} + JU_{AB},\tag{5.115}$$

yields the even-parity power dissipation formula

$$P_{even} = \frac{1}{32\pi}\left\{\frac{1}{2r^4}(l-1)l(1+l)(2+l)\left(\partial_r J - \frac{2}{r}J\right)\partial_t J +\right.\tag{5.116}$$
$$+\frac{2f}{r^2}l(1+l)\left[\left(\partial_r Q_1 - \frac{1}{r}Q_1\right)\partial_t Q_1 - \left(\partial_r Q_0 - \frac{1}{r}Q_0\right)\partial_t Q_0\right] +$$
$$+\frac{f^2}{2}\left(\partial_r P_{01}\partial_t P_{01} - \partial_r P_{11}\partial_t P_{11}\right) +$$
$$\left.- \frac{2f}{r^2}\left[\partial_r P_{00}\partial_t H + \left(\partial_r H - \frac{2}{r}H\right)\partial_t P_{00}\right]\right\}.$$

---

[13]$|-i| = 1.$

131

Converting to frequency domain ($\partial_t = -i\omega$) and tortoise coordinate $\left(\partial_r = \frac{1}{f}\partial_{r_*}\right)$, one obtains

$$
\begin{aligned}
P_{even} &= \frac{-i\omega}{32\pi}\left\{\frac{1}{2r^4}(l-1)l(1+l)(2+l)\left(\frac{1}{f}\partial_{r_*}J - \frac{2}{r}J\right)J + \right. \\
&\quad + \frac{2f}{r^2}l(1+l)\left[\left(\frac{1}{f}\partial_{r_*}Q_1 - \frac{1}{r}Q_1\right)Q_1 - \left(\frac{1}{f}\partial_{r_*}Q_0 - \frac{1}{r}Q_0\right)Q_0\right] + \\
&\quad + \frac{f}{2}\left(P_{01}\partial_{r_*}P_{01} - P_{11}\partial_{r_*}P_{11}\right) + \\
&\quad \left. - \frac{2f}{r^2}\left[\frac{1}{f}H\partial_{r_*}P_{00} + \left(\frac{1}{f}\partial_{r_*}H - \frac{2}{r}H\right)P_{00}\right]\right\}.
\end{aligned}
\tag{5.117}
$$

5.4.4 Initial/Boundary Conditions

Applying the procedure developed in (4.4.3)[14] yields the boundary conditions for an in-falling, monochromatic wave however, before said procedure can be followed, Lorentz gauge condition must be cast into a soluble form.

Lorentz Gauge

Statement of the Lorentz gauge is

$$
\bar{h}_{\mu\nu|}{}^{\nu} = 0,
\tag{5.118}
$$

$\mathcal{M}^2 \times \mathcal{S}^2$ decomposition of this statement is given by (3.316) and (3.317)

$$
\bar{h}_{M\nu|}{}^{\nu} = \nabla^n \bar{h}_{Mn} + \nabla^N \bar{h}_{MN} + \frac{2}{r}\rho^n \bar{h}_{nM} = 0;
\tag{5.119}
$$

$$
\bar{h}_{m\nu|}{}^{\nu} = \nabla^n \bar{h}_{mn} + \nabla^N \bar{h}_{mN} + \frac{2}{r}\rho^n \bar{h}_{nm} - \frac{1}{r}\rho_m g^{MN}\bar{h}_{MN} = 0.
\tag{5.120}
$$

---

[14]Substituting in-falling, monochromatic waves of undetermined amplitudes into the perturbation field equations and using the gauge to uniquely, within a multiplicative constant, determine said amplitudes.

Inserting the decomposed perturbation metric $\bar{h}_{\mu\nu}$ (5.69)-(5.71) yields the Lorentz gauge conditions on Schwarzschild background

$$0 = \tau^n \nabla_n R_0 + \rho^n \nabla_n R_1 + \frac{2}{r}\left(1 - \frac{m}{r}\right)R_1 + \frac{1}{r^2}\left(1 - \frac{1}{2}\beta\right)K; \tag{5.121}$$

$$0 = \tau^n \nabla_n Q_0 + \rho^n \nabla_n Q_1 + \frac{2}{r}\left(1 - \frac{m}{r}\right)Q_1 + \frac{1}{r^2}H + J\frac{1}{r^2}\left(1 - \frac{1}{2}\beta\right); \tag{5.122}$$

$$0 = \rho^n \nabla_n P_{00} + \frac{1}{2}\rho^n \nabla_n P_{01} + \frac{1}{2}\tau^n \nabla_n P_{11} - \frac{\beta}{r^2}Q_1 + \frac{2}{r}\left(1 - \frac{m}{r}\right)P_{00} + \frac{1}{r}P_{01} + \tag{5.123}$$
$$-\frac{2}{r^3}H;$$

$$0 = \tau^n \nabla_n P_{00} - \frac{1}{2}\tau^n \nabla_n P_{01} - \frac{1}{2}\rho^n \nabla_n P_{11} + \frac{\beta}{r^2}Q_0 + \frac{1}{r}P_{11}. \tag{5.124}$$

Converted to Schwarzschild [tortoise] coordinates and frequency-domain, the four Lorentz conditions take the form

$$0 = -i\omega R_0 + \partial_{r_*} R_1 + \frac{2}{r}\left(1 - \frac{m}{r}\right)R_1 + \frac{1}{r^2}\left(1 - \frac{1}{2}\beta\right)K; \tag{5.125}$$

$$0 = -i\omega Q_0 + \partial_{r_*} Q_1 + \frac{2}{r}\left(1 - \frac{m}{r}\right)Q_1 + \frac{1}{r^2}H + J\frac{1}{r^2}\left(1 - \frac{1}{2}\beta\right); \tag{5.126}$$

$$0 = \partial_{r_*} P_{00} + \frac{1}{2}\partial_{r_*} P_{01} - \frac{i\omega}{2}P_{11} - \frac{\beta}{r^2}Q_1 + \frac{2}{r}\left(1 - \frac{m}{r}\right)P_{00} + \frac{1}{r}P_{01} - \frac{2}{r^3}H; \tag{5.127}$$

$$0 = i\omega\left(\frac{1}{2}P_{01} - P_{00}\right) - \frac{1}{2}\partial_{r_*} P_{11} + \frac{\beta}{r^2}Q_0 + \frac{1}{r}P_{11}. \tag{5.128}$$

The In-falling Wave

Identical to (4.4.3), the form of the in-falling wave is assumed

$$R_0(r_* \to -\infty) \quad \to \quad C_1 e^{-i\omega r_*}; \tag{5.129}$$

$$R_1(r_* \to -\infty) \quad \to \quad C_2 e^{-i\omega r_*}; \tag{5.130}$$

$$K(r_* \to -\infty) \quad \to \quad C_3 e^{-i\omega r_*}; \tag{5.131}$$

$$P_{00}(r_* \to -\infty) \quad \to \quad C_4 e^{-i\omega r_*}; \tag{5.132}$$

133

$$P_{01}(r_* \to -\infty) \quad \to \quad C_5 e^{-i\omega r_*}; \tag{5.133}$$

$$P_{11}(r_* \to -\infty) \quad \to \quad C_6 e^{-i\omega r_*}; \tag{5.134}$$

$$Q_0(r_* \to -\infty) \quad \to \quad C_7 e^{-i\omega r_*}; \tag{5.135}$$

$$Q_1(r_* \to -\infty) \quad \to \quad C_8 e^{-i\omega r_*}; \tag{5.136}$$

$$J(r_* \to -\infty) \quad \to \quad C_9 e^{-i\omega r_*}; \tag{5.137}$$

$$H(r_* \to -\infty) \quad \to \quad C_{10} e^{-i\omega r_*}. \tag{5.138}$$

Taking the limits of (5.94)-(5.103) as $r_* \to -\infty$, $f \to 0$, and $r \to 2m$; inserting (5.129)-(5.138) into (5.94)-(5.103) and (5.125)-(5.128), yields the non-unique, in-falling perturbation field conforming to the perturbation field equations (5.94)-(5.103) and the Lorentz gauge

$$R_0(r_* \to -\infty) \quad \to \quad \frac{1}{4m}\frac{2-\beta}{4mi\omega - 1}e^{-i\omega r_*}; \tag{5.139}$$

$$R_1(r_* \to -\infty) \quad \to \quad \frac{1}{4m}\frac{2-\beta}{4mi\omega - 1}e^{-i\omega r_*}; \tag{5.140}$$

$$K(r_* \to -\infty) \quad \to \quad e^{-i\omega r_*}; \tag{5.141}$$

$$P_{00}(r_* \to -\infty) \quad \to \quad e^{-i\omega r_*}; \tag{5.142}$$

$$P_{01}(r_* \to -\infty) \quad \to \quad 0; \tag{5.143}$$

$$P_{11}(r_* \to -\infty) \quad \to \quad 0; \tag{5.144}$$

$$Q_0(r_* \to -\infty) \quad \to \quad i\frac{4m^2\omega}{\beta}e^{-i\omega r_*}; \tag{5.145}$$

$$Q_1(r_* \to -\infty) \quad \to \quad i\frac{4m^2\omega}{\beta}e^{-i\omega r_*}; \tag{5.146}$$

$$J(r_* \to -\infty) \quad \to \quad \frac{4m^2(4m\omega + i)(4m\omega - i\beta)}{\beta(\beta - 2)}e^{-i\omega r_*}; \tag{5.147}$$

$$H(r_* \to -\infty) \quad \to \quad 2m^2\left(1 - 4im\omega\right)e^{-i\omega r_*}, \tag{5.148}$$

where C_3 and C_4 are set to 1. Such residual gauge freedom is present because, ultimately, the amplitude of the wave is determined by whatever source or initial conditions produced it. Two constants are free (as opposed to one) because *even* and *odd* perturbations are independent.

5.5 Numerical Implementation

5.5.1 The Field Equations

Cognizant of the precedent of unprocessed fields not behaving as plane waves with $r \to r_* \to \pm\infty$ (4.5.1), one expects the field functions of (5.94)-(5.103) to be enveloped. Indeed, after integration, one discovers that $r^2 P_{00}, \frac{r}{f} P_{01}, \frac{r}{f} P_{11}, \frac{1}{r} K, \frac{1}{r} H$, and $\frac{1}{r} J$ behave like plane waves, *e.g.* $Ce^{\pm i\omega r_*}$; $R_{0,1}$ and $Q_{0,1}$ are not enveloped. To simplify numerical treatment of the perturbation field functions, the following substitutions are made to force all functions of (5.94)-(5.103) to plane waves as $r_* \to \pm\infty$

$$P'_{01} = \frac{r}{f} P_{01}; \tag{5.149}$$

$$P'_{11} = \frac{r}{f} P_{11}; \tag{5.150}$$

$$P'_{00} = r^2 P_{00}; \tag{5.151}$$

$$K' = \frac{1}{r} K; \tag{5.152}$$

$$H' = \frac{1}{r} H; \tag{5.153}$$

$$J' = \frac{1}{r} J. \tag{5.154}$$

Using (5.149)-(5.154) in (5.94)-(5.103) produces the perturbation equations where all fields approach plane waves as $r_* \to \pm\infty$.

$$0 = \left(\omega^2 + \partial_{r_*}^2\right)K' + \frac{2f}{r^2}\left(1 - \frac{m}{r} - \frac{1}{2}\beta\right)K' + \frac{4f^2}{r^2}R_1; \tag{5.155}$$

$$0 = \left(\omega^2 + \partial_{r_*}^2\right)R_0 + \frac{2m}{r^2}\partial_{r_*}R_0 - \beta\frac{f}{r^2}R_0 + i\frac{2m\omega}{r^2}R_1; \tag{5.156}$$

$$0 = \left(\omega^2 + \partial_{r_*}^2\right)R_1 + \frac{2m}{r^2}\partial_{r_*}R_1 - (4f+\beta)R_1\frac{f}{r^2} + i\frac{2m\omega}{r^2}R_0 - (2-\beta)\frac{f}{r^2}K'; \tag{5.157}$$

$$0 = \left(\omega^2 + \partial_{r_*}^2\right)P'_{00} - \frac{2}{r}\left(1 - \frac{4m}{r}\right)\partial_{r_*}P'_{00} - \frac{1}{r^2}\left[\frac{4m}{r}\left(2 - \frac{5m}{r}\right) + \beta f\right]P'_{00} + \tag{5.158}$$

$$-\frac{f^3}{r}P'_{01} + \frac{2f\beta}{r}Q_1 + \frac{2}{r}\left(1 - \frac{4m}{r}\right)H';$$

$$0 = \left(\omega^2 + \partial_{r_*}^2\right)P'_{01} + \frac{8m}{r^2}\partial_{r_*}P'_{01} + \frac{2}{r^2}\left[\frac{16m^2}{r^2} - \frac{3m}{r} - 1 - f\frac{1}{2}\beta\right]P'_{01} + \tag{5.159}$$

$$+i\frac{4m\omega}{r^2}P'_{11} + \frac{4\beta}{r^2}Q_1 + \frac{4}{r^2}H' - \frac{4f}{r^3}P'_{00};$$

$$0 = \left(\omega^2 + \partial_{r_*}^2\right)P'_{11} + \frac{8m}{r^2}\partial_{r_*}P'_{11} + \frac{2}{r^2}\left[\frac{16m^2}{r^2} - \frac{3m}{r} - 1 - f\frac{1}{2}\beta\right]P'_{11} + \tag{5.160}$$

$$+i\frac{4m\omega}{r^2}P'_{01} + \frac{4\beta}{r^2}Q_0;$$

$$0 = \left(\omega^2 + \partial_{r_*}^2\right)Q_0 + \frac{2m}{r^2}\left(i\omega Q_1 + \partial_{r_*}Q_0\right) - \frac{\beta f}{r^2}Q_0 + \frac{f^3}{r^2}P'_{11}; \tag{5.161}$$

$$0 = \left(\omega^2 + \partial_{r_*}^2\right)Q_1 + \frac{2m}{r^2}\left(\partial_{r_*}Q_1 + i\omega Q_0\right) - \frac{f}{r^2}(\beta + 4f)Q_1 + \tag{5.162}$$

$$-\frac{2f}{r^2}\left[H' + J'\left(1 - \frac{1}{2}\beta\right)\right] + \frac{f^2}{r^2}\left(\frac{2}{r}P'_{00} + fP'_{01}\right);$$

$$0 = \left(\omega^2 + \partial_{r_*}^2\right)J' + \frac{2f}{r^2}\left(1 - \frac{m}{r} - \frac{1}{2}\beta\right)J' + \frac{4f^2}{r^2}Q_1; \tag{5.163}$$

$$0 = \left(\omega^2 + \partial_{r_*}^2\right)H' - \frac{2f}{r^2}\left(1 - \frac{3m}{r} + \frac{1}{2}\beta\right)H' - \frac{2\beta f^2}{r^2}Q_1 + \tag{5.164}$$

$$+\frac{2f^2}{r^3}\left(1 - \frac{4m}{r}\right)P'_{00} + \frac{f^4}{r^2}P'_{01}.$$

Lorentz gauge must also be modified accordingly

$$0 = -i\omega R_0 + \partial_{r_*}R_1 + \frac{2}{r}\left(1 - \frac{m}{r}\right)R_1 + \frac{1}{r}\left(1 - \frac{1}{2}\beta\right)K'; \tag{5.165}$$

136

$$0 = -i\omega Q_0 + \partial_{r_*} Q_1 + \frac{2}{r}\left(1 - \frac{m}{r}\right)Q_1 + \frac{1}{r}H' + J'\frac{1}{r}\left(1 - \frac{1}{2}\beta\right); \tag{5.166}$$

$$0 = \partial_{r_*} P'_{00} + \frac{rf}{2}\partial_{r_*} P'_{01} + \frac{2m}{r^2}P'_{00} + \frac{f}{2}\left(1 + \frac{4m}{r}\right)P'_{01} - \frac{i\omega}{2}rfP'_{11} - \beta Q_1 + \tag{5.167}$$

$$-2H';$$

$$0 = i\omega\left(\frac{f}{2}P'_{01} - \frac{1}{r}P'_{00}\right) - \frac{f}{2}\partial_{r_*} P'_{11} + \frac{\beta}{r}Q_0 - \frac{f}{2r}\left(1 + \frac{4m}{r}\right)P'_{11}. \tag{5.168}$$

Same for the initial/boundary conditions

$$R_0(r_* \to -\infty) \;\to\; \frac{1}{4m}\frac{2 - \beta}{4mi\omega - 1}e^{-i\omega r_*}; \tag{5.169}$$

$$R_1(r_* \to -\infty) \;\to\; \frac{1}{4m}\frac{2 - \beta}{4mi\omega - 1}e^{-i\omega r_*}; \tag{5.170}$$

$$K'(r_* \to -\infty) \;\to\; \frac{1}{2m}e^{-i\omega r_*}; \tag{5.171}$$

$$P'_{00}(r_* \to -\infty) \;\to\; e^{-i\omega r_*}; \tag{5.172}$$

$$P'_{01}(r_* \to -\infty) \;\to\; \frac{1}{3m}\frac{4m\omega - 3i}{4m\omega + 3i}e^{-i\omega r_*}; \tag{5.173}$$

$$P'_{11}(r_* \to -\infty) \;\to\; \frac{8}{3}\frac{\omega}{4m\omega + 3i}e^{-i\omega r_*}; \tag{5.174}$$

$$Q_0(r_* \to -\infty) \;\to\; \frac{i\omega}{\beta}e^{-i\omega r_*}; \tag{5.175}$$

$$Q_1(r_* \to -\infty) \;\to\; \frac{i\omega}{\beta}e^{-i\omega r_*}; \tag{5.176}$$

$$J'(r_* \to -\infty) \;\to\; \frac{(\beta + 4im\omega)(1 - 4im\omega)}{2\beta(\beta - 2)}e^{-i\omega r_*}; \tag{5.177}$$

$$H'(r_* \to -\infty) \;\to\; \left(\frac{1}{4m} - i\omega\right)e^{-i\omega r_*}. \tag{5.178}$$

And finally the gravitational energy flux

$$P_{odd} = -i\omega\frac{l(l + 1)}{32\pi r^2}\left[\frac{1}{2}(l - 1)(l + 2)\left(\frac{1}{f}\partial_{r_*}K' - \frac{1}{r}K'\right)K' + \right. \tag{5.179}$$

$$\left. + 2\left(\frac{1}{f}\partial_{r_*}R_1 - \frac{1}{r}R_1\right)R_1 - 2\left(\frac{1}{f}\partial_{r_*}R_0 - \frac{1}{r}R_0\right)R_0\right];$$

$$P_{even} = \frac{-i\omega}{32\pi}\left\{\frac{1}{2r^2}(l - 1)l(1 + l)(2 + l)\left(\frac{1}{f}\partial_{r_*}J' - \frac{1}{r}J'\right)J' + \right. \tag{5.180}$$
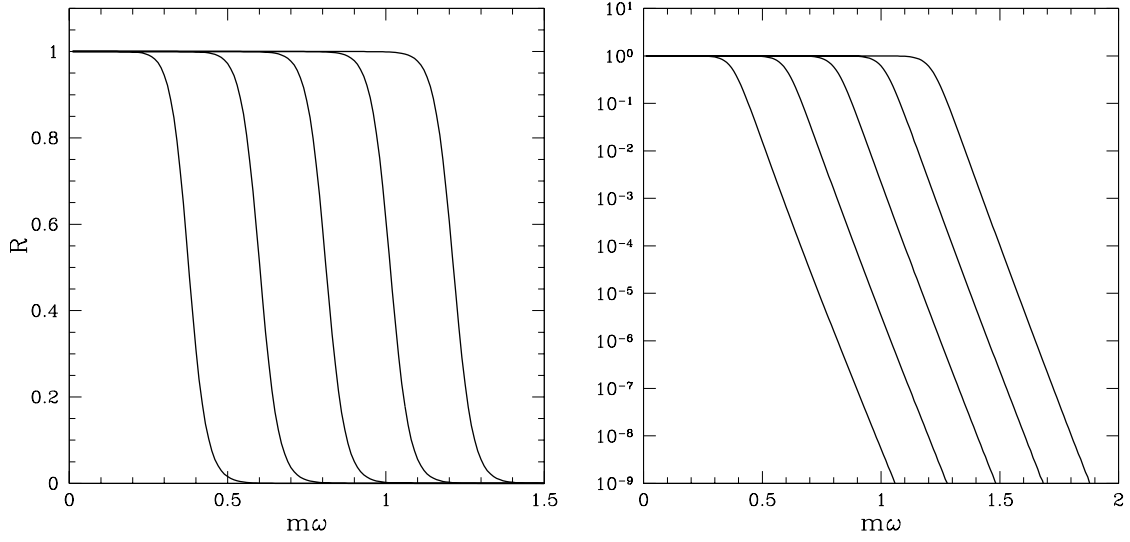
Figure 5.1: Reflection of gravitational radiation from a Schwarzschild black hole for (left to right) $l = 2, 3, 4, 5, 6$.

$$
\begin{aligned}
&+ \frac{2f}{r^2} l(1+l) \left[\left(\frac{1}{f} \partial_{r_*} Q_1 - \frac{1}{r} Q_1 \right) Q_1 - \left(\frac{1}{f} \partial_{r_*} Q_0 - \frac{1}{r} Q_0 \right) Q_0 \right] + \\
&+ \frac{f^3}{2r^2} \left[P'_{01} \partial_{r_*} P'_{01} - P'_{11} \partial_{r_*} P'_{11} - \frac{1}{r} \left(1 - \frac{4m}{r} \right) \left(P'^2_{01} - P'^2_{11} \right) \right] + \\
&- \frac{2f}{r^3} \left[\frac{1}{f} \left(H' \partial_{r_*} P'_{00} + P'_{00} \partial_{r_*} H' \right) - \frac{3}{r} P'_{00} H' \right] \Bigg\} .
\end{aligned}
$$

(5.155)-(5.165) are integrated with RK4 in a manner identical to that described in (4.5.2).

5.6   Conclusion

In order not to repeat the counterpart (sub)sections of the electromagnetic chapter, one can say that the perturbation field differential equations, boundary conditions, and power dissipation (energy flux) formulae developed in this chapter yield the accepted reflection coefficients of gravitational radiation from a Schwarzschild black

hole thus, once more, proving that direct metric perturbation along with $\mathcal{M}^2 \times \mathcal{S}^2$ decomposition is a valid method for working with gravitational radiation on curved spacetimes. Demonstrated advantage of the $\mathcal{M}^2 \times \mathcal{S}^2$ decomposition is that it provides coordinateless field equations on Schwarzschild space. Once the coordinate system is chosen, conversion of the equations is effortless.

Future work includes full self-force calculation of particles orbiting Schwarzschild black holes in circular and eccentric orbits.

Chapter 6

Conclusion

This thesis concludes with several major accomplishments. Quasinormal modes of an acoustic black hole comprised of a perfect, inviscid, relativistic, ideal gas spherically accreting onto a Schwarzschild black hole are computed. Enhancing on the previous research by introducing a fully-relativistic, physical accretion flow and relativistic equation of state. It is also shown that in the limit of the equation of state $p = \rho$, sound propagating in such ideal gas reduces to a Regge-Wheeler scalar wave traveling at the speed of light.

$\mathcal{M}^2 \times \mathcal{S}^2$ metric decomposition formalism, which operates on Schwarzschild spacetime but, not necessarily in Schwarzschild coordinates, is explored in detail. A relatively new mathematical tool, it required significant analytical review, for the identities associated with the concept are not tabulated in literature and/or publications.

$\mathcal{M}^2 \times \mathcal{S}^2$ decomposition is applied to the electromagnetic field propagating in the vicinity of a Schwarzschild black hole. Four field equations, one for each vector potential component A_μ, are obtained in Lorenz gauge and used to compute the reflection from the Schwarzschild curvature. Results match to those obtained previously via traditional methods, *e.g.* Regge-Wheeler potential/equation.

$\mathcal{M}^2 \times \mathcal{S}^2$ decomposition is applied to gravitational waves propagating in the vicinity of a Schwarzschild black hole. Ten field equations, one for each perturbation metric component $\bar{h}_{\mu\nu}$, are obtained in Lorentz gauge and used to compute the reflection from the Schwarzschild curvature. Results match to those obtained previously via traditional methods, *e.g.* Regge-Wheeler potential/equation.

Bibliography

[1] E. Abdalla, R. A. Konoplya, and A. Zhidenko. Perturbations of schwarzschild black holes in laboratories, 2007.

[2] Leor Barack and Carlos O. Lousto. Perturbations of schwarzschild black holes in the lorenz gauge: Formulation and numerical implementation. *Physical Review D*, 72:104026, 2005.

[3] Leor Barack and Amos Ori. Regularization parameters for the self force in schwarzschild spacetime: Ii. gravitational and electromagnetic cases. *Physical Review D*, 67:024029, 2003.

[4] Leor Barack and Norichika Sago. Gravitational self-force correction to the innermost stable circular orbit of a schwarzschild black hole, 2009.

[5] Mark V. Berndtson. Harmonic gauge perturbations of the schwarzschild metric, 2009.

[6] Emanuele Berti, Vitor Cardoso, and Jose' P. S. Lemos. Quasinormal modes and classical wave propagation in analogue black holes. *Physical Review D*, 70:124006, 2004.

[7] Gerold Betschart and Chris A. Clarkson. Scalar field and electromagnetic perturbations on locally rotationally symmetric spacetimes. *Classical and Quantum Gravity*, 21:5587, 2004.

[8] N. Bilic. Relativistic acoustic geometry. *Classical and Quantum Gravity*, 16:3953–3964, December 1999.

[9] H. Bondi. On spherically symmetrical accretion. *Monthly Notices of the Royal Astronomical Society*, 112:195–204, October 1952.

[10] W. Brinkmann. Adiabatic accretion onto a Schwarzschild black hole. *Astronomy and Astrophysics*, 85:146–148, May 1980.

[11] M. Campanelli, C. O. Lousto, P. Marronetti, and Y. Zlochower. Accurate evolutions of orbiting black-hole binaries without excision. *Physical Review Letters*, 96:111101, 2006.

[12] Vitor Cardoso, Jose' P. S. Lemos, and Shijun Yoshida. Quasinormal modes and stability of the rotating acoustic black hole: numerical analysis. *Physical Review D*, 70:124032, 2004.

[13] Jorge Castineiras, Luis C. B. Crispino, George E. A. Matsas, and Rodrigo Murta. Semiclassical approach to black hole absorption of electromagnetic radiation emitted by a rotating charge. *Physical Review D*, 71:104013, 2005.

[14] L. L. Cowie, J. P. Ostriker, and A. A. Stark. Time-dependent spherically symmetric accretion onto compact X-ray sources. *Astrophysical Journal*, 226:1041–1062, December 1978.

[15] Ernst Nils Dorband. Computing and Analyzing Gravitational Radiation in Black Hole Simulations using a New Multi-Block Approach to Numerical Relativity. AAT-3256317.

[16] T. Foglizzo. Entropic-acoustic instability of shocked Bondi accretion I. What does perturbed Bondi accretion sound like? *Astronomy and Astrophysics*, 368:311–324, March 2001.

[17] S.W. Hawking. Black hole explosions? *Nature*, 248:30–31, 1974.

[18] Benjamin Aylott *et al.* Testing gravitational-wave searches with numerical relativity waveforms: Results from the first numerical injection analysis (ninja) project, 2009.

[19] Kunihito Ioka and Hiroyuki Nakano. Second and higher-order quasi-normal modes in binary black hole mergers. *Physical Review D*, 76:061503, 2007.

[20] John David Jackson. *Classical Electrodynamics*. Wiley, 1998.

[21] Samuel Lepe and Joel Saavedra. Quasinormal modes, superradiance and area spectrum for 2+1 acoustic black holes. *Physics Letters B*, 617:174, 2005.

[22] L. Lorenz. On the identity of the vibrations of light with electrical currents. *Philos. Mag.*, 34:287–301, 1867.

[23] Carlos O. Lousto and Hiroyuki Nakano. Regular second order perturbations of binary black holes: The extreme mass ratio regime. *CLASS.QUANT.GRAV*, 015007, 2009.

[24] J. F. Lu. Sound horizon of accretion onto a Kerr black hole. *General Relativity and Gravitation*, 18:45–51, January 1986.

[25] Edward Malec. How much of the outgoing radiation can be intercepted by schwarzschildean black holes? *ACTA PHYS.POLON.B*, 32:47, 2001.

[26] Karl Martel. Gravitational waveforms from a point particle orbiting a schwarzschild black hole. *Physical Review D*, 69:044025, 2004.

[27] Karl Martel and Eric Poisson. Gravitational perturbations of the schwarzschild spacetime: A practical covariant and gauge-invariant formalism. *Physical Review D*, 71:104003, 2005.

[28] Yasushi Mino, Hiroyuki Nakano, and Misao Sasaki. Covariant self-force regularization of a particle orbiting a schwarzschild black hole - mode decomposition regularization -. *Progress of Theoretical Physics*, 108:1039, 2003.

[29] Charles W. Misner, Kip S. Thorne, and John Archibald Wheeler. *Gravitation*. W. H. Freeman, 1973.

[30] V. Moncrief. Stability of stationary, spherical accretion onto a Schwarzschild black hole. *Astrophysical Journal*, 235:1038–1046, February 1980.

[31] Alessandro Nagar and Luciano Rezzolla. Gauge-invariant non-spherical metric perturbations of schwarzschild black-hole spacetimes. *ERRATUM-IBID.*, 23:4297, 2006.

[32] Alessandro Nagar, Olindo Zanotti, Jose A. Font, and Luciano Rezzolla. On the accretion-induced qnm excitation of a schwarzschild black hole. *Physical Review D*, 75:044016, 2007.

[33] Hiroyuki Nakano, Manuela Campanelli, Carlos O. Lousto, and Yosef Zlochower. Comparison of post-newtonian and numerical evolutions of black-hole binaries, 2009.

[34] Hiroyuki Nakano, Yasunari Kurita, Kouji Ogawa, and Chul-Moon Yoo. Quasinormal ringing for acoustic black holes at low temperature. *Physical Review D*, 71:084006, 2005.

[35] T. Naskar, N. Chakravarty, J. K. Bhattacharjee, and A. K. Ray. Acoustic perturbations on steady spherical accretion in Schwarzschild geometry. *Physical Review D*, 76(12):123002–+, December 2007.

[36] L. Nobili, R. Turolla, and L. Zampieri. Spherical accretion onto black holes - A

complete analysis of stationary solutions. *Astrophysical Journal*, 383:250–262, December 1991.

[37] Satoshi Okuzumi and Masa aki Sakagami. Quasinormal ringing of acoustic black holes in laval nozzles: Numerical simulations. *Physical Review D*, 76:084027, 2007.

[38] Tullio Regge and John A. Wheeler. Stability of a schwarzschild singularity. *Phys. Rev.*, 108(4):1063–1069, Nov 1957.

[39] Joel Saavedra. Quasinormal modes of unruh's acoustic black hole. *MOD.PHYS.LETT.A*, 21:1601, 2006.

[40] Norichika Sago, Leor Barack, and Steven Detweiler. Two approaches for the gravitational self force in black hole spacetime: Comparison of numerical results. *Physical Review D*, 78:124024, 2008.

[41] S. L. Shapiro. Potential flows in general relativity: Some exact solutions. *Phys. Rev. D*, 39:2839–2847, May 1989.

[42] Carlos F. Sopuerta and Pablo Laguna. A finite element computation of the gravitational radiation emitted by a point-like object orbiting a non-rotating black hole. *Physical Review D*, 73:044028, 2006.

[43] Pranesh A. Sundararajan, Gaurav Khanna, and Scott A. Hughes. Towards adiabatic waveforms for inspiral into kerr black holes: I. a new model of the source for the time domain perturbation equation. *Physical Review D*, 76:104005, 2007.

[44] Kip S. Thorne. Multipole expansions of gravitational radiation. *Reviews of Modern Physics*, 52(2):299–339, 1980.

[45] W. G. Unruh. Experimental black-hole evaporation? *Phys. Rev. Lett.*, 46(21):1351–1353, May 1981.

[46] Matt Visser. Acoustic black holes: horizons, ergospheres, and hawking radiation. *Classical and Quantum Gravity*, 15:1767, 1998.

[47] L. Zampieri, J. C. Miller, and R. Turolla. Time-dependent analysis of spherical accretion on to black holes. *Monthly Notices of the Royal Astronomical Society*, 281:1183–1196, August 1996.

[48] Frank J. Zerilli. Effective potential for even-parity regge-wheeler gravitational perturbation equations. *Phys. Rev. Lett.*, 24(13):737–738, Mar 1970.

[49] Yu Zhang, Yuanxing Gui, Fei Yu, and Fenglin Li. Quasinormal modes of a schwarzschild black hole surrounded by free static spherically symmetric quintessence: Electromagnetic perturbations, 2006.